Conjuntos Limite e Bifurcações de Campos de Vetores Suaves por Partes no Plano.

Tiago de Carvalho

Tiago de Carvalho

Conjuntos Limite e Bifurcações de Campos de Vetores Suaves por Partes no Plano

Orientador: ***Prof. Dr. Claudio Aguinaldo Buzzi***

Tese apresentada para obtenção do título de Doutor em Matemática, área de Matemática junto ao Programa de Pós-Graduação em Matemática do Instituto de Biociências, Letras e Ciências Exatas da Universidade Estadual Paulista "Júlio de Mesquita Filho", Campus de São José do Rio Preto.

Banca Examinadora

Prof. Dr. Claudio Aguinaldo Buzzi
UNESP - São José do Rio Preto
Orientador

Prof. Dr. Marco Antonio Teixeira
UNICAMP - Campinas

Prof. Dr. Ronaldo Alves Garcia
UFG - Goiânia

Prof. Dr. João Carlos da Rocha Medrado
UFG - Goiânia

Prof. Dr. Paulo Ricardo da Silva
UNESP - São José do Rio Preto

UNESP - São José do Rio Preto
20 de Janeiro de 2011

Agradecimentos

Gostaria de lembrar aqui de, alguns, daqueles que tornaram possível a realização deste trabalho. Por mais que eu me esforçasse jamais conseguiria colocar aqui uma lista completa das pessoas que me ajudaram, direta ou indiretamente, para a obtenção deste título. Fica aqui meu profundo agradecimento a todos, porém gostaria de destacar algumas pessoas.

Primeiramente, aos meus pais, Geraldo e Neuza, pelo apoio e amor incondicionais, aos quais não só agradeço como também dedico este trabalho.

Ao meu orientador Claudio Buzzi, pelas críticas valiosas e sempre construtivas, pelo suporte, apoio, paciência, dedicação e principalmente por contar com sua amizade.

Aos colegas do IBILCE, em especial ao pessoal da primeira turma de doutorado do IBILCE. Ao Pedro pela importantíssima companhia em Barcelona, ao nosso "chefe" Rafael pelas dicas no espanhol e ao Eduardo que se tornou um grande amigo durante esses últimos anos, inclusive me aturando em sua casa por alguns dias.

Aos professores e funcionários do IBILCE que, de forma muito prestativa e educada, sempre forneceram o suporte acadêmico necessário. Em especial agradeço à Neuza Kakuta pela oportunidade no início de minha graduação quando me apoiou no grupo PET e ao Paulo Ricardo que cuidou da minha iniciação científica e que ainda hoje se dedica a me auxiliar em meus trabalhos.

Ao meu orientador do mestrado, o saudoso Carlos Gutierrez, sem o qual não teria chegado até aqui.

A agência FAPESP pelo apoio financeiro durante o Doutorado (e também durante a Iniciação Científica e o Mestrado).

Resumo

Este trabalho está relacionado com a Teoria Qualitativa de Sistemas Dinâmicos suaves por partes. Estudamos a existência de conjuntos limite, chamados ciclos canard, para esta classe de sistemas definidos no plano e analisamos quando ciclos limite de campos suaves convergem para estes. O conceito de Índice de Poincaré foi generalizado para campos suaves por partes no plano. Seguindo o programa de Thom-Smale, exibimos famílias a 3-parâmetros, bem como os respectivos diagramas de bifurcação, das singularidades planares denominadas Dobra-Sela e Dobra-Cúspide. Também aplicamos o Método Averaging de Primeira Ordem para quantificar os ciclos limite e ciclos canard de uma classe de campos lineares por partes no espaço n-dimensional.

Abstract

This work is related to Qualitative Theory of non-smooth Dynamical Systems. We study the existence os limit sets, named canard cycles, for this class of planar systems. And we analyze when limit cycles of smooth vector fields converge to them. The concept of Poincaré Index was generalized for planar non-smooth systems. Following the Thom-Smale program we exhibit 3-parameter families, and its bifurcation diagrams, of the planar singularities called Fold-Saddle and Fold-Cusp. We apply the First Order Averaging Method to obtain an upper bound to the number of limit cycles and canard cycles for a special class of piecewise linear differential systems in the n-dimensional space.

Sumário

Introdução

É extremamente difundida a idéia que equações diferenciais modelam sistemas de caráter geral nas mais diversas áreas do conhecimento. Muito se fez no sentido de desenvolver uma teoria sólida nesse contexto (veja [1], [33], [38] ou [42]). Entretanto somente recentemente uma nova classe de tais sistemas ganhou notoriedade, são os chamados *Sistemas Dinâmicos suaves por partes*. Nestes admite−se que exista uma subvariedade $(n-1)-$dimensional Σ do espaço $\mathbb{R}^n$ onde o campo de vetores deixa de ser suave e em alguns casos deixa inclusive de ser contínuo. A esta variedade damos o nome de *Variedade de Descontinuidade* (ou curva/superfície de descontinuidade segundo $n = 2$ ou $n = 3$).

Este trabalho está relacionado com a Teoria Qualitativa das Equações Diferenciais Ordinárias visando obter propriedades qualitativas dos Sistemas Dinâmicos suaves por partes no plano. Apesar de existirem diversos trabalhos nesta linha de pesquisa, muito ainda resta a fazer e pretendemos aqui contribuir com essa teoria, quer seja estendendo para esse contexto resultados clássicos estabelecidos para campos suaves em geral, quer seja apresentando resultados que não tem análogo para campos suaves em geral e que só fazem sentido quando inseridos no universo dos campos de vetores suaves por partes.

Em termos mais formais, consideraremos $\Sigma = f^{-1}(0)$ onde $f : \mathbb{R}^n \longrightarrow \mathbb{R}$ é uma função suave que tem $0 \in \mathbb{R}$ como um valor regular, isto é, $\nabla f(p) \neq 0$ para todo $p \in f^{-1}(0)$ e $\Sigma = f^{-1}(0)$. Dessa forma a subvariedade Σ divide $\mathbb{R}^n$ em duas regiões: $\Sigma_+ = \{q \in \mathbb{R}^n | f(q) \geq 0\}$ e $\Sigma_- = \{q \in \mathbb{R}^n | f(q) \leq 0\}$. Localmente sempre podemos identificar Σ com $\{x = (x_1, x_2, \ldots, x_n) \in \mathbb{R}^n | x_1 = 0\}$.

Em cada uma das sub−regiões Σ_+ e Σ_- atuará ou o campo X ou o campo Y, ambos de classe C^r, com $r \geq 1$ grande o suficiente ou $r = \infty$. Definimos o campo de vetores C^r por

partes (ou descontínuo) $Z : \mathbb{R}^n \setminus \Sigma \longrightarrow \mathbb{R}^n$ da seguinte forma:

$$Z(x,y) = \begin{cases} X(x), & \text{se} \quad x \in \Sigma_+, \\ Y(x), & \text{se} \quad x \in \Sigma_-. \end{cases}$$

Usaremos a notação $Z = (X, Y)$. O conjunto de todos os campos descontínuos $Z = (X, Y)$ será denotado por Ω^r.

Para o que segue, considere a notação $X.f(p) = \langle \nabla f(p), X(p) \rangle$. A subvariedade Σ pode ser particionada em três tipos de regiões:

(i) As *regiões de costura* caracterizadas por $(X.f)(Y.f) > 0$.

(ii) As *regiões de escape* caracterizadas por $(X.f) > 0$ e $(Y.f) < 0$.

(iii) As *regiões de deslize* caracterizadas por $(X.f) < 0$ and $(Y.f) > 0$.

Nos pontos p das regiões de deslize e escape, para descrever o comportamento de Z utilizamos o *Campo de Vetores de Filippov* F, que é uma combinação convexa dos vetores $X(p)$ e $Y(p)$ (para mais detalhes veja Figura 1.1 e comentários que a precedem). Note que, dada essa configuração, é latente a relação que existe entre campos de vetores suaves por partes e campos de vetores definidos em variedades com fronteira (veja [39]).

Em busca de propriedades qualitativas que descrevam o comportamento das órbitas destes campos de vetores é de suma importância que estejam bem caracterizados os pontos regulares, os pontos singulares e, em especial, os chamados *Conjuntos Limite*. Fora da curva de descontinuidade Σ temos os conjuntos limite clássicos como pontos de equilíbrio ou ciclos limite (entre outros). Já sobre Σ, ou passando por Σ, aparecem novos pontos e/ou conjuntos distinguíveis que não estavam presentes quando consideramos X ou Y individualmente. Diremos que $q \in \Sigma$ é um *Ponto* $\Sigma-$*Regular* se:

(i) $(X.f(q))(Y.f(q)) > 0$ ou se

(ii) $(X.f(q))(Y.f(q)) < 0$ e q não é um ponto de equilíbrio de F.

Os pontos de Σ que não são $\Sigma-$regulares são chamados de *Pontos* $\Sigma-$*singulares*. O conjunto dos pontos $\Sigma-$singulares é subdividido em dois:

(i) O conjunto dos *Pseudo Equilíbrios*, que é onde $F = 0$ e

(ii) O conjunto das *Singularidades Tangenciais* que é onde $F \neq 0$ e $(X.f(q))(Y.f(q)) = 0$.

Os pseudo equilíbrios atuam como pontos de equilíbrio do campo de Filippov e as singularidades tangencias são pontos de Σ para os quais X e/ou Y são tangentes. Em [40] Teixeira caracteriza os pontos de pseudo equilíbrio genéricos de F. Ao longo desta tese tais pseudo equilíbrios genéricos receberão o nome de $\Sigma-$atrator, $\Sigma-$repulsor e $\Sigma-$sela. Existem vários

tipos de singularidades tangencias, de acordo com a ordem de contato de X e/ou Y com Σ. Os mais relevantes para nós são os pontos de *dobra* e de *cúspide*, onde X e/ou Y têm contatos quadrático e cúbico com Σ, respectivamente. De modo mais formal, dizemos que um ponto $p \in \Sigma$ é um ponto de dobra para X se $X.f(p) = 0$ mas $X^2.f(p) \neq 0$ (caso $X^2.f(p) > 0$ diremos que a dobra é invisível e caso $X^2.f(p) < 0$ diremos que a dobra é visível). Analogamente, dizemos que um ponto $p \in \Sigma$ é um ponto de cúspide para X se $X.f(p) = X^2.f(p) = 0$ mas $X^3.f(p) \neq 0$.

Outro tipo conjuntos limite importante no estudo dos campos descontínuo são os que chamamos de *ciclos canard*. Tais ciclos são trajetórias fechadas que passam por Σ (para maiores detalhes veja a definição 1.2). Em [34] estão caracterizados os ciclos canard genéricos (ou hiperbólicos). Os ciclos canard hiperbólicos descritos na referência acima citada serão chamados nesta tese de ciclos canard hiperbólicos do tipo I, II e III (veja ilustrações nas figuras 1.2, 1.3 e 1.4, respectivamente).

No Capítulo 1 damos as noções básicas sobre a teoria de sistemas dinâmicos suaves por partes, principalmente no plano, necessárias ao bom entendimento do restante do trabalho. Esta teoria foi consolidada ao longo dos anos em trabalhos como [4], [21], [26], [41], entre outros.

No Capítulo 2 apresentamos em detalhes o processo de regularização, introduzido por Sotomayor e Teixeira em [35], e relacionamos campos descontínuos no plano com campos regularizados planares suaves. Este processo diz que dado um campo descontínuo $Z = (X, Y)$, podemos associar a este, uma família a um parâmetro de campos de vetores regularizados Z_ε, de classe C^r, que é uma aproximação do campo descontínuo original Z. De fato, para cada $q \in \mathbb{R}^2$ tome

$$Z_\varepsilon(q) = \varphi_\varepsilon(f(q))Y(q) + (1 - \varphi_\varepsilon(f(q)))X(q),$$

onde $\varphi_\varepsilon(x) = \varphi(x/\varepsilon)$ com φ uma função de transição suave que vale 0 se $x \leq -1$, vale 1 se $x \geq 1$ e $\varphi'(x) > 0$ se $x \in (-1, 1)$. Note que Z_ε coincide com X nos pontos de Σ_+ que estão a uma distância maior que ε de Σ e Z_ε coincide com Y nos pontos de Σ_- que estão a uma distância maior que ε de Σ.

No primeiro resultado inédito que apresentamos na tese (veja Teorema 2.1 no Capítulo 2, ou sua tradução abaixo) obtivemos condições necessárias e suficientes para a ocorrência de um certo tipo de ciclo canard. Desta forma, através de condições intrínsecas a Z, somos capazes de dizer se ocorre ou não um ciclo canard conforme o especificado no dito teorema. O resultado é o seguinte (a numeração dos teoremas enunciados nesta introdução é a mesma que aparece mais adiante nesta tese):

Teorema 2.1 *Seja $Z = (X, Y) \in \Omega^r$ um campo de vetores suave por partes apresentando apenas uma dobra A, onde esta é visível. Denote por γ_1 o arco do campo de vetores W ($W = X$ ou $W = Y$) que passa por A e chame de B o ponto de contato transversal de γ_1 com Σ. Então Z tem um ciclo canard Γ se e somente se as seguintes condições são satisfeitas (veja Figura 1):*

(i) *a componente γ_1 de Γ que passa por A é um arco do tipo focal (veja a definição 2.2);*

(ii) *$X.f(q).Y.f(q) < 0$ para todo $q \in \widehat{AB}/\{A\}$ onde $\widehat{AB}$ representa o arco de Σ ligando os pontos A e B (neste arco inclui-se os extremos A e B);*

(iii) *$\{X(q), Y(q)\}$ é um conjunto linearmente independente para todo $q \in \widehat{AB}$.*

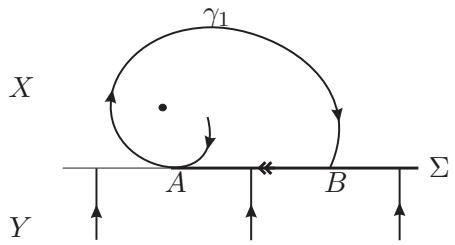

Figure 1: Ciclo canard com apenas uma dobra.

Em [34] os autores provam que se o campo descontínuo tem um ciclo canard hiperbólico então o campo contínuo regularizado também apresenta um ciclo limite hiperbólico. No segundo resultado inédito desta tese (veja o Teorema 2.2 no Capítulo 2, ou sua tradução abaixo), provamos a convergência destes ciclos limite hiperbólicos dos campos regularizados para os ciclos canard hiperbólicos dos campos descontínuos, de acordo com a distância de Hausdorff. Observamos que a distância de Hausdorff entre compactos de $\mathbb{R}^2$ é dada por

$$D(K_1, K_2) = \max_{z_1 \in K_1, z_2 \in K_2} \{d(z_1, K_2), d(z_2, K_1)\}.$$

O resultado obtido é o seguinte:

Teorema 2.2 *Seja Γ_0 um ciclo canard hiperbólico de $Z_0 \in \Omega^r$. Então para todo $\epsilon > 0$ o campo de vetores regularizado Z_ϵ tem um ciclo limite hiperbólico Γ_ϵ tal que $\Gamma_\epsilon \to \Gamma_0$ quando $\epsilon \to 0$.*

Para finalizar o Capítulo 2 apresentamos a Teoria Geométrica das Perturbações Singulares e sua correlação com campos vetoriais suaves por partes. Em [13] os autores conjecturam que dado um ciclo canard Γ de um campo de vetores descontínuo Z, é possível obter, via técnicas de perturbação singular, uma família de ciclos limite Γ_ϵ dos campos regularizados Z_ϵ de modo que $\Gamma_\epsilon \to \Gamma$. O Teorema 2.2 acima responde parcialmente a essa questão, ou seja, de fato

existe a família de ciclos limite Γ_ϵ com as propriedades procuradas, entretanto não utilizamos das técnicas de perturbação singular para obtê-la.

No Capítulo 3 utilizamos o teorema anterior para obter propriedades topológicas de campos de vetores descontínuos. Toda a teoria presente neste capítulo é inédita. Apresentamos aqui o conceito de Índice de Poincaré para o caso de campos vetoriais planares suaves por partes. Salientamos que para adaptar a teoria para o nosso contexto, precisamos realizar adaptações na definição de índice de um caminho com relação a um dado campo de vetores. Tais adaptações só seriam de fato úteis se ao realizarmos a regularização do campo de vetores descontínuo obtivermos que o índice para o caso dos campos descontínuos converge para o índice clássico. Este importante fato é provado na Proposição 3.1 do Capítulo 3. Veja abaixo o enunciado deste resultado:

Proposição 3.1 *Seja Z_0 um campo de vetores suave por partes e Z_ϵ sua regularização, onde $\epsilon > 0$ é um número real suficientemente pequeno. Se $\sigma : [0,1] \to \mathcal{U}$ é um caminho contínuo fechado então o índice de Poincaré de σ em relação ao campo Z_ϵ coincide com o índice de Poincaré da curva σ com relação ao campo Z_0.*

Como terceiro resultado inédito presente nesta tese (veja o Teorema 3.1 do Capítulo 3 ou sua tradução abaixo) estabelecemos um resultado análogo ao que se tem para o caso clássico também para o nosso contexto.

Teorema 3.1 *Seja $Z_0 = (X, Y)$ um campo de vetores suave por partes. Seja $\sigma : [0,1] \to \mathcal{U}$ um caminho contínuo fechado e simples. Se $\{p_1, \ldots, p_k\}$ é o conjunto de pontos de equilíbrio ou de pontos de pseudo equilíbrio de Z_0 no interior de σ então o índice da curva σ com relação ao campo Z_0 é a soma dos índices de p_i, para $i = 1, \ldots, k$.*

Este Teorema possui diversas aplicações. Por exemplo, esse resultado garante que se o caminho σ for um ciclo canard hiperbólico então a soma dos índices dos pontos de equilíbrio no interior de σ é igual a 1, ou ainda que não existe pseudo ciclo limitando uma única singularidade que é uma $\Sigma-$sela. Esta última aplicação pode ser melhorada dizendo que se σ for um ciclo canard hiperbólico, então existem $(2n+1)$ pontos de equilíbrio ou pseudo equilíbrio, todos hiperbólicos, no interior de σ; mais ainda, destes n são selas ou $\Sigma-$selas e $(n+1)$ são focos, $\Sigma-$atratores ou $\Sigma-$repulsores.

Na literatura, existem resultados bem estabelecidos que dizem quais dos pontos de pseudo equilíbrio ou quais dos ciclos canard são genéricos ou hiperbólicos (veja [40] e [34]). O próximo passo é seguir, assim como já foi feito na teoria clássica, o programa de Thom−Smale e encontrar os conjuntos estruturalmente estáveis e dentre os conjuntos limite não genéricos

quais tem codimensão 1, 2 ou maior.

Assim como no caso clássico temos o Teorema de Peixoto (veja [32]), para o caso de campos de vetores descontínuos $Z = (X, Y)$ também temos um resultado, presente na referência [34], que nos diz que se adicionarmos às condições dadas no Teorema de Peixoto os seguintes fatos:

- todos os pontos de pseudo equilíbrio são hiperbólicos e nenhum ponto de equilíbrio de X ou de Y está sobre Σ,
- todos os ciclos canard são hiperbólicos e nenhum ciclo limite de X ou de Y tem contato com Σ,
- as singularidades tangenciais, caso ocorram, são $\Sigma-$dobras isoladas, ou seja, não permite-se que um mesmo ponto seja $\Sigma-$dobra de X e de Y,
- não existem conexões entre as $\Sigma-$dobras, entre separatrizes de selas ou entre uma separatriz de sela e uma $\Sigma-$dobra,

então o conjunto dos campos de vetores descontínuos com essas propriedades é aberto e denso em Ω^r e torna-se dessa forma um conjunto genérico.

Com o objetivo de estudar bifurcações de campos de vetores descontínuos precisamos, antes de mais nada, definir qual a relação de equivalência empregada. Diremos que dois campos descontínuos Z e $\widetilde{Z}$, apresentando curvas de descontinuidade Σ e $\widetilde{\Sigma}$, são $\Sigma-$*equivalentes* se existir um homeomorfismo h preservando orientação que leva Σ em $\widetilde{\Sigma}$ e leva órbitas de Z em órbitas de $\widetilde{\Sigma}$. Observe que segundo esta relação de equivalência, órbitas regulares são mandadas em órbitas regulares e pontos de equilíbrio ou pontos $\Sigma-$singulares são mandados em pontos de equilíbrio ou pontos $\Sigma-$singulares. Mais ainda, como esta relação preserva a orientação, as regiões de escape, deslize e costura são preservadas, assim como são preservadas as separatrizes, as conexões de separatrizes, conexões de tangencias, os ciclos limite, as órbitas periódicas e os ciclos canard.

Singularidades dos campos suaves por partes cujo desdobramento de sua forma normal pode ser conseguido usando 1 parâmetro foram estudadas, além de outros, em [27], onde de modo geral se considera X apresentando um ponto de equilíbrio hiperbólico P sobre Σ e Y transversal a Σ. Desta forma, pequenas perturbações nos campos fazem com que o ponto P esteja situado em Σ_+ ou em Σ_-, produzindo assim uma bifurcação no retrato de fase.

Singularidades cujo desdobramento de sua forma normal envolvem 2 parâmetros, também entre outros, foram estudadas em [24], onde se consideram pontos que são simultaneamente $\Sigma-$dobras de X e de Y, ou pontos de equilíbrio não hiperbólicos de X sobre Σ sendo Y transversal, dentre outros casos.

O Capítulo 4 desta tese é o único trabalho que conhecemos que trata do desdobramento de singularidades de campos de vetores suaves por partes envolvendo mais de 2 parâmetros. Mais especificamente, estabelecemos um método sistemático usado para estudar algumas bifurcações envolvendo singularidades que só aparecem quando tratamos de campos vetoriais suaves por partes. Além de bifurcações mais simples, podemos fazer colidir em um mesmo ponto de Σ um ponto de equilíbrio de X e uma singularidade tangencial de Y (como exemplo, veja o primeiro e o terceiro casos na figura 2, chamados de singularidades Sela−dobra e Foco−dobra respectivamente; ou ainda o terceiro caso da parte superior ou o primeiro caso da parte inferior da figura 3, chamados de singularidades Foco−cúspide e Sela−cúspide respectivamente), ou colidir em um mesmo ponto de Σ um ponto de equilíbrio de X e um ponto de equilíbrio de Y (como exemplo, veja os dois primeiros casos da parte superior ou o segundo caso da parte inferior da figura 3, chamados respectivamente singularidades Sela−foco, Foco−foco e Sela−sela respectivamente), ou ainda colidir em um mesmo ponto de Σ uma singularidade tangencial de X e outra de Y (veja o segundo caso na figura 2 ou o terceiro caso da parte inferior da figura 3, chamados de singularidades Cúspide−dobra e Cúspide−cúspide).

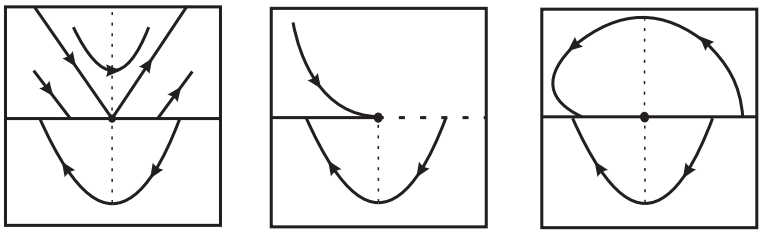

Figure 2: Singularidades com Y apresentando uma Σ−dobra invisível.

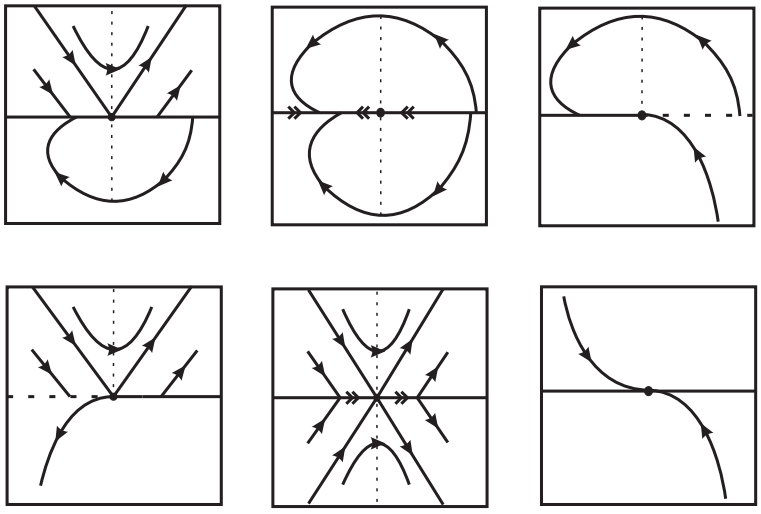

Figure 3: Singularidades de $Z = (X, Y)$.

Considerando os pontos de equilíbrio hiperbólicos e analisando os campos isoladamente, temos o seguinte:

- Para o caso de um foco sobre Σ, impondo pequenas perturbações ao campo concluímos que o foco translada para Σ_+ ou para Σ_- (veja Figura 4). Uma forma normal que representa este desdobramento é dada por

$$\begin{pmatrix} -x-(y-\epsilon) \\ x-(y-\epsilon) \end{pmatrix}$$

onde para $\epsilon > 0$ o foco pertence a Σ_+ e para $\epsilon < 0$ o foco pertence a Σ_-.

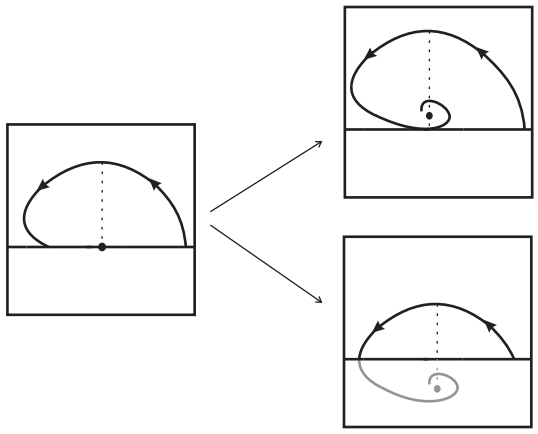

Figure 4: Desdobramento do foco hiperbólico sobre Σ.

- Para o caso de uma sela sobre Σ, impondo pequenas perturbações ao campo concluímos que esta é transladada para Σ_+ ou para Σ_- (veja Figura 5). Uma forma normal que representa este desdobramento é dada por

$$\begin{pmatrix} (y-\theta) \\ x \end{pmatrix}$$

onde para $\theta > 0$ a sela pertence a Σ_+ e para $\theta < 0$ a sela pertence a Σ_-.

- Para o caso de uma cúspide sobre Σ, impondo pequenas perturbações ao campo concluímos que a cúspide pode tornar-se transversal a Σ ou passar a ter uma dobra visível e mais um ponto de contato transversal com Σ. (veja Figura 6). Uma forma normal que representa este desdobramento é dada por

$$\begin{pmatrix} 1 \\ -x^2+\rho \end{pmatrix}$$

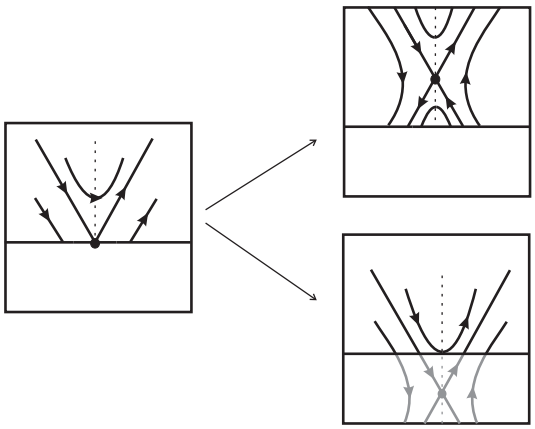

Figure 5: Desdobramento da sela hiperbólica sobre Σ.

onde para $\rho > 0$ temos uma dobra visível e um ponto de contato transversal com Σ e para $\rho < 0$ temos apenas contatos transversais com Σ.

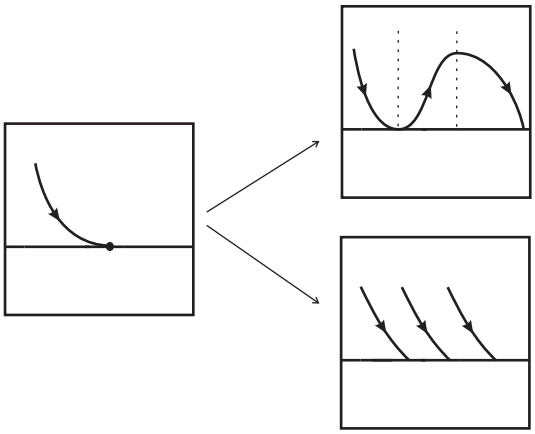

Figure 6: Desdobramento da cúspide sobre Σ.

Dos desdobramentos destas singularidades podem surgir os mais diversos comportamentos topológicos, de acordo com as posições relativas dos pontos envolvidos. Evidente que a passagem de um caso para o outro pode produzir bifurcações de codimensão baixa, como o mostrado na figura 7 onde nota-se uma bifurcação do tipo *Hopf*.

Nesta tese, tratamos em detalhes as singularidades Dobra−Sela e Dobra−Cúspide. Em ambos os casos damos famílias a três parâmetros que as representam, analisamos seu desdobramento e estabelecemos os diagramas de bifurcação.

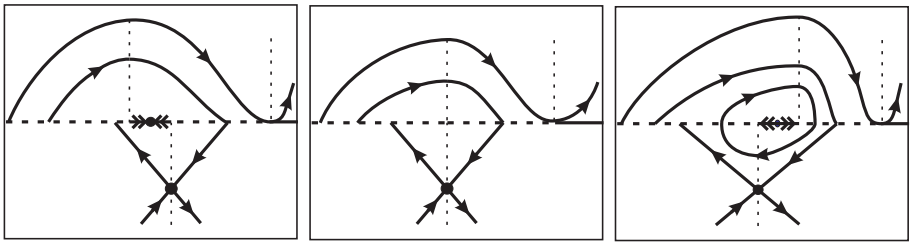

Figure 7: Bifurcação do tipo Hopf.

Para as singularidades Dobra−Sela representadas nas figuras 8 e 9 temos a seguinte família a 3 parâmetros que as representam:

$$\overline{Z}^{\tau}_{\lambda,\mu,\beta} = \begin{cases} X_{\lambda} = \begin{pmatrix} 1 \\ \alpha_1(\tau)(x-\lambda) + \alpha_2(\tau)(x-\lambda)^2 \end{pmatrix} & \text{if } y \geq 0, \\ Y_{\mu,\beta} = \begin{pmatrix} \frac{\mu}{2}x + \frac{(\mu-2)}{2}(y+\beta) \\ \frac{(\mu-2)}{2}x + \frac{\mu}{2}(y+\beta) \end{pmatrix} & \text{if } y \leq 0, \end{cases}$$

onde λ, $\beta \in (-1,1)$, $\tau = inv$ quando a $\Sigma-$dobra de X é invisível, $\tau = vis$ quando a $\Sigma-$dobra de X é visível, $\alpha_1(inv) = -1$, $\alpha_1(vis) = 1$, $\alpha_2(inv) = 1$, $\alpha_2(vis) = 0$ e $\mu \in (\varepsilon_0, 1)$ com $\varepsilon_0 < 0$ (maiores detalhes sobre a função de cada parâmetro podem ser encontrados na seção 4.2).

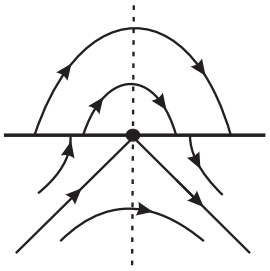

Figure 8: Singularidade Dobra−Sela com a $\Sigma-$dobra invisível.

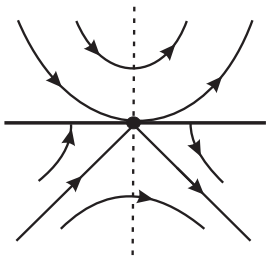

Figure 9: Singularidade Dobra−Sela com a $\Sigma-$dobra visível.

Variando os parâmetros λ, μ e β encontramos configurações com nenhum, um ou dois ciclos canard; com pseudo equilíbrio do tipo $\Sigma-$atrator ou $\Sigma-$repulsor, dentre outros. De fato, os principais resultados a respeito destas singularidades são os seguintes teoremas (que também podem ser encontrados, com maiores detalhes, na seção 4.2 do Capítulo 4):

Teorema 4.7 *O diagrama de bifurcação da singularidade Dobra−Sela, com esta dobra sendo invisível, apresenta* 61 *casos sendo que estes representam* 25 *comportamentos topológicos distintos.*

Teorema 4.8 *O diagrama de bifurcação da singularidade Dobra−Sela, com esta dobra sendo visível, apresenta* 39 *casos sendo que cada um deles representa um comportamento topológico*

distinto.

Para as singularidades Dobra−cúspide representadas nas figuras 10 e 11 temos a seguinte família a 3 parâmetros que as representam:

$$Z^{\tau,\rho}_{\lambda,\beta,\mu} = \begin{cases} X^{\tau}_{\lambda} = \begin{pmatrix} 1 \\ \omega_1(\tau)(x-\lambda) \end{pmatrix} & \text{if } y \geq 0, \\ Y^{\rho}_{\mu,\beta} = \begin{pmatrix} \alpha_2(\rho) \\ -x^2 + \beta - \frac{\partial B^{\rho}}{\partial x}(x,\beta,\mu)) \end{pmatrix} & \text{if } y \leq 0, \end{cases}$$

onde $(\lambda,\beta) \in (-1/8,1/8) \times (-1/8,1/8)$, $\mu \in (-\mu_0,\mu_0)$, com $\mu_0 > 0$, B uma bump function apropriada, $\tau = ivb$ quando a $\Sigma-$dobra de X é invisível, $\tau = vis$ quando a $\Sigma-$dobra de X é visível, $\rho = k1$ quando a curva integral da cúspide é crescente, $\rho = k2$ quando a curva integral da cúspide é decrescente, $(\tau,\rho) = (ivb,k1)$ e $\alpha_2(k1) = -1$ ou $(\tau,\rho) = (vis,k2)$ e $\alpha_2(k2) = 1$ (maiores detalhes sobre a função de cada parâmetro, bem como a função da bump function B, podem ser encontrados na seção 4.3 do Capítulo 4).

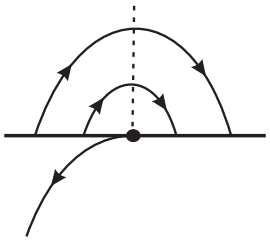

Figure 10: Singularidade Dobra−cúspide com a $\Sigma-$dobra invisível.

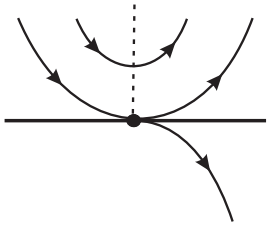

Figure 11: Singularidade Dobra−cúspide com a $\Sigma-$dobra visível.

Variando os parâmetros λ, μ e β encontramos os mais diversos tipos de configurações. Os principais resultados a respeito destas singularidades são os seguintes teoremas (que também podem ser encontrados, com maiores detalhes, na seção 4.3 do Capítulo 4):

Teorema 4.12 *O diagrama de bifurcação da singularidade Dobra− Cúspide, com esta dobra sendo invisível, apresenta* 51 *casos representando* 23 *comportamentos topológicos distintos.*

Teorema 4.13 *O diagrama de bifurcação da singularidade Dobra− Cúspide, com esta dobra sendo visível, apresenta* 11 *casos, sendo que cada um deles representa um comportamento topológico distinto.*

Para futuros trabalhos pretendemos estudar as outras singularidades apresentadas anteriormente bem como utilizar a teoria geométrica das perturbações singulares ou o processo de regularização para descrever suas bifurcações. Salientamos que em [31] estuda-se, utilizando o processo de regularização descrito anteriormente, uma sela−nó de X sobre Σ com Y transversal. Já em [16] estuda-se bifurcações envolvendo singularidades onde ocorre a colisão de uma

$\Sigma-$dobra de X com uma $\Sigma-$dobra de Y utilizando a teoria geométrica das perturbações singulares. Ainda como objetivo futuro, gostaríamos de estender para campos de vetores descontínuos em $\mathbb{R}^3$ os resultados sobre bifurcações presentes nesta tese.

Para analisar o comportamento qualitativo de um dado sistema dinâmico é sempre conveniente obter informações sobre seus conjuntos minimais, ou seja, pontos de equilíbrio, ciclos limite, dentre outros. De um modo geral, não é elementar saber a quantidade de ciclos limite de um campo de vetores a partir das equações que o definem. Um dos métodos mais relevantes para esse fim é o chamado *Método Averaging*, onde pode-se deduzir a quantidade de ciclos limite de um dado campo de vetores a partir da quantidade de zeros de uma equação. Este será o escopo do Capítulo 5, onde utilizamos o *Método Averaging de primeira ordem* para estabelecer uma cota de ciclos limite ou ciclos canard para certas classes de campos em $\mathbb{R}^n$ (veja maiores detalhes a respeito do método averaging na seção 5.1 do Capítulo 5).

Mais especificamente, nosso objetivo é estudar a existência de ciclos canard para o sistema

$$\dot{x} = A_0 x + \varepsilon F(x), \tag{0.1}$$

onde A_0 é igual a

$$A_0^1 = \begin{pmatrix} 0 & -1 & 0 & \cdots & 0 \\ 1 & 0 & 0 & \cdots & 0 \\ 0 & 0 & 0 & \cdots & 0 \\ \vdots & \vdots & \vdots & \ddots & \vdots \\ 0 & 0 & 0 & \cdots & 0 \end{pmatrix}$$

ou

$$A_0^2 = \begin{pmatrix} 0 & -1 & 0 & 0 & 0 & \cdots & 0 \\ 1 & 0 & 0 & 0 & 0 & \cdots & 0 \\ 0 & 0 & 0 & -1 & 0 & \cdots & 0 \\ 0 & 0 & 1 & 0 & 0 & \cdots & 0 \\ 0 & 0 & 0 & 0 & 0 & \cdots & 0 \\ \vdots & \vdots & \vdots & \vdots & \vdots & \ddots & \vdots \\ 0 & 0 & 0 & 0 & 0 & \cdots & 0 \end{pmatrix}$$

e $F : \mathbb{R}^n \to \mathbb{R}^n$ é dada por $F(x) = Ax + \varphi_0(k^T x)b$, com $A \in \mathcal{M}_n(\mathbb{R})$, $k, b \in \mathbb{R}^n \backslash \{0\}$ e $\varphi_0 : \mathbb{R} \to \mathbb{R}$ é a função descontínua

$$\varphi_0(x_1) = \begin{cases} -1 & \text{se } x_1 \in (-\infty, 0), \\ 1 & \text{se } x_1 \in (0, \infty), \end{cases}$$

onde $x = (x_1, \ldots, x_n)^T$.

Com este fim, inicialmente estudamos o sistema

$$\dot{x} = A_0 x + \varepsilon F_\alpha(x), \tag{0.2}$$

onde F_α é igual a F trocando φ_0 pela função linear por partes $\varphi_\alpha : \mathbb{R} \longrightarrow \mathbb{R}$ dada por

$$\varphi_\alpha(x_1) = \begin{cases} -1 & \text{se } x_1 \in (-\infty, -\alpha), \\ \dfrac{x_1}{\alpha} & \text{se } x_1 \in [-\alpha, \alpha], \\ 1 & \text{se } x_1 \in (\alpha, \infty), \end{cases}$$

onde $\alpha > 0$, e depois faremos α tender a 0. Os gráficos de φ_0 e φ_α estão ilustrados na figura 12.

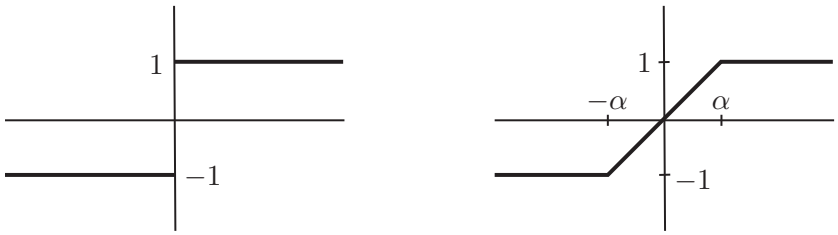

Figure 12: À esquerda temos o gráfico de φ_0 e à direita o gráfico de φ_α.

Para $\varepsilon = 0$ e $A_0 = A_0^1$, o sistema (0.1) fica da forma

$$\dot{x}_1 = -x_2,\ \dot{x}_2 = x_1,\ \dot{x}_i = 0 \text{ para } i = 3, \ldots, n \tag{0.3}$$

e para $\varepsilon = 0$ e $A_0 = A_0^2$, o sistema (0.1) fica da forma

$$\dot{x}_1 = -x_2,\ \dot{x}_2 = x_1,\ \dot{x}_3 = -x_4,\ \dot{x}_4 = x_3,\ \dot{x}_i = 0 \tag{0.4}$$

para $i = 5, \ldots, n$.

Diante disso, temos os seguintes resultados:

Teorema 5.1 *Considere $A_0 = A_0^1$. Para $n \geq 2$ no máximo um ciclo limite do sistema diferencial linear por partes* (0.2) *bifurca das órbitas periódicas do sistema* (0.3). *Mais ainda, existem sistemas cujo número de ciclos limite que bifurcam é* 1.

Corolário 5.1 *Considere $A_0 = A_0^1$. Para $n \geq 2$ no máximo um ciclo limite do sistema diferencial linear por partes descontínuo* (0.1) *bifurca das órbitas periódicas do sistema* (0.3). *Mais ainda, existem sistemas cujo número de ciclos limite que bifurcam é* 1.

Teorema 5.2 *Considere $A_0 = A_0^2$. Para $n \geq 4$ no máximo* 3 *ciclos limite do sistema diferencial linear por partes* (0.2) *bifurcam das órbitas periódicas do sistema* (0.4). *Mais ainda, existem sistemas cujo número de ciclos limite que bifurcam é* 3.

Corolário 5.2 *Considere $A_0 = A_0^2$. Para $n \geq 4$ no máximo* 3 *ciclos limite do sistema diferencial linear por partes descontínuo* (0.1) *bifurcam das órbitas periódicas do sistema* (0.4).

Mais ainda, existem sistemas cujo número de ciclos limite que bifurcam é 3.

Considere agora o sistema (0.1) com F dada por $F(x) = Ax + \varphi(k^T x)b$, onde $A \in \mathcal{M}_n(\mathbb{R})$, $k, b \in \mathbb{R}^n \backslash \{0\}$ e $\varphi : \mathbb{R} \longrightarrow \mathbb{R}$ é uma função linear por partes tal que

$$\varphi(x_1) = \begin{cases} -1 & \text{se } x_1 \in (-\infty, -1), \\ x_1 & \text{se } x_1 \in [-1, 1], \\ 1 & \text{se } x_1 \in (1, \infty). \end{cases}$$

Além disso, tome

$$A_0 = A_0^3 = \begin{pmatrix} 0 & -1 & 0 & 0 & \cdots & 0 & 0 \\ 1 & 0 & 0 & 0 & \cdots & 0 & 0 \\ 0 & 0 & 0 & -1 & \cdots & 0 & 0 \\ 0 & 0 & 1 & 0 & \cdots & 0 & 0 \\ \vdots & \vdots & \vdots & \vdots & \ddots & \vdots & \vdots \\ 0 & 0 & 0 & 0 & \cdots & 0 & -1 \\ 0 & 0 & 0 & 0 & \cdots & 1 & 0 \end{pmatrix}.$$

Para $\varepsilon = 0$ o sistema (0.1) fica da forma

$$\dot{x}_1 = -x_2, \quad \dot{x}_2 = x_1, \quad \ldots \quad , \dot{x}_{n-1} = -x_n, \quad \dot{x}_n = x_{n-1}. \tag{0.5}$$

Teorema 5.3 *Considere $A_0 = A_0^3$. Para $n \geq 6$, com n par, no máximo $(4n-6)^{n/2-1}$ ciclos limite do sistema diferencial linear por partes* (0.1) *bifurcam das órbitas periódicas do sistema* (0.5).

Gostaríamos de destacar ainda que os capítulos 2, 3 e a primeira seção do Capítulo 4 fazem parte do trabalho [8] submetido para publicação. A seção 4.2 faz parte do trabalho [10] submetido para publicação. A seção 4.3 faz parte do trabalho [9] submetido para publicação. As seções 5.2 e 5.3 fazem parte do trabalho [15] submetido para publicação. A seção 5.4 faz parte do trabalho [14] também submetido para publicação.

Chapter

1

Basic Theory about Non−Smooth Vector Fields

1.1 Motivation

Non−Smooth Dynamical Systems (abbreviated by NSDS) has become certainly one of the common frontiers between Mathematics and Physics, Engineering, Economics, Medicine, Biology or Ecology. The dynamics of several such non−smooth systems are relevant in applications. Problems involving impact or friction are piecewise−smooth, as are many control systems with thresholds.

The most common piecewise−smooth systems involve either a discontinuity in the vector field, or in the orbit given by the integral solution $x(t)$. In this thesis we consider the former, that is, general systems where the vector field is independently defined on either side of a smooth codimension one switching manifold. Three possible regions of the manifold are apparent. At a crossing region the component of the vector field normal to the switching manifold has the same direction on both sides of the manifold (sometimes called sewing instead of crossing). At a stable sliding region both normal components of the vector field point toward the manifold. At an unstable sliding region both normal components point away from the manifold. Piecewise−smooth systems with sliding are also known as Filippov Systems (see [21]). Clearly these three distinct scenarios lead to vastly distinct dynamics. An orbit that meets the switching manifold at a crossing region passes through it, but is non−differentiable at the crossing point. An orbit that impacts at a stable sliding region becomes constrained

(sticks) to the manifold. An orbit in an unstable sliding region slides along the switching manifold, but will depart it under any infinitesimal perturbation. Consequently, the only means by which a stable sliding orbit can escape the switching manifold is tangentially, at the boundary of the sliding region. This leads to the observation that, under parameter variation, orbits in Filippov systems can undergo a large variety of bifurcations, commonly called sliding bifurcations.

We focus our attention on Filippov systems on the plane, which are systems modeled by ordinary differential equations with discontinuous righthand sides. Many authors have contributed to the study of Filippov systems (see for instance [21] and [26]). One of the starting points for a systematic approach in the geometric and qualitative analysis of NSDS is the work [39], of M. A Teixeira, on smooth systems in 2−dimensional manifolds with boundary. See [41] or [4] for a survey on NSDS and references there in.

The generic singularities that appear in NSDS, as well as we know, were first studied in [40]. Bifurcations and related problems involving or not sliding regions are studied in papers like [18] and [22]. Bifurcation theory describes how continuous variations of parameter values in a dynamical system can, through topological changes, cause the phase portrait to change suddenly. In this thesis we focus on certain unstable non−smooth vector fields within a generic context. The framework in which we shall pursue these unstable systems is sometimes called generic bifurcation theory. In [1] the concept of $k^{\text{th}}-$order structural stability is presented; in a local approach such setting gives rise to the notion of a codimension$-k$ singularity. Observe that, so far, bifurcation and normal form theories for non−smooth vector fields have not been extensively studied in a systematic way.

In the present work the bifurcation diagrams of some typical singularities of NSDS in the plane are discussed. We study in this setting a set of typical bifurcations which are not found in smooth systems. It is well known that many of these models (see for instance [2] and [3]) occur in generic $k-$parameter families and therefore they typically undergo generic codimension$-k$ bifurcations. The classification of codimension-1 local and some global bifurcations for planar systems was given in [27]. In [24] is shown how to construct the homeomorphisms which lead to equivalences between two non−smooth systems when the discontinuity set is a planar smooth curve. In that work codimension-2 singularities were discussed and an amazing phenomena on its bifurcation diagrams appeared in the form of infinite many branches of codimension-1 global bifurcations. These bifurcations, that also appear in the present work, called ST−bifurcations, are characterized by the connection between a saddle critical point and a tangency singularity or between two specific tangency singularities.

1.2 Preliminaries

Let $K \subseteq \mathbb{R}^2$ be a compact set and $\Sigma \subseteq K$ given by $\Sigma = f^{-1}(0)$, where $f : K \to \mathbb{R}$ is a smooth function having $0 \in \mathbb{R}$ as a regular value (i.e. $\nabla f(p) \neq 0$, for any $p \in f^{-1}(0)$) such that $\partial K \cap \Sigma = \emptyset$ or $\partial K \pitchfork \Sigma$. Clearly Σ is the separating boundary of the regions

$\Sigma_+ = \{q \in K | f(q) \geq 0\}$ and $\Sigma_- = \{q \in K | f(q) \leq 0\}$. We can assume that Σ is represented, locally around a point $q = (x, y)$, by the function $f(x, y) = y$.

Designate by χ^r the space of structurally stable (see [32]) C^r-vector fields on K endowed with the C^r-topology with $r \geq 1$ or $r = \infty$, large enough for our purposes. Call $\Omega^r = \Omega^r(K, f)$ the space of vector fields $Z : K \to \mathbb{R}^2$ such that

$$Z(x, y) = \begin{cases} X(x, y), & \text{for} \quad (x, y) \in \Sigma_+, \\ Y(x, y), & \text{for} \quad (x, y) \in \Sigma_-, \end{cases}$$

where $X = (f_1, g_1)$, $Y = (f_2, g_2)$ are in χ^r. We write $Z = (X, Y)$, which we will accept to be multivalued in points of Σ. The trajectories of Z are solutions of $\dot{q} = Z(q)$, which has, in general, discontinuous right−hand side. The basic results of differential equations, in this context, were stated by Filippov in [21]. Related theories can be found in [26, 35, 40].

Definition 1.1. *Two non−smooth vector fields Z, $\widetilde{Z} \in \Omega^r(K, f)$ defined in open sets U, $\widetilde{U} \in K$ and with switching manifolds $\Sigma \subset U$ and $\widetilde{\Sigma} \subset \widetilde{U}$ respectively are $\Sigma-$**equivalent** if there exists an orientation preserving homeomorphism $h : U \to \widetilde{U}$ which sends Σ to $\widetilde{\Sigma}$ and sends orbits of Z to orbits of $\widetilde{Z}$.*

We say that two unfoldings $\Theta_\lambda : \mathbb{R}^2 \times \mathbb{R}^k \to \mathbb{R}^2$ and $\Xi_\mu : \mathbb{R}^2 \times \mathbb{R}^l \to \mathbb{R}^2$, where $\lambda \in \mathbb{R}^k, 0$ and $\mu \in \mathbb{R}^l, 0$, are topologically equivalent if for each $\lambda \in \mathbb{R}^k, 0$ there exists $A(\lambda) \in \mathbb{R}^l, 0$ such that the vector fields Θ_λ and $\Xi_{A(\lambda)}$ are $\Sigma-$equivalent. And we say that an unfolding Θ_λ is generic if in a neighborhood of Θ_λ any other unfolding Ξ_μ is topologically equivalent to Θ_λ.

In what follows we will use the notation

$$X.f(p) = \langle \nabla f(p), X(p) \rangle \quad \text{and} \quad Y.f(p) = \langle \nabla f(p), Y(p) \rangle .$$

We distinguish the following regions on the discontinuity set Σ:

(i) $\Sigma_1 \subseteq \Sigma$ is the *sewing region* if $(X.f)(Y.f) > 0$ on Σ_1 .

(ii) $\Sigma_2 \subseteq \Sigma$ is the *escaping region* if $(X.f) > 0$ and $(Y.f) < 0$ on Σ_2.

(iii) $\Sigma_3 \subseteq \Sigma$ is the *sliding region* if $(X.f) < 0$ and $(Y.f) > 0$ on Σ_3.

Consider $Z \in \Omega^r$. The *sliding vector field* associated to Z is the vector field Z^s tangent to Σ_3 and defined at $q \in \Sigma_3$ by $Z^s(q) = m - q$ with m being the point where the segment joining $q + X(q)$ and $q + Y(q)$ is tangent to Σ_3 (see Figure 1.1). It is clear that if $q \in \Sigma_3$ then $q \in \Sigma_2$ for $-Z$ and then we can define the *escaping vector field* on Σ_2 associated to Z by $Z^e = -(-Z)^s$. In what follows we use the notation Z^Σ for both cases. The *sewing vector field* associated to Z is the vector field Z^w defined in $q \in \Sigma_1$ as an arbitrary convex combination

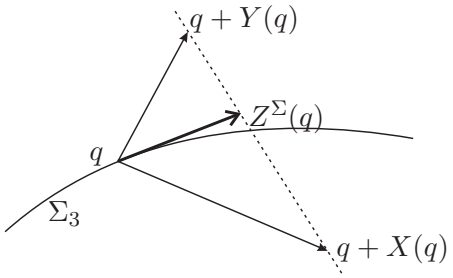

Figure 1.1: Fillipov's convention.

of $X(q)$ and $Y(q)$, i.e., $Z^w(q) = \lambda X(q) + (1-\lambda)Y(q)$ where $\lambda \in [0,1]$.

We say that $q \in \Sigma$ is a $\Sigma-$*regular point* if

(i) $(X.f(q))(Y.f(q)) > 0$ or

(ii) $(X.f(q))(Y.f(q)) < 0$ and $Z^{\Sigma}(q) \neq 0$ (that is $q \in \Sigma_2 \cup \Sigma_3$ and it is not a equilibrium point of Z^{Σ}).

The points of Σ which are not $\Sigma-$regular are called $\Sigma-$*singular*. We distinguish two subsets in the set of $\Sigma-$singular points: Σ^t and Σ^p. Any $q \in \Sigma^p$ is called a *pseudo equilibrium of* Z and it is characterized by $Z^{\Sigma}(q) = 0$. Any $q \in \Sigma^t$ is called a *tangential singularity* and is characterized by $Z^{\Sigma}(q) \neq 0$ and $(X.f(q))(Y.f(q)) = 0$ (q is a contact point of Z^{Σ}).

A pseudo equilibrium $q \in \Sigma^p$ is a $\Sigma-$*saddle* provided one of the following condition is satisfied: (i) $q \in \Sigma_2$ and q is an attractor for Z^{Σ} or (ii) $q \in \Sigma_3$ and q is a repeller for Z^{Σ}. A pseudo equilibrium $q \in \Sigma^p$ is a $\Sigma-$*repeller* (resp. $\Sigma-$*attractor*) provided $q \in \Sigma_2$ (resp. $q \in \Sigma_3$) and q is a repeller (resp. attractor) equilibrium point for Z^{Σ}.

On Σ_1 can happens that q is a $\Sigma-$regular point and $\{X(q), Y(q)\}$ is linearly dependent. These points are called *virtual pseudo equilibria*.

Let X be a smooth vector field defined in Σ_+. We say that a point $p \in \Sigma$ is a $\Sigma-$*fold point* of X if $X.f(p) = 0$ but $X^2.f(p) \neq 0$. Moreover, a $\Sigma-$fold point p of X is called *visible* (respectively *invisible*) if $X.f(p) = 0$ and $X^2.f(p) > 0$ (resp. $X^2.f(p) < 0$). We say that a point $q \in \Sigma$ is a $\Sigma-$*cusp point* of X if $X.f(q) = X^2.f(q) = 0$ and $X^3.f(q) \neq 0$. Moreover, a $\Sigma-$cusp point q of X is called of *kind 1* (respectively *kind 2*) if $X^3.f(q) > 0$ (resp. $X^3.f(q) < 0$).

In particular, $\Sigma-$fold and $\Sigma-$cusp points are tangential singularities.

Definition 1.2. *Consider* $Z \in \Omega^r$.

1. *A curve* Γ *is a* ***canard cycle*** *if* Γ *is closed and*

- Γ *contains arcs of at least two of the vector fields* $X|_{\Sigma_+}$, $Y|_{\Sigma_-}$ *and* Z^Σ *or is composed by a single arc of* Z^Σ*;*
- *the transition between arcs of* X *and arcs of* Y *happens in sewing points;*
- *the transition between arcs of* X *(or* Y*) and arcs of* Z^Σ *happens through* $\Sigma-$*fold points or regular points in the escape or sliding arc, respecting the orientation. Moreover if* $\Gamma \neq \Sigma$ *then there exists at least one visible* $\Sigma-$*fold point on each connected component of* $\Gamma \cap \Sigma$*.*

2. *Let* Γ *be a canard cycle of* Z*. We say that*

   - Γ *is a* ***canard cycle of kind I*** *if* Γ *meets* Σ *just in sewing points;*
   - Γ *is a* ***canard cycle of kind II*** *if* $\Gamma = \Sigma$*;*
   - Γ *is a* ***canard cycle of kind III*** *if* Γ *contains at least one visible* $\Sigma-$*fold point of* Z*.*

   In Figures 1.2, 1.3 and 1.4 arise canard cycles of kind I, II and III respectively.

3. *Let* Γ *be a canard cycle. We say that* Γ *is* ***hyperbolic*** *if*

   - Γ *is of kind I and* $\eta'(p) \neq 1$*, where* η *is the first return map defined on a segment* T *with* $p \in T \pitchfork \gamma$*;*
   - Γ *is of kind II;*
   - Γ *is of kind III,* $\overline{\Sigma_2} \cap \overline{\Sigma_3} \cap \Gamma = \emptyset$ *and either* $\Gamma \cap \Sigma \subseteq \Sigma_1 \cup \Sigma_2 \cup \Sigma^t$ *or* $\Gamma \cap \Sigma \subseteq \Sigma_1 \cup \Sigma_3 \cup \Sigma^t$*.*

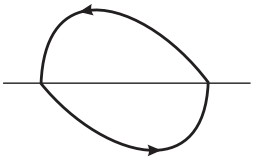

Figure 1.2: Canard cycle of kind I.

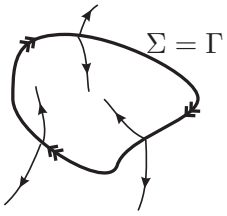

Figure 1.3: Canard cycle of kind II.

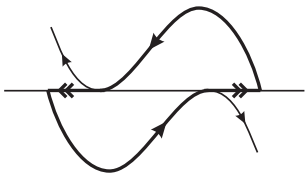

Figure 1.4: Canard cycle of kind III.

Remark 1. *Observe that a canard cycle does not need to be a simple curve. In fact, consider a non−smooth vector field* $Z = (X, Y)$ *presenting the configuration described in Figure 1.5. Let* γ_1 *be an arc of* X *joining the* $\Sigma-$*fold points* a *and* b *of* X*;* e *the* $\Sigma-$*fold point of* Y*;* c *and* d *points in the escaping region* $\overline{e\,b}$*;* g*,* h *and* i *points in the sliding region* $\overline{f\,a}$ *where* f *is a invisible* $\Sigma-$*fold point of* X*;* δ_2 *the arc of* Y *joining* c *and* h*,* δ_1 *the arc of* X *joining* d *and* g*; and* γ_2 *the arc of* Y *joining* e *and* i*. Consider the fixed point of* Y *named by* p_2 *in Figure 1.5. Take the path* $\overline{i\,a} \cup \gamma_1 \cup \overline{b\,c} \cup \delta_2 \cup \overline{h\,a} \cup \gamma_1 \cup \overline{b\,e} \cup \gamma_2$*. So, it has some self intersections. For example,* $\overline{h\,a} \cup \gamma_1 \cup \overline{b\,c}$*.*

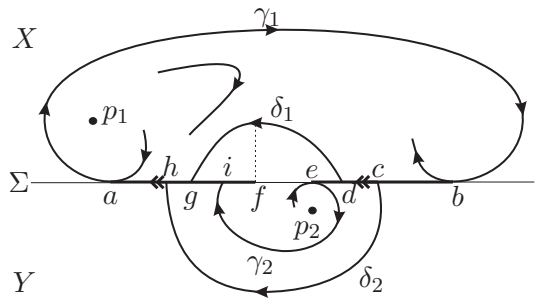

Figure 1.5: Non−hyperbolic canard cycle that is not a simple curve.

Definition 1.3. *Consider $Z \in \Omega^r$. A point $q \in \Sigma$ is a $\Sigma-$**center** if there is a neighborhood U of q such that an one parameter family of canard cycles encircles q and foliates U. See Figure 1.6.*

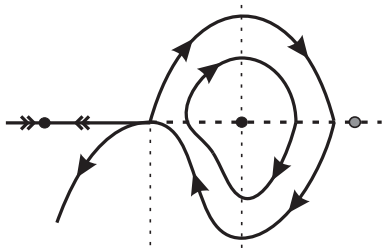

Figure 1.6: Σ−center.

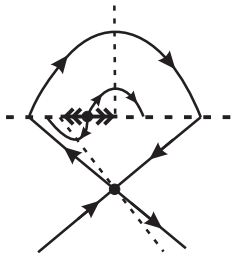

Figure 1.7: Σ−graph of kind I.

Definition 1.4. *Consider $Z \in \Omega^r$. A closed path Δ is a $\Sigma-$**graph** if it is a union of equilibria, pseudo equilibria, tangential singularities of Z and arcs of Z joining these points in such a way that $\Delta \cap \Sigma \neq \emptyset$. Like for canard cycles, we say that Δ is a $\Sigma-$**graph of kind I** if $\Delta \cap \Sigma \subset \Sigma_1$, Δ is a $\Sigma-$**graph of kind II** if $\Delta \cap \Sigma = \Delta$ and Δ is a $\Sigma-$**graph of kind III** if $\Delta \cap \Sigma \subsetneqq \Sigma_2 \cup \Sigma_3$.*

1.3 The Direction Function

The properties of the function defined in this section will be extremely useful in what follows. It will be important to describe the dynamic on Σ.

In $(a,b) \subset \Sigma_2 \cup \Sigma_3$, consider the point $c = (c_1, c_2)$, the vectors $X(c) = (d_1, d_2)$ and $Y(c) = (e_1, e_2)$ (as illustrated in Figure 1.8). The straight line passing through $c + X(c)$ and $c + Y(c)$ meets Σ in a point $p(c)$. We define the map

$$\begin{array}{rccc} p: & (a,b) & \longrightarrow & \Sigma \\ & z & \longmapsto & p(z). \end{array}$$

We can choose local coordinates such that Σ is the $x-$axis; so $c = (c_1, 0)$ and $p(c) \in \mathbb{R} \times \{0\}$ can be identified with points in $\mathbb{R}$. According with this identification, the *direction function* on Σ is defined by

$$\begin{array}{rccc} H: & (a,b) & \longrightarrow & \mathbb{R} \\ & z & \longmapsto & p(z) - z. \end{array}$$

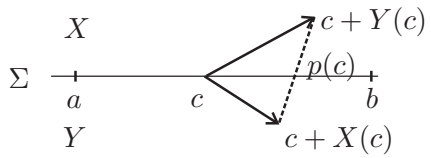

Figure 1.8: Direction function.

Remark 2. *We obtain that*

- *if $H(c) < 0$ then the orientation of Z^Σ in a small neighborhood of c is from b to a;*
- *if $H(c) = 0$ or if c is a discontinuity of H then $c \in \Sigma^p$;*
- *if $H(c) > 0$ then the orientation of Z^Σ in a small neighborhood of c is from a to b.*

Simple calculations show that $p(c_1) = \frac{e_2(d_1+c_1)-d_2(e_1+c_1)}{e_2-d_2}$ and consequently,

$$H(c_1) = \frac{e_2 d_1 - d_2 e_1}{e_2 - d_2}. \tag{1.1}$$

Remark 3. *If $X.f(p) = 0$ and $Y.f(p) \neq 0$ then, in a neighborhood V_p of p in Σ, the direction function H has the same signal of d_1, where $X = (d_1, d_2)$. In fact, $X.f(p) = 0$ and $Y.f(p) \neq 0$ are equivalent to $d_2 = 0$ and $e_2 \neq 0$ in (1.1). So, $\lim\limits_{(d_2,e_2)\to(0,k_0)} H(p_1) = d_1$, where $k_0 \neq 0$ and $p = (p_1, p_2)$.*

Remark 4. *Observe that we can extend H to points of Σ_1. In these situation, it is possible that the straight line connecting $c + X(c)$ and $c + Y(c)$ does not return to Σ. So, H is not defined in c.*

The following property is immediate.

Proposition 1.1. *If n_1 is the number of pseudo equilibria and n_2 is the number of virtual pseudo equilibria then $n_1 + n_2 = v_1 + v_2$ where v_1 is the number of zeros of H and v_2 is the number of points of Σ_1 for which H is not defined.*

Proof. Straightforward according with Remark 2, Remark 4 and (1.1).

Chapter

2

Limit Sets and Convergence

Our main interest in this chapter is to study a special kind of typical minimal sets of non−smooth vector fields called canard cycles.

2.1 Regularization

An approximation of the non−smooth vector field $Z_0 = (X, Y)$ by a 1−parameter family $Z_\epsilon \in \chi^r(K, \mathbb{R}^2)$ of smooth vector fields is called an *$\epsilon-$regularization of Z_0*. This regularization process was developed by Sotomayor and Teixeira in [35]. A transition function is used to average X and Y in order to get a family of smooth vector fields that approximates Z_0. The main aim is to deduce certain dynamical properties of the NSDS from the regularized system.

The regularization gives the mathematical tool to study the stability of these systems, according to the program introduced by Peixoto. For each $\varepsilon_0 > 0$ fixed we have

(i) Z_{ε_0} is equal to X in all points of Σ_+ whose distance to Σ is bigger than ε_0;

(ii) Z_{ε_0} is equal to Y in all points of Σ_- whose distance to Σ is bigger than ε_0.

Definition 2.1. *A C^∞ function $\varphi : \mathbb{R} \longrightarrow \mathbb{R}$ is a transition function if $\varphi(x) = -1$ for $x \leqslant -1$, $\varphi(x) = 1$ for $x \geqslant 1$ and $\varphi'(x) > 0$ if $x \in (-1, 1)$. The $\epsilon-$regularization of $Z_0 = (X, Y)$ is the 1−parameter family $X_\varepsilon \in \chi^r$ given by*

$$Z_\varepsilon(q) = \left(\frac{1}{2} + \frac{\varphi_\varepsilon(f(q))}{2}\right) X(q) + \left(\frac{1}{2} - \frac{\varphi_\varepsilon(f(q))}{2}\right) Y(q) \tag{2.1}$$

with $\varphi_\varepsilon(x) = \varphi(x/\varepsilon)$, *for* $\varepsilon > 0$.

2.2 On the Existence of Canard Cycles

In this section, for a subclass of non−smooth vector fields, we provide necessary and sufficient conditions for the existence of a kind of canard cycles.

We remark that for a hyperbolic canard cycle Γ we have that each connected component of $\Gamma \cap \Sigma$ has only one Σ−fold point (See [34] for more details).

Definition 2.2. *Let* γ_{A,X_i} *be the orbit of* X_i *passing through a visible* Σ*-fold point* A*. Let* B *be the first return (for positive or negative time) of* γ_{A,X_i} *to* Σ*. Let* $(\overrightarrow{AB})_{X_i}$ *be the arc of* X_i *joining* A *to* B*. We say that* $(\overrightarrow{AB})_{X_i}$ *has* ***focal kind*** *if* $B = \gamma_{A,X_i} \pitchfork \Sigma$ *and there are not* Σ*-fold points between* A *and* B *(see Figure 2.1). And we say that* $(\overrightarrow{AB})_{X_i}$ *has* ***graphic kind*** *if* $B = \gamma_{A,X_i} \pitchfork \Sigma$ *and* X_i *has only one* Σ*-fold point between* A *and* B *(see Figure 2.2),* $i = 1, 2$.

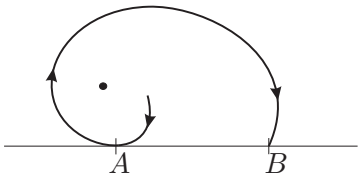

Figure 2.1: Focal kind arc.

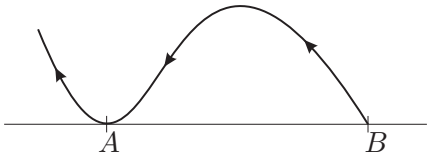

Figure 2.2: Graphic kind arc.

By using the previous notation, our result is:

Theorem 2.1. *Let* $Z_0 = (X, Y) \in \Omega^r$ *presenting only one* $\Sigma-$*fold point* A *which is visible. Then* Z_0 *has a canard cycle* Γ *if and only if the following conditions are satisfied:*

(i) *the component* γ_1 *of* Γ *which passes through* A *is a focal kind arc* $(\overrightarrow{AB})_{X_i}$, $i = 1$ *or* $i = 2$,

(ii) $X_1 f . X_2 f < 0$ *in* $\widehat{AB}/\{A\} \subset \Sigma$, *where* $\widehat{AB}$ *is the arc of* Σ *connecting* A *and* B, *including the points* A *and* B, *and*

(iii) $\{X_1(q), X_2(q)\}$ *is a linearly independent set for all* $q \in \widehat{AB}$.

Moreover, Γ *is of kind III.*

Proof. Consider Σ the $x-$axis. First we prove that (i),(ii) and (iii) imply the existence of the canard cycle. Since $X.f(q).Y.f(q) < 0$ for all $q \in (A, B]$ the piece of Σ between A and B is part of a escaping region or a sliding region. Moreover since $\{X, Y\}$ is a linearly independent set in $[A, B]$ the system does not have pseudo equilibrium points in $[A, B]$. Without loss of generality, $[A, B]$ is part of the sliding region like in Figure 2.3. The curve $\Gamma = \gamma_1 \cup [B, A]$ is a hyperbolic canard cycle of kind III. We remark that this canard cycle takes place in just one side of Σ.

Now we prove that (i),(ii) and (iii) are necessary conditions for the existence of this particular kind of canard cycle. Since Γ is a hyperbolic canard cycle of kind III with just one $\Sigma-$fold point, Γ takes place in just one side of Σ. In fact, if it does not holds, then Γ returns to Σ at least twice and so there exists at least a second $\Sigma-$fold point. Without loss of generality we suppose that Γ is on the side corresponding to X. We denote by γ_1 the part of the cycle Γ which is a trajectory of X. Thus we have that γ_1 is a focal kind arc because if it is a graphic kind arc then there is another $\Sigma-$fold point on (A, B) (see Figure 2.3). Since Γ has no one arc of Y, the point B belongs to an escaping region or a sliding region and so $X.f(B).Y.f(B) < 0$. Let us assume that $B \in \Sigma_3$. Since γ_1 meets Σ in the point B, the flow slides via Z_0^Σ until the point A because there are no $\Sigma-$fold points between A and B; therefore $X.f(q).Y.f(q) < 0$ for all $q \in (A, B]$. Moreover, the linear independence of $\{X, Y\}$ on $[A, B]$ follows from the non existence of pseudo equilibrium points on $[A, B]$. ∎

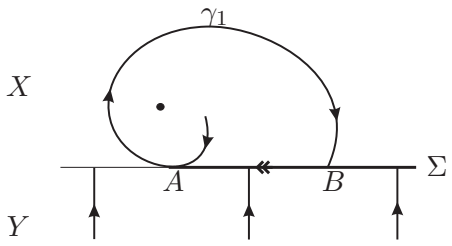

Figure 2.3: Closed poly-trajectory with just one $\Sigma-$fold point.

Assuming all the hypothesis of Theorem 2.1 we have immediately the following corollary.

Corollary 2.1. *The non−smooth vector field Z_0 has a canard cycle Γ if and only if the direction function $H : \widehat{AB} \longrightarrow \mathbb{R}$ is a well defined function and it has no zeros. Moreover, Γ is of kind III.*

2.3 On the Convergence of Limit Cycles to Canard Cycles

Consider $Z_0 = (X, Y) \in \Omega^r$ and Z_ϵ a regularization. In [34] is proved that the $\epsilon-$regularization of non−smooth vector fields Z_0 with hyperbolic canard cycles has hyperbolic limit cycles. The next result answer what happens with these limit cycles when $\epsilon \to 0$. Following the ideas exposed in [34], we prove that hyperbolic canard cycles are limit sets, according Hausdorff distance, of families of (smooth) hyperbolic limit cycles (this fact is not proved in [34])

Theorem 2.2. *Let Γ_0 be a hyperbolic canard cycle of Z_0. Then for any $\epsilon > 0$ the regularized vector field Z_ϵ, has a hyperbolic limit cycle Γ_ϵ such that $\Gamma_\epsilon \to \Gamma_0$ when $\epsilon \to 0$.*

This convergence is obtained considering the Hausdorff distance. Observe that the Hausdorff distance between compact sets of $\mathbb{R}^2$ is characterized by:

$$D(K_1, K_2) = \max_{z_1 \in K_1, z_2 \in K_2} \{d(z_1, K_2), d(z_2, K_1)\}. \tag{2.2}$$

In order to prove Theorem 2.2 we need to construct a special neighborhood of arbitrary diameter for hyperbolic canard cycles.

2.3.1 Construction of a neighborhood of diameter μ around a hyperbolic canard cycle.

Here we describe a method to construct a tubular neighborhood of diameter μ around a hyperbolic canard cycle. This presentation is done for canard cycles of kind III, but the ideas can also be extended for kinds I or II. We will be particularly interested in two of them: the ones that take place on just one side of Σ and with just one visible $\Sigma-$fold point and the ones that take place on the two sides of Σ with two visible $\Sigma-$fold points (one for X and another one for Y).

Case 1- One $\Sigma-$fold point. Denote by Γ the hyperbolic canard cycle of kind III with just one $\Sigma-$fold point and with orientation showed in Figure 2.4 (the reverse orientation is treated in a similar way). Consider the strip of diameter μ around $\Sigma = \{y = 0\}$. Let p_1 and q_1 be points in $\{y = \mu\} \cap \Gamma$. Take an arc γ_2 of the vector field X passing to the point $p_2 \in \{y = \mu\}$ in such a way that p_2 stays on the left of p_1 and such that γ_2 returns to the line $y = \mu$ in a point q_2 which is in a neighborhood of q_1. Take this trajectory satisfying $d(\Gamma, \gamma_2) < \frac{\mu}{2}$ (this is possible by the continuity of X). Let r_1 be the point where the arc of X through by p_1 first meets the straight line $y = \mu$ for negative time. Analogously take an arc γ_1 of the field X passing by the point r_2 in such a way that r_2 stays on the left of r_1 and such that γ_1 has second return to $y = \mu$ in a point q_3 which is in a neighborhood of q_1. Take this trajectory satisfying $d(\Gamma, \gamma_1) < \frac{\mu}{2}$. On Σ, on the left of the $\Sigma-$fold point A, the flow of X is oriented to up, so it is possible to construct a transversal section σ_2 joining p_2 to the straight line $y = 0$ in such a way that the same trajectories of X cross transversally σ_2 and the segment $\overline{p_2\, p_1}$. Take t_2 the point where σ_2 meets the straight line $y = 0$ satisfying $d(\Gamma, \sigma_2) < \mu$, as before. Moreover, on Σ, on the right of the point B, the flow of X is oriented for down, so it is possible to construct a transversal section θ_2 joining q_2 to the straight line $y = 0$ in such a way that the trajectories of X that cross transversally θ_2 do not cross the segment $\overline{q_1\, q_2}$. Let s_2 be the point where θ_2 meets the straight line $y = 0$ (here we also need to take care for $d(\Gamma, \theta_2) < \mu$). Since $[A, B]$ is a sliding region, the flow of Y is transversal to Σ. In the straight line $y = -\mu$, consider the points u_2 and v_2 (u_2 is on the left of v_2) satisfying that the trajectories of Y crossing the transversal sections $\lambda_2 = \overline{t_2\, u_2}$ and $\delta_2 = \overline{s_2\, v_2}$ meet transversally Σ at the segment $\overline{t_2\, s_2}$ (again, we need to take care for $d(\Gamma, \lambda_2) < \mu$ and $d(\Gamma, \delta_2) < \mu$).

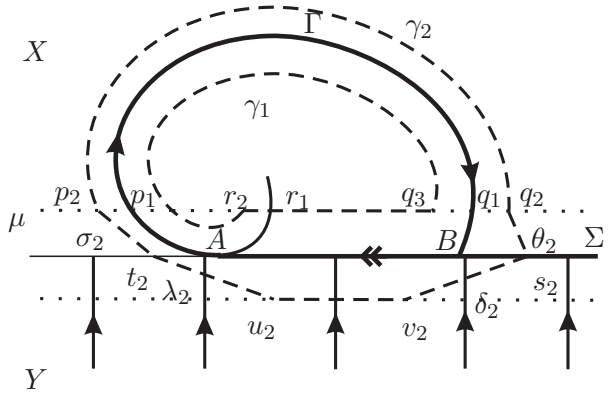

Figure 2.4: Tubular neighborhood of a canard cycle with one Σ−fold.

In this way, the strip defined by the closed curve $\gamma_1 \cup \overline{q_3\, r_2}$ and by the closed curve $\gamma_2 \cup \theta_2 \cup \delta_2 \cup \overline{v_2\, u_2} \cup \lambda_2 \cup \sigma_2$ is a tubular neighborhood of Γ of diameter μ. Note that the flow of $Z_0 = (X, Y)$ is arriving in this neighborhood and never departs from it.

Case 2- Two Σ−fold points. Now we study the hyperbolic canard cycles of kind III with two visible Σ−fold points, being one for X and the other one for Y, like showed in Figure 2.5. We work with canard cycles Γ that have only escaping regions on $\Sigma = \{y = 0\}$ (the case with sliding regions is treated similarly). Consider the strip of diameter μ around Σ. Let p_1 and q_1 be points in $\{y = \mu\} \cap \Gamma$. Take an arc γ_1 of the vector field X through $t_1 \in \{y = \mu\}$ satisfying that t_1 stays on the left of p_1 and such that γ_1 returns to the line $y = \mu$ in a point u_1 which is in a neighborhood of q_1. Take this trajectory satisfying that $d(\Gamma, \gamma_1) < \frac{\mu}{2}$. Take an arc σ_1 of the vector field X through $v_1 \in \{y = \mu\}$ satisfying that v_1 stays on the right of p_1 and such that σ_1 has second return on the straight line $y = \mu$ in a point x_1, even take this trajectory with the particularity that $d(\Gamma, \sigma_1) < \frac{\mu}{2}$. We repeat the same argument for the vector field Y and we found the points p_2, q_2, t_2, u_2, v_2 and x_2 respectively, and the curves γ_2 and σ_2. Let c be the point on $\Sigma \cap \sigma_2$, d be the point on $\Sigma \cap \gamma_1$, e be the point on $\Sigma \cap \gamma_2$ and f be the point on $\Sigma \cap \sigma_1$ as indicated in Figure 2.5. On Σ, take the points g on the left of c, h between A and d, i between e and A' and j on the right of f; satisfying that the arcs θ_1 (joining g to x_1), ρ_1 (joining u_1 to h), η_1 (joining i to t_1) and π_1 (joining v_1 to j) are transversal sections for X and the arcs θ_2 (joining g to v_2), ρ_2 (joining h to t_2), η_2 (joining u_2 to i) and π_2 (joining j and x_2) are transversal sections for Y with the distance from Γ to any one of this arcs less than μ.

In this way, the strip defined by the closed curve $\gamma_1 \cup \rho_1 \cup \rho_2 \cup \gamma_2 \cup \eta_2 \cup \eta_1$ and by the closed curve $\sigma_1 \cup \theta_1 \cup \theta_2 \cup \sigma_2 \cup \pi_2 \cup \pi_1$ is a tubular neighborhood for Γ of diameter μ. Note that the flow of $Z_0 = (X, Y)$ is departing from the tubular neighborhood and never arrives in it.

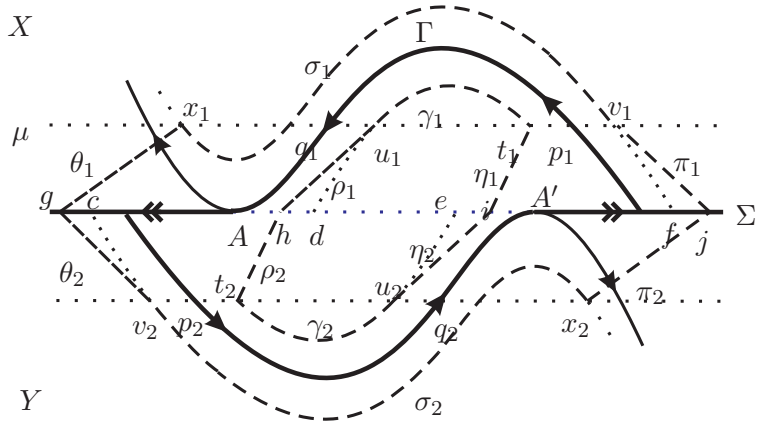

Figure 2.5: Tubular neighborhood for canard cycles of kind III with two $\Sigma-$fold points.

- Since this neighborhood bounds a region where the non$-$smooth vector field $Z_0 = (X, Y)$ is arriving in or it is departing from them, it makes sense to say *attractor canard cycles* or *repeller canard cycle*.

- In the neighborhoods constructed before we allow that trajectories can make part of them, however it is possible to do it with the flow of Z_0 being transversal to the boundaries of the tubular neighborhoods. In fact, it is enough to replace the trajectories by transversal curves. It is important for the construction of the tubular neighborhood of the canard cycles of kind I. Thus we make a construction like we made before but now we can use for this, the first return map η and thus if $\eta' < 1$ we have an attractor canard cycle and if $\eta' > 1$ we have a repeller canard cycle.

- For canard cycles of kind II it is enough to take the strip of diameter μ in the beginning of the construction as the tubular neighborhood.

- Any other hyperbolic canard cycle is an arrangement of pieces of the canard cycles described above and so we can construct a tubular neighborhood for it arranging the previous tubular neighborhoods.

Proof of Theorem 2.2. Let Γ_0 be a canard cycle of Z_0 and let V_ε be a tubular neighborhood of diameter ε around Γ_0. Since Z_0 is transversal to the boundary of V_ε, by continuity, the regularized vector field Z_ε is also transversal to the boundary of V_ε. Assume that Γ_0 is an attractor canard cycle, so the flow of Z_0 is arriving in the neighborhood V_ε and consequently the flow of X_ε is also arriving in the neighborhood V_ε. As there are not fixed points in V_ε, applying the Poincaré-Bendixson Theorem we conclude that there exists an attractor limit cycle Γ_ε inside V_ε. Moreover with a more detailed analysis we can prove that it is hyperbolic (see [34] for instance). Since every paths that compose V_ε depends continuously of ε we have that the diameter of the tubular neighborhood is a continuous function of the variable ε.

Therefore making $\epsilon \to 0$ we conclude that $\Gamma_\epsilon \to \Gamma_0$ (see Figure 2.6). ∎

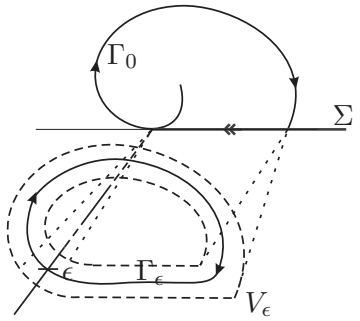

Figure 2.6: Cycles convergence.

We remark that if Γ_0 is an attractor (resp. repeller) hyperbolic canard cycle of Z_0, then the same occurs for Γ_ϵ and Z_ϵ.

2.4 Geometric Singular Perturbation Theory

In this section we show how the regularization process gives a singular perturbation problem. In this context, the canard cycles can be considered as *limit periodic sets* of singular problems. First of all we present some basic definitions.

Definition 2.3. *Let $U \subseteq \mathbb{R}^2$ be an open subset and take $\varepsilon \geqslant 0$. A singular perturbation problem in U (SP−Problem) is a differential system which can be written like*

$$x' = dx/d\tau = l(x, y, \varepsilon), \quad y' = dy/d\tau = \varepsilon m(x, y, \varepsilon) \tag{2.3}$$

or equivalently, after the time re−scaling $t = \varepsilon\tau$

$$\varepsilon\dot{x} = \varepsilon dx/dt = l(x, y, \varepsilon), \quad \dot{y} = dy/dt = m(x, y, \varepsilon), \tag{2.4}$$

with $(x, y) \in U$ and l, m smooth in all variables.

The understanding of the phase portrait of the vector field associated to a SP−problem is the main goal of the *geometric singular perturbation theory* (GSP−theory). The techniques of GSP−theory can be used to obtain information on the dynamics of (2.3) for small values of $\varepsilon > 0$, mainly in searching limit cycles. System (2.3) is called the *fast system*, and (2.4) the *slow system* of the SP−problem. Observe that for $\varepsilon > 0$ the phase portraits of the fast and the slow systems coincide. For $\varepsilon = 0$, let $\mathcal{S}$ be the set

$$\mathcal{S} = \{(x, y) : f(x, y, 0) = 0\} \tag{2.5}$$

of all singular points of (2.3). We call $\mathcal{S}$ the *slow manifold* of the singular perturbation problem and it is important to notice that equation (2.4) defines a dynamical system, on $\mathcal{S}$,

called the *reduced problem*:

$$f(x,y,0)=0, \quad \dot{y}=g(x,y,0). \tag{2.6}$$

Combining results on the dynamics of these two limiting problems, with $\varepsilon=0$, one obtains information on the dynamics of X_ε for small values of ε. We refer to [20] for an introduction to the general theory of singular perturbations. Related problems can be seen in [12], [19] and [37]. Let us apply the techniques of GSP−Theory to study hyperbolic canard cycles.

Example. Consider the non−smooth vector field $Z_0=(X,Y)$ with $X(x,y)=(x+y-1,-x+y+1)$, $Y(x,y)=(1,2)$ and $f(x,y)=x$. The regularized vector field becomes

$$\begin{array}{rcl}\dot{x} &=& \frac{x+y}{2}+\varphi\left(\frac{x}{\epsilon}\right)\frac{x+y-2}{2},\\ \dot{y} &=& \frac{-x+y+3}{2}+\varphi\left(\frac{x}{\epsilon}\right)\frac{-x+y-1}{2}.\end{array}$$

where $\varphi(\frac{x}{\epsilon})$ is the transition function. Making the change of variables $x=r.\cos\theta$ and $\epsilon=r.\mathrm{sen}\,\theta$ we obtain

$$\begin{array}{rcl}r\dot{\theta} &=& -\mathrm{sen}\,\theta\left(\frac{r.\cos\theta+y}{2}+\varphi(\cot\theta)\frac{r.\cos\theta+y-2}{2}\right),\\ \dot{y} &=& \frac{-r.\cos\theta+y+3}{2}+\varphi(\cot\theta)\frac{-r.\cos\theta+y-1}{2}.\end{array} \tag{2.7}$$

In the blowing up locus $r=0$ the fast dynamics is determined by the system

$$\theta'=-\mathrm{sen}\,\theta\left(\frac{y}{2}+\varphi(\cot\theta)\frac{y-2}{2}\right), \quad y'=0\,;$$

and the slow dynamics on the slow manifold is determined by the reduced system

$$\frac{y}{2}+\varphi(\cot\theta)\frac{y-2}{2}=0\,, \quad \dot{y}=\frac{y+3}{2}+\varphi(\cot\theta)\frac{y-1}{2}.$$

We remark that the slow manifold is implicitly defined by $\frac{y}{2}+\varphi(\cot\theta)\frac{y-2}{2}=0$ and $y(\theta)$ defined in this way is such that $\lim\limits_{\theta\longrightarrow\pi/4}y(\theta)=1$, $\lim\limits_{\theta\longrightarrow3\pi/4}y(\theta)=-\infty$.

In the phase portrait on the blowing up locus double arrow over one the trajectory means that the trajectory is of the fast dynamical system, and simple arrow means that the trajectory is of the slow dynamical system. So, we can draw the slow variety and its orientation and give the orientation of the fast flow (see Figures 2.7 and 2.8).

We known that the slow flow is given by the solutions of $r\dot{\theta}=0$ and the fast flow in $S^1_+\times\mathbb{R}$ is given by the solutions of $y'=0$, after the time re−scaling in the equation 2.7. In same way (like in the final example of [13]) we conclude that $\lim\limits_{\theta\longrightarrow\pi/4}y(\theta)=1$, $\lim\limits_{\theta\longrightarrow3\pi/4}y(\theta)=-\infty$, $\dot{y}(\theta)>0$, $\theta'(y)<0$ for $y>r.\dot{\theta}(y)$ and $\theta'(y)>0$ for $y<r.\dot{\theta}(y)$.

In [29] the authors prove that $\Sigma_2\cap\Sigma_3$ is homeomorphic to the slow manifold and that the sliding vector field Z_0^Σ is topologically equivalent to the reduced problem.

In the final example of the paper [13], the authors apply the GSP−Theory to the non−smooth vector field $Z_0(x,y)=(X(x,y),Y(x,y))=((3y^2-y-2,1),(-3y^2-y+2,-1))$ and obtain

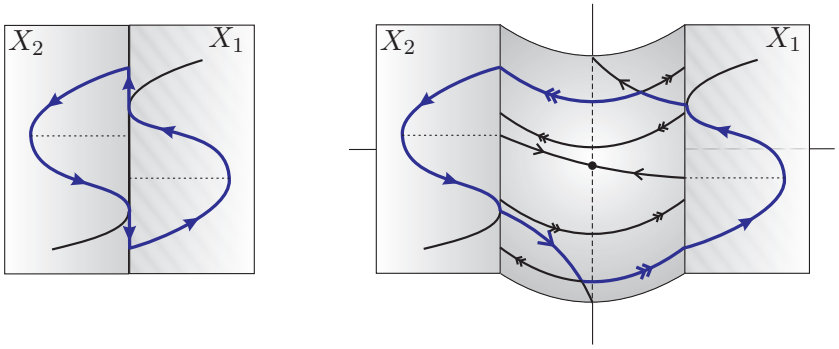

Figure 2.7: Canard cycle Γ and the correspondent limit periodic set of a singular perturbation problem.

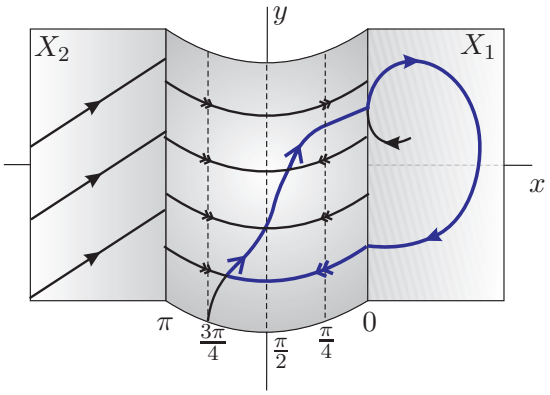

Figure 2.8: Limit periodic set of a singular perturbation problem.

the SP−problem which behavior is described in Figure 2.7. Moreover, they suggest that is possible to obtain, via GSP techniques, a family of limit cycles Γ_ϵ of the regularizated vector field Z_ϵ satisfying that $\Gamma_\epsilon \to \Gamma$, where Γ is a canard cycle, according with Hausdorff distance (see (2.2)).

From Theorem 2.2 a partial answer of this question is obtained. In fact, there exist such family Γ_ϵ, however it was not obtained via GSP−theory.

Chapter

3

Poincaré Index for Non−Smooth Vector Fields

In this chapter we extend the concept of Poincaré Index to non−smooth vector fields.

Let $I = [0, 1]$ be an interval and $\sigma : I \to \mathcal{U}$ be an oriented closed continuous path, where $\mathcal{U} \subset K$ is an open subset. Suppose that there are no equilibria or pseudo equilibria points of $Z = (X, Y)$ on σ. Let us move a point P along the curve in the counterclockwise direction. The vector $Z(P)$ will rotate during the motion. When P returns to its starting position after one rotation along the curve σ, $Z(P)$ also returns to its original position. During the journey $Z(P)$ will make some whole number of revolutions. Counting these revolutions positively if they are counterclockwise, negatively if they are clockwise, the resulting algebraic sum of the number of revolutions is called the *index of σ with respect to Z*, and is denoted by $I(Z, \sigma)$.

In order to calculate $I(Z, \sigma)$ in $\mathbb{R}^2 \backslash \Sigma$ is convenient normalize $Z(\sigma(t))$ as an unit vector at the origin. In this way, we can define a function θ such that

$$\lim_{t \to \tilde{t}} \frac{Z(\sigma(t))}{\|Z(\sigma(t))\|} = \lim_{t \to \tilde{t}} (\cos \theta(t), \operatorname{sen} \theta(t))$$

where $t \in I$. The function θ is called *angle function*.

We observe that in the case of smooth vector fields, the angle function is always continuous in the whole interval I, but in the case of non−smooth vector fields we assume that it has finitely many “jumps" on Σ.

When σ touches Σ in an isolated point $s_i = \sigma(t_i)$, with $i \in \{1, \ldots, k\}$, we obtain, in general, that

$$\theta(t_i^-) = \lim_{t \to t_i^-} \theta(t) \neq \lim_{t \to t_i^+} \theta(t) = \theta(t_i^+).$$

In this case we define the "jump" at the point s_i by

$$j(s_i) = \theta(t_i^+) - \theta(t_i^-).$$

When σ touches Σ in an interval $I_j = (\sigma(\alpha_j), \sigma(\beta_j))$, with $j \in \{1, \ldots, l\}$, we obtain, in general, that

$$\theta(\alpha_j^-) = \lim_{t \to \alpha_j^-} \theta(t) \neq \lim_{t \to \beta_j^+} \theta(t) = \theta(\beta_j^+).$$

In this case we define the "jump" at the interval I_j by

$$j(I_j) = \theta(\beta_j^+) - \theta(\alpha_j^-).$$

Let $\{\tau_1 < \ldots < \tau_{k+l}\} \subset (0,1)$ be a rearrangement of the times t_i, $i \in \{1, \ldots, k\}$, and α_j, $j \in \{1, \ldots, l\}$. We make the conventions $\theta(0) = \theta(\tau_0^+)$, $\theta(1) = \theta(\tau_{k+l+1}^-)$ and when $\tau_m = \alpha_j$ we use the notation $\tau_m^- = \alpha_j^-$ and $\tau_m^+ = \beta_j^+$. Now we define

$$I(Z, \sigma) = \frac{\displaystyle\sum_{m=0}^{k+l+1} [\theta(\tau_{m+1}^-) - \theta(\tau_m^+)] + \sum_{i=1}^{k} j(s_i) + \sum_{j=1}^{l} j(I_j)}{2\pi}.$$

Note that $I(Z, \sigma)$ is an integer modulo 2π, independent of the chosen $\sigma-$parametrization. This number also is called *Poincaré Index of the curve σ with relation to the non-smooth vector field Z.*

Moreover, this definition coincides with those one for smooth vector fields when Z is continuous. In fact, in this case, $k = l = 0$, the "jumps" are null and so $I(Z, \sigma) = (\theta(1) - \theta(0))/2\pi$.

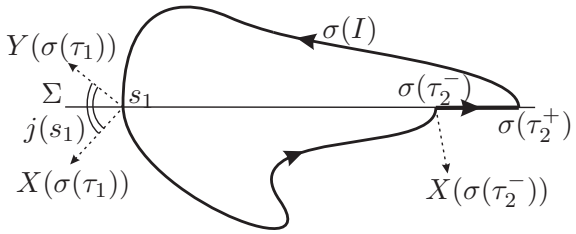

Figure 3.1: Angle function: at s_1 it has a jump of size $j(s_1)$ and from $\sigma(\tau_2^-)$ to $\sigma(\tau_2^+)$ it has a jump of size $j(I_1)$.

Example 3.1. *Consider $Z = (X, Y) \in \Omega^r$ presenting a configuration like in Figure 3.2. Here there exists a canard cycle Γ. Observe that $X(A)$ is tangent to Σ. Moreover, consider that $X(B)$ is orthogonal to Σ. The Poincaré Index of Γ with relation to Z is given by*

$$I(Z,\Gamma) = \frac{(\theta(\tau_1^-) - \theta(\tau_0^+)) + j(I)}{2\pi} = \frac{(2\pi - (\pi/2)) + (\pi/2 - 0)}{2\pi} = 1$$

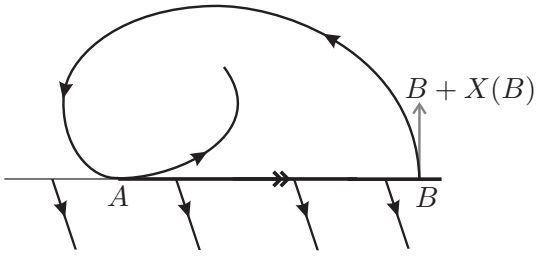

Figure 3.2: Example.

Proposition 3.1. *Let Z_0 be a non−smooth vector field and Z_ϵ its regularization, where $\epsilon > 0$ is a sufficiently small real number. If $\sigma : [0,1] \to \mathcal{U}$ is a closed continuous path then $I(Z_\epsilon, \sigma) = I(Z_0, \sigma)$.*

Proof. Since Z_ϵ is a C^r vector field, by the classical theory, the index $I(Z_\epsilon, \sigma)$ is given by $(\theta(1) - \theta(0))/2\pi$. Without loss of generality, consider that σ crosses Σ (here Σ is the $x-$axis) in an unique point $s_1 = \sigma(\tau_1)$ and σ has an unique interval $I = (\sigma(\alpha), \sigma(\beta))$ in common with Σ. The other cases are treated in a similar way. So, we obtain

$$\begin{aligned} 2\pi I(Z_\epsilon, \sigma) &= \theta(1) - \theta(0) = \theta(1) - \theta(w_4) + \theta(w_4) - \theta(w_3) + \theta(w_3) + \\ &\quad -\theta(w_2) + \theta(w_2) - \theta(w_1) + \theta(w_1) - \theta(0) \end{aligned}$$

where w_1 and w_4 are the times t for which $\sigma(t) \in \{y = \epsilon\}$ and w_2 and w_3 are the times t for which $\sigma(t) \in \{y = -\epsilon\}$. Since the angle function θ is continuous in this situation, we can rewrite the previous sentence as

$$\begin{aligned} 2\pi I(Z_\epsilon, \sigma) &= \theta(1) - \theta(0) = \theta(1) - \theta(w_4^+) + \theta(w_4^+) - \theta(w_3^-) + \theta(w_3^-) + \\ &\quad -\theta(w_2^+) + \theta(w_2^+) - \theta(w_1^-) + \theta(w_1^-) - \theta(0) \end{aligned}$$

where we use the notation $\theta(u^\pm) = \lim_{t \to u^\pm} \theta(t)$. When ϵ tends to 0 we have that w_1 and w_2 tend to τ_1, w_3 tends to α and w_4 tends to β. So, with our previous conventions,

$$2\pi \lim_{\epsilon \to 0} I(Z_\epsilon, \sigma) = \sum_{m=0}^{3} [\theta(\tau_{m+1}^-) - \theta(\tau_m^+)] + j(s_1) + j(I_1) = 2\pi I(Z_0, \sigma).$$

Since $I(Z_\epsilon, \sigma)$ and $I(Z_0, \sigma)$ are natural numbers follow that $I(Z_\epsilon, \sigma) = I(Z_0, \sigma)$. ∎

Remark 5. We recall that if Z_0 has a hyperbolic $\Sigma-$saddle (or a hyperbolic $\Sigma-$focus) s_0 then the regularized vector field Z_ϵ has a hyperbolic saddle (hyperbolic focus) s_ϵ where $s_\epsilon \to s_0$

when $\epsilon \to 0$ (for details see [34]). Moreover, we can verify that if s_0 is a saddle or a $\Sigma-$saddle then we can take a sufficiently small closed path σ_{s_0} around s_0 and prove that $I(Z_0, \sigma_{s_0}) = -1$ (and if s_0 is a focus or a $\Sigma-$attractor or a $\Sigma-$repeller then we can take a sufficiently small closed path $\widetilde{\sigma}_{s_0}$ around s_0 and prove that $I(Z_0, \widetilde{\sigma}_{s_0}) = 1$). When the path σ_{s_0} is sufficiently small to have just one critical point of Z_0, named s_0, in its interior we use the notation $I_{s_0}(Z_0)$ to denote its Poincaré Index $I(Z_0, \sigma_{s_0})$.

We are now in position to state the main result of this chapter.

Theorem 3.1. *Consider $Z_0 = (X, Y)$ a non−smooth vector field. Let $\sigma : [0, 1] \to \mathcal{U}$ be a closed simple continuous path. If $\{p_1, \ldots, p_k\}$ is the set of critical or pseudo equilibria points of Z_0 inside σ then the index of σ with respect to Z_0 is the sum of the indexes of p_i, for $i = 1, ..., k$.*

Proof. We want to prove that if σ is a closed single continuous path and if $p_1, \ldots, p_k$ are the only ones equilibria or pseudo equilibria points of Z_0 inside σ then

$$I(Z_0, \sigma) = \sum_{i=1}^{k} I_{p_i}(Z_0).$$

Suppose that Z_0 has some non−hyperbolic equilibria or pseudo equilibria points. So, by [34], there exists $\widetilde{Z}_0$ near Z_0 such that all its equilibria or pseudo equilibria $\widetilde{p}_1, \ldots, \widetilde{p}_l$ are hyperbolic. Moreover, by continuity, $I(Z_0, \sigma) = I(\widetilde{Z}_0, \sigma)$ (remember that these are natural numbers). The regularized vector field $\widetilde{Z}_\epsilon$ has all its equilibria $q_1, \ldots, q_l$ hyperbolic and

$$I(\widetilde{Z}_\epsilon, \sigma) = \sum_{i=1}^{l} I_{q_i}(\widetilde{Z}_\epsilon).$$

By consequence

$$I(\widetilde{Z}_\epsilon, \sigma) = I(\widetilde{Z}_0, \sigma) = I(Z_0, \sigma)$$

and

$$\sum_{i=1}^{k} I_{p_i}(Z_0) = \sum_{i=1}^{k} I(Z_0, \sigma_{p_i}) = \sum_{i=1}^{k} I(Z_\epsilon, \sigma_{p_i}) = \sum_{i=1}^{l} I(\widetilde{Z}_\epsilon, \sigma_{q_i}) =$$

$$= \sum_{i=1}^{l} I_{q_i}(\widetilde{Z}_\epsilon) = I(\widetilde{Z}_\epsilon, \sigma) = I(Z_0, \sigma). \blacksquare$$

Corollary 3.1. *With the hypothesis of Theorem 3.1, assume that $\sigma = \Gamma$ where Γ is a hyperbolic canard cycle. Then*

$$I(Z_0, \Gamma) = 1.$$

Proof. The regularized vector field Z_ϵ has a hyperbolic limit cycle Γ_ϵ. So, by the Poincaré Index Theorem for smooth vector fields the index calculated in Γ_ϵ in relation to Z_ϵ is the sum of the indexes of the fixed points of Z_ϵ inside Γ_ϵ and this sum is equal to 1. By continuity $I(Z_0, \Gamma) = I(Z_0, \Gamma_\epsilon)$ and by Proposition 3.1 we obtain that $I(Z_0, \Gamma_\epsilon) = I(Z_\epsilon, \Gamma_\epsilon)$. Therefore,

$$I(Z_0, \Gamma) = I(Z_0, \Gamma_\epsilon) = I(Z_\epsilon, \Gamma_\epsilon) = 1. \blacksquare$$

Corollary 3.2. *Under the hypothesis of Theorem 3.1 and assuming that all canard cycles of Z_0 are hyperbolic, we have that:*

1. *If Γ_0 is a canard cycle then inside Γ_0 there exist $(2n+1)$ hyperbolic critical points of Z_0, being n saddles or $\Sigma-$saddles and $(n+1)$ focus, $\Sigma-$repeller or $\Sigma-$attractor.*

2. *If all critical points of Z_0 are saddle or $\Sigma-$saddle then Z_0 does not have canard cycles.*

Proof. Since the index of each saddle and each $\Sigma-$saddle point is equal to -1 and the index of each other critical point of Z_0 is equal to 1 the result is an immediate consequence of Theorem 3.1. ∎

Chapter

4

Bifurcations

In this chapter we focus on bifurcations of non−smooth vector fields in the plane. At this point is convenient to read again Section "Motivation" on Chapter 1.

The main aim of this chapter is to study the bifurcation scenarios that present the Fold−Saddle and the Fold−Cusp singularities. Such singularities, occurs generically in 3−parameter families of NSDS and we exhibit, in details, its bifurcation diagrams. It has been observed that such classes of dynamical system can exhibit complex dynamical transitions whenever bifurcations take place. In particular, many interesting global phenomena have been observed in the bifurcation diagram. We follow basically the terminology and the approach of [27] or [24]. The used tools and techniques involve just basic concepts in ordinary differential equations and differential topology. In fact, in almost whole chapter, only geometrical tools are enough to establish our results.

4.1 Heteroclinic Orbits and Bifurcations

This section is dedicated to some application of Theorem 2.1. Consider the notation of this theorem. We give now an example of a curve that satisfies all the hypothesis of this theorem except that there exists a point $C \in (A, B)$ such that the vectors $X(C)$ and $Y(C)$ are not linearly independent; instead of Γ obtained in the theorem we have here a *"$\Sigma-loop$"*, that is a $\Sigma-saddle-attractor$ with connection between $\Sigma-$separatrices.

Example 4.1. . *Consider the non−smooth vector field* $Z = (X, Y)$ *with* $X(x, z) = (x + z - 1, -x + z - 1)$, $Y(x, z) = (-x^2 + \frac{3}{2}x - \frac{1}{2}, 1)$ *and discontinuity set given by the* $x-$*axis, i.e.,* $f(x, z) = z$. *On* $z = 0$, *we have* $X(x, 0) = (x - 1, -x - 1)$ *and* $Y(x, 0) = (-x^2 + \frac{3}{2}x - \frac{1}{2}, 1)$ *and so,*

$$X.f(x, 0) = -x - 1\,, \quad Y.f(x, 0) = 1. \tag{4.1}$$

In this way, we can conclude that $x = -1$ *is a* $\Sigma-$*fold point of* X *which determines a focal kind arc. For* $x > -1$ *we have that* Σ *is a sliding region and for* $x < -1$ *it is a sewing region (see Figure 4.1). We show now that there exists a point* C *in the semi straight line* $x > -1$ *for which* $X(C) = \lambda Y(C)$. *In fact, if* $X(x, 0) = \lambda Y(x, 0)$ *then* $h(x) = (x - 1)^2(x + \frac{3}{2}) = 0$. *The graphic of* $h(x)$ *is given in Figure 4.2. We observe that* h *is equal to* $-H$, *where* H *is the direction function defined previously. So, we have the situation described in the Theorem 2.1, except that* X *and* Y *are not linearly independent in* $x = 1$ *where* Z^Σ *has a pseudo equilibrium point. The orientation of* Z^Σ *is in direction to the* $\Sigma-$*fold point because for* $x = \frac{1}{2}$ *we have* $X(\frac{1}{2}, 0) = (\frac{-1}{2}, \frac{-3}{2})$, $Y(\frac{1}{2}, 0) = (0, 1)$ *and so, the direction function* H *is negative* $(H(\frac{1}{2}) = -\frac{1}{5})$, *analogously for* $x = \frac{3}{2}$ *we have* $X(\frac{3}{2}, 0) = (\frac{1}{2}, \frac{-5}{2})$, $Y(\frac{1}{2}, 0) = (\frac{-1}{2}, 1)$ *and so, the direction function* H *also is negative* $(H(\frac{3}{2}) = -\frac{3}{14})$. *The pseudo equilibrium* $p = (1, 0)$ *is a* $\Sigma-$*saddle−attractor where the* $\Sigma-$*separatrices are connected.*

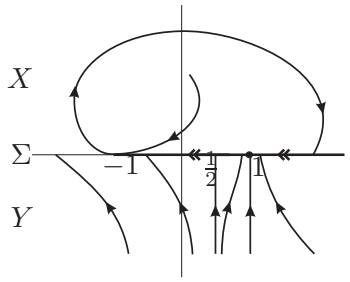

Figure 4.1: Σ−loop. There exists a pseudo equilibrium $C = (1, 0)$.

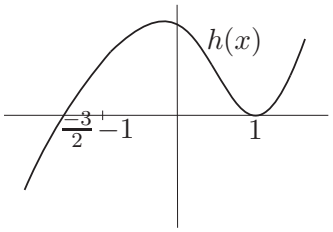

Figure 4.2: Graphic of h.

Example 4.2. *(Bifurcation of the previous example) In the previous example, the pseudo equilibrium with a "loop" was found because the function* h *has a double−zero at* $x = 1$. *So, we can conclude that putting small variations on the vector fields* X *and* Y *a new function* h *appears, with two simple real zeros (see Figure 4.6) or without real zeros (see Figure 4.4) in a neighborhood of* $x = 1$. *The phase portrait of* Z *for small variations on* X *and* XY *are showed in Figures 4.3 and 4.5. Note that for the case showed in Figure 4.3, the direction function* H *is always negative in a neighborhood of* $x = 1$ *and we can apply the corollary 2.1 to conclude that there exists a hyperbolic canard cycle of kind III and, for the case showed in Figure 4.5, the direction function* H *has two simple real zeros in a neighborhood of* $x = 1$ *and assumes positive values between this two points and negative values in the rest of the sliding region. In this way we have a bifurcation model where imposing small variations we can have a hyperbolic*

canard cycle or we can have two pseudo equilibrium points with a stable connection between its separatrices. We call this a $\Sigma-$***Loop Bifurcation***.

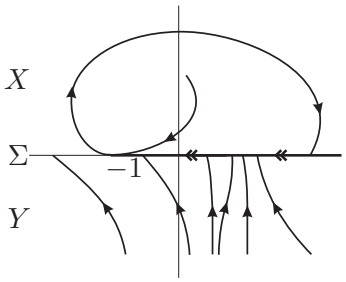

Figure 4.3: Hyperbolic canard cycle of kind III.

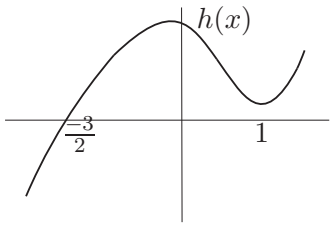

Figure 4.4: Graphic of h.

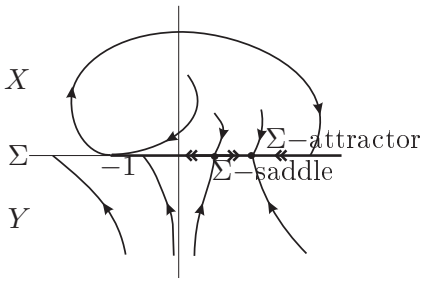

Figure 4.5: $\Sigma-$saddle and $\Sigma-$attractor with $\Sigma-$separatrices connection.

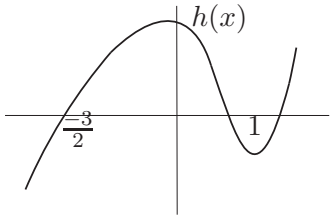

Figure 4.6: Graphic of h.

Following the notation of Theorem 2.1 and the ideas just exposed we can state the next Proposition:

Proposition 4.1. *Let* $Z = (X, Y) \in \Omega^r$ *and* A, B *like in Definition 2.2. Then:*

1. *Z has an unstable configuration topologically equivalent to that one in Figure 4.1 if and only if (i) the direction function H is well defined in $[A, B]$, (ii) H has a single zero in the arc $\widehat{AB} \subset \Sigma$ and (iii) $H(B) < 0$.*

2. *Z has a stable configuration topologically equivalent to that one in Figure 4.7 if and only if (i) the direction function H is well defined in $[A, B]$, (ii) H has a single zero in the arc $\widehat{AB} \subset \Sigma$ and (iii) $H(B) > 0$.*

3. *Z has an unstable configuration topologically equivalent to that one in Figure 4.8 if and only if (i) the direction function H is well defined in the arc $\widehat{AB} \subset \Sigma$, (ii) H do not have zeros in the arc $\widehat{AB} \subset \Sigma$ and (iii) $H(B) = 0$.*

Proof. It is straightforward following what is done in the previous example. ∎

Moreover, concerning with the item (1) of Proposition 4.1, small perturbations in Z produce the effects showed in the previous example and concerning with the item (3) of this

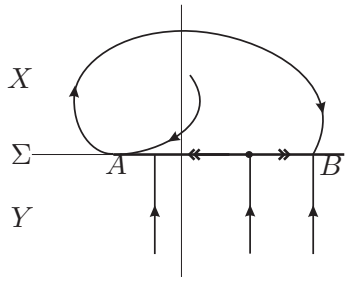

Figure 4.7: Stable configuration.

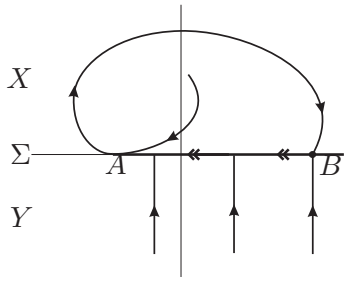

Figure 4.8: Unstable configuration.

proposition, small perturbations in Z produce effects described in Theorem 2.1, in the previous example and in the item (2) of Proposition 4.1.

4.2 The Fold−Saddle Singularity

The specific topic addressed in this section is the characterization of the *Fold−Saddle bifurcation diagram.*

4.2.1 Setting the problem

Let X_0 be a smooth vector field defined in Σ_+. We denote the set of all vector fields defined in Σ_+ presenting a $\Sigma-$fold point by $\Gamma^F_{\Sigma_+}$. We endow $\Gamma^F_{\Sigma_+}$ with the C^r-topology. In this universe a $\Sigma-$fold point has codimension zero. It is possible to consider $f(x,y)=y$ and the following generic normal forms $X_0(x,y)=(\alpha_1,\beta_1 x)$ with $\alpha_1=\pm 1$ and $\beta_1=\pm 1$ (see [43], Theorem 2).

Let Y_0 be a smooth vector field defined in Σ_-. Assume that Y_0 has a hyperbolic saddle point S_{Y_0} on Σ and that the eigenspaces of $DY_0(S_{Y_0})$ are transverse to Σ at S_{Y_0}. We denote the set of all vector fields defined in Σ_- presenting a hyperbolic saddle with the eigenspaces transverse to Σ by $\Gamma^S_{\Sigma_-}$. We endow $\Gamma^S_{\Sigma_-}$ with the C^r-topology. In this universe a saddle point S_{Y_0} has codimension one. By Grobman−Hartman's Theorem any hyperbolic saddle is topologically conjugated to its linearization. And the linear saddle with eigenspaces transverse to the $x-$axis is topologically equivalent to the generic normal forms $Y_0(x,y)=(\alpha_2 y,\alpha_2 x)$ with $\alpha_2=\pm 1$. So the generic unfolding of the singularity is given by $Y_\beta=(\alpha_2(y+\beta),\alpha_2 x)$ where $\beta\in\mathbb{R}$.

Let U be a small neighborhood of Y_0 in $\Gamma^S_{\Sigma_-}$. Then:

(a) There exists a smooth function $L:U\to\mathbb{R}$, such that DL_{Y_0} is surjective.

(b) The correspondence $Y\to S_Y$ is smooth, where S_Y is a saddle point of Y.

(c) If $L(Y)>0$ then $S_Y\in\Sigma_-$.

(d) If $L(Y)=0$ then $S_Y\in\Sigma$.

(e) If $L(Y)<0$ then $S_Y\in\Sigma_+$.

In this section we are concerned with the bifurcation diagram of systems $Z_0 = (X_0, Y_0)$ in Ω^r such that $p_0 = S_{Y_0} \in \Sigma$. This singularity will be called **Fold − Saddle** singularity (see Figures 4.9 and 4.10 − the dotted lines in these and later figures represent the points where $X.f = 0$ and $Y.f = 0$).

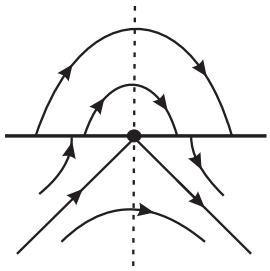

Figure 4.9: (Invisible) Fold-Saddle Singularity.

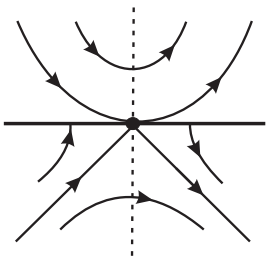

Figure 4.10: (Visible) Fold-Saddle Singularity.

Let $p = (0,0)$ be a fold−saddle singularity of $Z = (X,Y)$. We denote the set of all non−smooth vector fields $Z = (X,Y)$ such that $X \in \Gamma^F_{\Sigma_+}$ and $Y \in \Gamma^S_{\Sigma_-}$ by Γ^{F-S}. We endow Γ^{F-S} with the product topology. Let $Z_0 = (X_0, Y_0) \in \Gamma^{F-S}_0$. That means that we may fix coordinates such that $X_0(x,y) = (-1, \pm x)$ and $f(x,y) = y$. Observe that 0 is the unique singularity of X_0 around a neighborhood W_0 of the origin in $\mathbb{R}^2$. There exists a neighborhood U_0 of Z_0 in Ω^r such that for any $Z = (X,Y) \in U_0$ we may find a Σ−fold point $p_Z = (k_Z, 0) \in W_0$ such that it is the unique singularity of X in W_0. Moreover the correspondence $Z \to p_Z$ is C^r.

In the same way, for any $Z = (X,Y) \in U_0$ we find a C^r−correspondence $B : U_0 \to \mathbb{R}^2$ where $B(Z) = s_Z = (a_Z, b_Z)$ is the (unique) equilibrium (saddle) of Y in U_0. We are assuming that the eigenspaces of $DY_{s_Z}(q_Z)$ are transverse to Σ at s_Z. We have to distinguish the cases: (i) $b_Z < 0$, (ii) $b_Z = 0$ and (iii) $b_Z > 0$. Observe that when $b_Z < 0$ (resp. $b_Z > 0$) there is associated to Z an invisible (resp. visible) Σ−fold point of Y given by $q_Y = (c_Z, 0) \in W_0$. Moreover $lim_{b_Z \to 0} c_Z = a_Z$.

Define $F(Z) = (k_Z - a_Z, b_Z)$. We get:

(i) The derivative $DF : U_0 \to R^2$ is surjective;

(ii) $F^{-1}(0) = \Omega_2$ is a codimension−two submanifold of Ω^r.

Then this fold−saddle singularity occurs generically in two−parameter families of vector fields in Ω^r.

Consider

$$Z^\tau = \begin{cases} X^\tau = \begin{pmatrix} \pm 1 \\ \alpha_1(\tau)x \end{pmatrix} & \text{if } y \geq 0, \\ Y = \begin{pmatrix} -y \\ -x \end{pmatrix} & \text{if } y \leq 0, \end{cases} \tag{4.2}$$

where $\alpha_1(inv) = -1$ and $\alpha_1(vis) = 1$.

Lemma 4.1. *If $Z \in \Omega_2$ then Z is $\Sigma-$equivalent to Z^τ given by* (4.2).

We prove the previous lemma in section 4.2.3.

Conjecture: *For any neighborhood $W \subset \Omega^r$ of Z^{inv}, given by* (4.2)*, and for any integer $k > 0$ there exists $\widetilde{Z} \in W$ such that the codimension of $\widetilde{Z}$ is k.*

So, based on the conjecture, we have to sharper our analysis. In order to get low codimension bifurcation we have to impose some generic assumption.

Consider an arbitrary non−smooth vector field $Z_0 = (X_0, Y_0)$ presenting a fold−saddle singularity p like above. When $\tau = inv$ we add the extra generic assumption $X_0^3.f(p) \neq 0$ on the $\Sigma-$fold point. In [43], Theorem 2, we can change the set called Q and to conclude that around the invisible $\Sigma-$fold point the vector field X_0 is expressed by $X_0 = (1, -x + a_1x^2)$ where $a_1 \neq 0$. We say that the $\Sigma-$fold point of X_0 is *contractive* (respectively, *expansive*) if $a_1 < 0$ (respectively $a_1 > 0$).

According to the previous discussion, we will consider $Z_0^{inv}, Z_0^{vis} \in \Omega^r$ written in the following forms:

$$Z_0^{inv} = \begin{cases} X_0^{inv} = \begin{pmatrix} 1 \\ -x + x^2 \end{pmatrix} & \text{if } y \geq 0, \\ Y_0 = \begin{pmatrix} -y \\ -x \end{pmatrix} & \text{if } y \leq 0, \text{ and} \end{cases} \tag{4.3}$$

$$Z_0^{vis} = \begin{cases} X_0^{vis} = \begin{pmatrix} 1 \\ x \end{pmatrix} & \text{if } y \geq 0, \\ Y_0 = \begin{pmatrix} -y \\ -x \end{pmatrix} & \text{if } y \leq 0. \end{cases} \tag{4.4}$$

Note that X_0^{inv} presents an invisible expansive $\Sigma-$fold point in its phase portrait and X_0^{vis} presents a visible one.

The main question is to exhibit the bifurcation diagram of Z_0^τ with either $\tau = inv$ or $\tau = vis$.

We obtain that:

I- There is a canonical imbedding $F_0^\tau : \mathbb{R}^2, 0 \to \chi^r, Z_0^\tau$ such that $F_0^\tau(\lambda, \beta) = Z_{\lambda,\beta}^\tau$ is expressed by:

$$Z_{\lambda,\beta}^\tau = \begin{cases} X_\lambda^\tau = \begin{pmatrix} 1 \\ \alpha_1(\tau)(x-\lambda) + \alpha_2(\tau)(x-\lambda)^2 \end{pmatrix} & \text{if } y \geq 0, \\ Y_\beta = \begin{pmatrix} -(y+\beta) \\ -x \end{pmatrix} & \text{if } y \leq 0, \end{cases} \tag{4.5}$$

where λ, $\beta \in (-1,1)$, $\alpha_1(inv) = -1$, $\alpha_1(vis) = 1$, $\alpha_2(inv) = 1$ and $\alpha_2(vis) = 0$. Moreover, the two−parameter family given by (4.5) is transversal to Ω_2 and its bifurcation diagram is exhibited (see Figures 4.24 and 4.31). We observe that there are some typical topological types nearby Z_0^τ that do not appear in the bifurcation diagram of $Z_{\lambda,\beta}^\tau$. For example, when $\tau = inv$ the configurations in Figures 4.11 and 4.12 are excluded and when $\tau = vis$ the configuration in Figure 4.13 also is excluded.

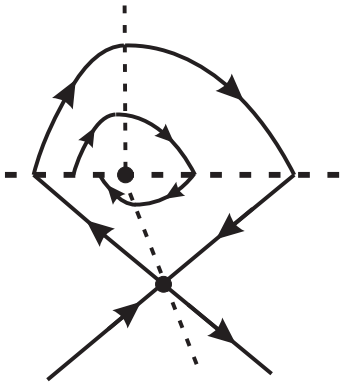

Figure 4.11:

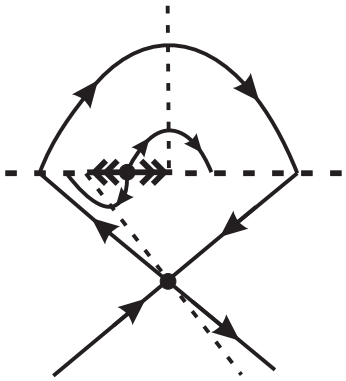

Figure 4.12:

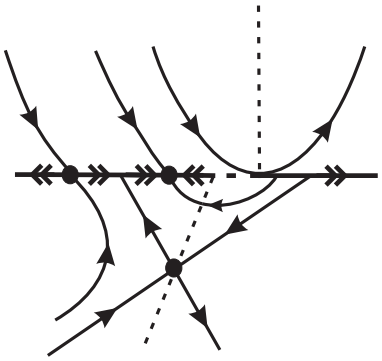

Figure 4.13:

II- We add an auxiliary parameter μ in the following way:

$$\overline{Z}_{\lambda,\mu,\beta}^\tau = \begin{cases} X_\lambda = \begin{pmatrix} 1 \\ \alpha_1(\tau)(x-\lambda) + \alpha_2(\tau)(x-\lambda)^2 \end{pmatrix} & \text{if } y \geq 0, \\ Y_{\mu,\beta} = \begin{pmatrix} \frac{\mu}{2}x + \frac{(\mu-2)}{2}(y+\beta) \\ \frac{(\mu-2)}{2}x + \frac{\mu}{2}(y+\beta) \end{pmatrix} & \text{if } y \leq 0, \end{cases} \tag{4.6}$$

where λ, $\beta \in (-1,1)$, $\alpha_1(inv) = -1$, $\alpha_1(vis) = 1$, $\alpha_2(inv) = 1$, $\alpha_2(vis) = 0$ and $\mu \in (\varepsilon_0, 1)$ with $\varepsilon_0 < 0$. By means of this latter unfolding its bifurcation diagram cover all topological types near $\overline{Z}_{0,0,0}^\tau$.

The configuration illustrated in Figure 4.11 plays a very important role in our analysis. In this *resonant* configuration we note, for example, a fold−fold singularity or even a loop passing through the saddle point. Only the bifurcation of these two unstable configurations already represents a relevant development (the fold−fold singularity is studied recently in [24]

and the *non−smooth loop bifurcation*, as long as we known, was not studied until the present work). In fact, this configuration is reached in (4.6), taking $\mu = \mu_0$ where

$$\mu_0 = 2 - (12\beta/(-3 + 6\beta + \sqrt{9 - 12\beta^2})) \tag{4.7}$$

and $\lambda = \lambda_0 = (-3 + \sqrt{9 - 12\beta^2})/6$.

In this section we consider just the cases described in Equations (4.3) and (4.4), where the first coordinate of X is equal to 1. When the first coordinate of X is equal to -1 a similar approach can be done.

It is worth mentioning that we detect branches of "*canard cycles*" in the bifurcation diagram of $\overline{Z}^{inv}_{\lambda,\mu,\beta}$. A canard cycle is a closed path composed by pieces of orbits of X, Y and Z^{Σ} (see Figures 1.2, 1.3 and 1.4).

4.2.2 Statement of the Main Results

Our results are now stated. Theorems 4.1, 4.2 and 4.3 are intermediate steps towards Theorem 4.7 and Theorems 4.4, 4.5 and 4.6 are intermediate steps towards Theorem 4.8. Here we follow Definition 1.1 to say when two non−smooth vector fields represent a same topological behavior.

Theorem 4.1. *Take $\tau = inv$ and $\mu = \mu_0$ in Equation (4.6), where μ_0 is given by (4.7). Its bifurcation diagram in the $(\lambda, \beta)-$plane contains essentially* 19 *distinct topological behaviors (see Figure 4.22).*

It is easy to see that the cases covered by Theorem 4.1 do not represent the full unfolding of the (Invisible) Fold−Saddle singularity. Because of this, the next two theorems are necessary. Each one of them describes a distinct generic codimension two singularity.

Theorem 4.2. *Take $\tau = inv$ and $\mu_0 < \mu < \varepsilon_0$ in Equation (4.6). Its bifurcation diagram in the $(\lambda, \beta)-$plane contains essentially* 21 *distinct topological behaviors (see Figure 4.24).*

Theorem 4.3. *Take $\tau = inv$ and $-\varepsilon_0 < \mu < \mu_0$ in Equation (4.6). Its bifurcation diagram in the $(\lambda, \beta)-$plane contains essentially* 21 *distinct topological behaviors (see Figure 4.24).*

Theorem 4.4. *Take $\tau = vis$ in Equation (4.5) or equivalently, take $\tau = vis$ and $\mu = 0$ in Equation (4.6). Its bifurcation diagram in the $(\lambda, \beta)-$plane contains essentially* 13 *distinct topological behaviors (see Figure 4.31).*

The cases covered by Theorem 4.4 do not represent the full unfolding of the (Visible) Fold−Saddle singularity. Because of this, the next two theorems are necessary. Each one of them describes a distinct generic codimension two singularity.

Theorem 4.5. *Take $\tau = vis$ and $0 < \mu < \varepsilon_0$ in Equation (4.6). Its bifurcation diagram in the $(\lambda, \beta)-$plane contains essentially* 13 *distinct topological behaviors on (see Figure 4.31).*

Theorem 4.6. *Take $\tau = vis$ and $-\varepsilon_0 < \mu < 0$ in Equation (4.6). Its bifurcation diagram in the $(\lambda, \beta)-$plane contains essentially 13 distinct topological behaviors (see Figure 4.31).*

Finally, we are able to state the main results of the section.

Theorem 4.7. *Equation (4.6) with $\tau = inv$ generically unfolds the (Invisible) Fold−Saddle singularity. Moreover, its bifurcation diagram exhibits 61 distinct cases representing 25 distinct topological behaviors (see Figure 4.26).*

Theorem 4.8. *Equation (4.6) with $\tau = vis$ generically unfolds the (Visible) Fold−Saddle singularity. Moreover, its bifurcation diagram exhibits 39 distinct topological behaviors (see Figure 4.33).*

In what follows, in order to simplify the calculations, we take $\mu = \alpha + 1$ in (4.6) and obtain the following expression

$$Z^{\tau}_{\lambda,\alpha,\beta} = \begin{cases} X_\lambda = \begin{pmatrix} 1 \\ \alpha_1(\tau)(x-\lambda) + \alpha_2(\tau)(x-\lambda)^2 \end{pmatrix} & \text{if } y \geq 0, \\ Y_{\alpha,\beta} = \begin{pmatrix} \frac{(1+\alpha)}{2}x + \frac{(-1+\alpha)}{2}(y+\beta) \\ \frac{(-1+\alpha)}{2}x + \frac{(1+\alpha)}{2}(y+\beta) \end{pmatrix} & \text{if } y \leq 0, \end{cases} \tag{4.8}$$

where $\lambda, \beta \in (-1, 1)$, $\alpha \in (-1+\varepsilon_0, 0)$, $\tau = inv$ or vis, $\alpha_1(inv) = -1$, $\alpha_1(vis) = 1$, $\alpha_2(inv) = 1$ and $\alpha_2(vis) = 0$. When it does not produce confusion, in order to simplify the notation we use $Z = (X, Y)$ or $Z_{\lambda,\alpha,\beta} = (X, Y)$ instead $Z^{\tau}_{\lambda,\alpha,\beta} = (X_\lambda, Y_{\alpha,\beta})$.

Since μ_0 is given by (4.7), we obtain that

$$\alpha_0 = 1 - (12\beta/(-3 + 6\beta + \sqrt{9 - 12\beta^2})). \tag{4.9}$$

Given $Z = (X, Y)$, we describe some properties of both $X = X_\lambda$ and $Y = Y_{\alpha,\beta}$.

The real number λ measures how the $\Sigma-$fold point $d = (\lambda, 0)$ of X is translated away from the origin. More specifically, if $\lambda < 0$ then d is translated to the left hand side and if $\lambda > 0$ then d is translated to the right hand side.

Some calculations show that the curve $Y.f = 0$ is given by $y = \frac{(1-\alpha)}{(1+\alpha)}x - \beta$. So the points of this curve are equidistant from the separatrices when $\alpha = -1$. It becomes closer to the stable separatrix of the saddle point $S = S_{\alpha,\beta} = (s_1, s_2)$ when $\alpha \in (-1, -1 + \varepsilon_0)$. It becomes closer to the unstable separatrix of S when $\alpha \in (-1 - \varepsilon_0, -1)$. Moreover, the smooth vector field Y has distinct types of contact with Σ according with the particular deformation considered. In this way, we have to consider the following behaviors:

- $\mathbf{Y^-}$: In this case $\beta < 0$. So S is translated to the $y-$direction with $y > 0$ (and S is not visible for Z). It has a visible $\Sigma-$fold point $e = e_{\alpha,\beta} = \left(\frac{(1+\alpha)}{(1-\alpha)}\beta, 0\right) = (e_1, 0)$ (see Figure 4.14).

- $\mathbf{Y^0}$: In this case $\beta = 0$. So S is not translated (see Figure 4.9).

- $\mathbf{Y}^+$: In this case $\beta > 0$. So S is translated to the $y-$direction with $y < 0$. It has an invisible $\Sigma-$fold point $i = (i_1, i_2) = i_{\alpha,\beta} = \left(\frac{(1+\alpha)}{(1-\alpha)}\beta, 0\right)$. Moreover, we distinguish two points: $h = h_\beta = (-\beta, 0)$ which is the intersection between the unstable separatrix with Σ and $j = j_\beta = (\beta, 0)$ which is the intersection between the stable separatrix with Σ (see Figure 4.15).

In Figure 4.15 we distinguish the arcs σ_1 of Y joining the saddle point S of Y to h and σ_2 of Y joining j to the saddle point S of Y.

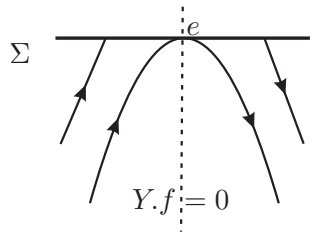

Figure 4.14: Case Y^-.

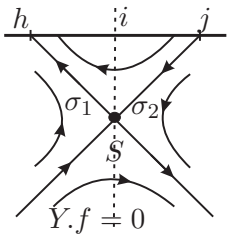

Figure 4.15: Case Y^+.

4.2.3 Proof of Theorem 4.1

Proof of Lemma 1. Here we construct a $\Sigma-$preserving homeomorphism h that sends orbits of $Z = (X, Y)$ to orbits of $\widetilde{Z} = (\widetilde{X}, \widetilde{Y})$, where $\widetilde{Z} = Z^{inv}$, given by (4.2), and the first coordinate of $\widetilde{X}$ is equal to 1. The other cases are treated in a similar way. Consider A_0 a fixed point of the stable separatrix of the saddle point S of Y (see Figure 4.16). Let T_1 be a transversal section of Y passing through A_0. The section T_1 also is transversal to $\widetilde{Y}$ and it crosses the stable separatrix of the saddle point $\widetilde{S}$ of $\widetilde{Y}$ in the point B_0. Let $A_1 \in T_1$ be a point on the left of A_0. The trajectory of Y passing through A_1 crosses Σ in a point A_2. In the same way, the trajectory of $\widetilde{Y}$ passing through A_1 crosses Σ in a point B_2. The trajectory of X that passes through A_2 crosses Σ in a point A_3. The trajectory of $\widetilde{X}$ that passes through B_2 crosses Σ in B_3. Consider A_4 a fixed point of the unstable separatrix of S. Let T_2 be a transversal section of Y passing through A_4. The section T_2 also is transversal to $\widetilde{Y}$ and it crosses the stable separatrix of $\widetilde{S}$ in the point B_4. The trajectory of Y passing through A_3 crosses T_2 in a point A_5. In the same way, the trajectory of $\widetilde{Y}$ passing through B_3 crosses T_2 in a point B_5. Let $A_6 \in T_1$ be a point at the right of A_0. The trajectory of Y passing through A_6 crosses T_2 in a point A_7. The trajectory of $\widetilde{Y}$ passing through A_6 crosses T_2 in a point B_7. The homeomorphism h sends T_1 to T_1, the arc $\gamma_1 = \widehat{A_1\, A5}$ to the arc $\widetilde{\gamma}_1 = \widehat{A_1\, B_5}$ and the arc $\gamma_2 = \widehat{A_6\, A_7}$ to the arc $\widetilde{\gamma}_2 = \widehat{A_6\, B_7}$. Now we can extend continuously h to the interior of the region limited by $T_1 \cup \gamma_1 \cup T_2 \cup \gamma_2$. In this way, there exists a $\Sigma-$preserving homeomorphism h that sends orbits of Z to orbits of $\widetilde{Z}$.

□

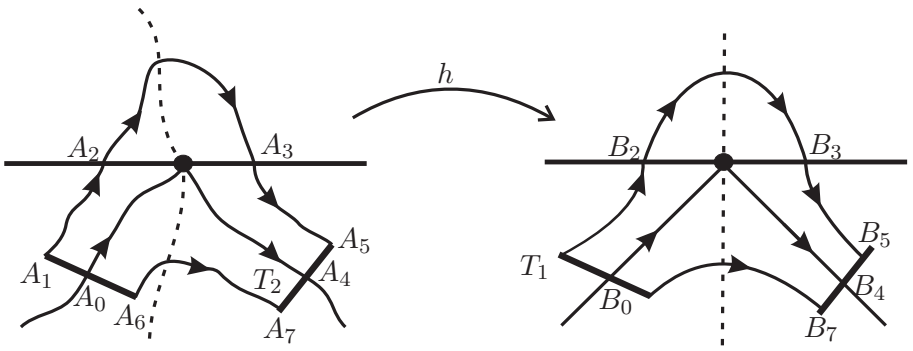

Figure 4.16: Construction of the homeomorphism.

Proof of Theorem 4.1. In Cases 1_1, 2_1 and 3_1 we assume that Y presents the behavior Y^-. In Cases 4_1, 5_1 and 6_1 we assume that Y presents the behavior Y^0. In these cases canard cycles do not arise.

$\diamond$ *Case* 1_1. $d_1 < e_1$, *Case* 2_1. $d_1 = e_1$ *and Case* 3_1. $d_1 > e_1$*:* The points of Σ outside the interval (d_1, e_1) or (e_1, d_1), according with the case, belong to Σ_1. The points inside this interval, when it is not degenerate, belong to Σ_3 in Case 1_1 and to Σ_2 in Case 3_1. In both cases $H(z) > 0$ for all $z \in \Sigma_2 \cup \Sigma_3$. See Figure 4.40.

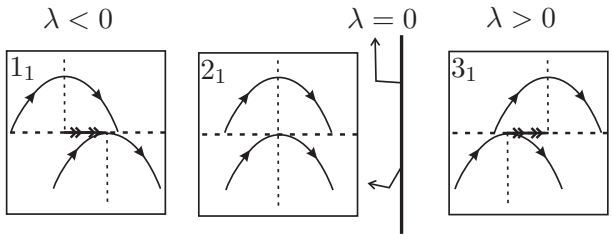

Figure 4.17: Cases 1_1, 2_1 and 3_1.

$\diamond$ *Case* 4_1. $d_1 < s_1$, *Case* 5_1. $d_1 = s_1$ *and Case* 6_1. $d_1 > s_1$*:* The points of Σ outside the interval (d_1, s_1) or (s_1, d_1), according with the case, belong to Σ_1. The points inside this interval, when it is not degenerate, belong to Σ_3 in Case 4_1 and to Σ_2 in Case 6_1. In both cases $H(z) > 0$ for all $z \in \Sigma_2 \cup \Sigma_3$. See Figure 4.18.

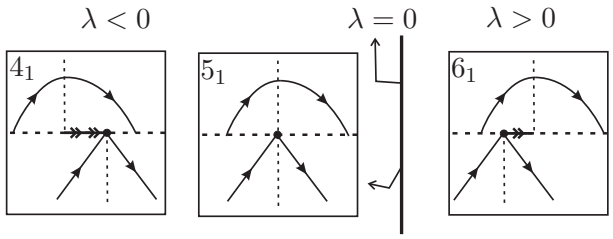

Figure 4.18: Cases 4_1, 5_1 and 6_1.

In Cases $7_1 - 19_1$ we assume that Y presents the behavior Y^+. Remember that $\alpha = 1 - (12\beta/(-3 + 6\beta + \sqrt{9-12\beta^2}))$. In what follows we call $L_0 = 1/12(-9-6\beta+\sqrt{9-12\beta^2}+\sqrt{2}\sqrt{15+\sqrt{9-12\beta^2}-2\beta(-3+2\beta+\sqrt{9-12\beta^2})})$, $L_1 = -1/2 + \sqrt{9-12\beta^2}/6$ and $L_2 = (-9 + 6\beta + \sqrt{9-12\beta^2} + +\sqrt{2}\sqrt{15+\sqrt{9-12\beta^2}+2\beta(-3+2\beta+\sqrt{9-12\beta^2})})/12$. Observe that when $\lambda = L_0$ there exists an arc of trajectory of X connecting h and i. When $\lambda = L_1$ there exists an arc of trajectory of X connecting h and j. When $\lambda = L_2$ there exists an arc of trajectory of X connecting i and j.

$\diamond$ *Case* 7_1. $\lambda < -\beta$, *Case* 8_1. $\lambda = -\beta$, *Case* 9_1. $-\beta < \lambda < L_0$, *Case* 10_1. $\lambda = L_0$ *and Case* 11_1. $L_0 < \lambda < L_1$*:* The points of Σ outside the interval (d_1, i_1) belong to Σ_1. The points inside this interval belong to Σ_3. The direction function H assumes positive values in a neighborhood of d_1, negative values in a neighborhood of i_1 and there exists only one value $\widetilde{P} = \widetilde{P}_{\lambda,\alpha,\beta}$ such that $H(\widetilde{P}) = 0$ (in fact, using the software *Mathematica*, we obtain explicitly the value of $\widetilde{P}$, but its expression is too large, so it will be omitted). So, by (1.1), the $\Sigma-$attractor $P = (\widetilde{P}, 0)$, nearby $(0,0)$, is the unique pseudo equilibrium of Z. In these cases canard cycles do not arise. See Figure 4.19.

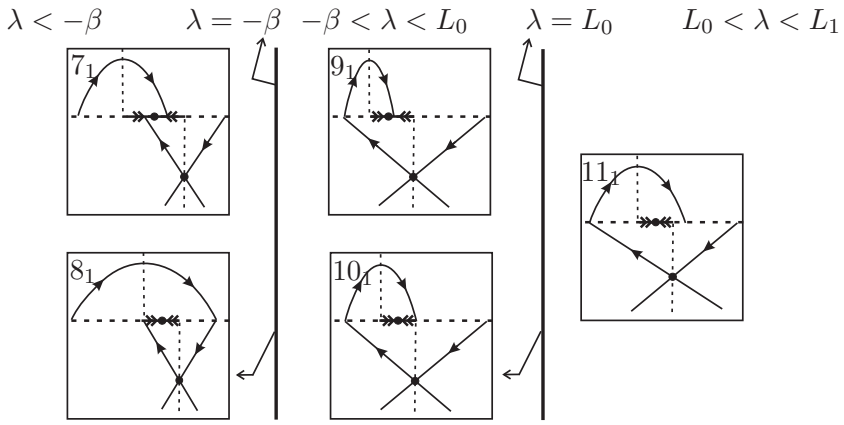

Figure 4.19: Cases $7_1 - 11_1$.

$\diamond$ *Case* 12_1. $\lambda = L_1$*:* Since $\lambda = L_1$ there is an arc γ_1^X of X connecting the points h and j. It generates a $\Sigma-$graph $\Gamma = \gamma_1^X \cup \sigma_2 \cup S \cup \sigma_1$ of kind I. Moreover, since $\alpha = \alpha_0$, where α_0 is given by (4.9), there exists a non generic tangential singularity at the point $d = i$. So, the points of $\Sigma/\{d\}$ belong to Σ_1. As the $\Sigma-$fold point of X is expansive, a direct calculus shows that the *First Return Map* $\eta : (h, d) \to (d, j)$ has derivative less than 1. As consequence, Γ is a repeller for the trajectories inside it, $d = i$ behavior itself like an attractor weak focus and canard cycles do not arise. See Figure 4.20.

$\diamond$ *Case* 13_1. $L_1 < \lambda < L_3$*:* The meanning of L_3 will be given below in this case. The points of Σ outside the interval (i_1, d_1) belong to Σ_1 and the points inside this interval belong to Σ_2. The direction function H assumes positive values in a neighborhood of d_1, negative values in

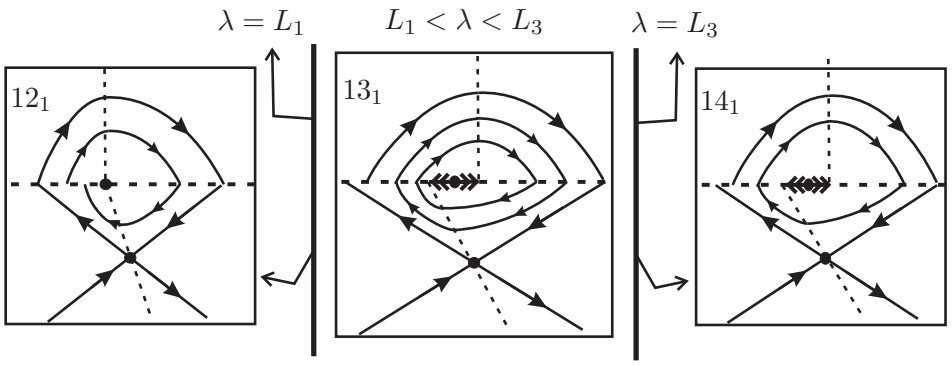

Figure 4.20: Cases 12_1, 13_1 and 14_1.

a neighborhood of i_1 and there exists a unique value $\widetilde{P} = \widetilde{P}_{\lambda,\alpha,\beta}$ such that $H(\widetilde{P}) = 0$. So $P = (\widetilde{P}, 0)$ is a $\Sigma-$repeller. When λ is a bit bigger than L_1, the First Return Map η has two fixed points, i.e., Z has two canard cycles. One of them, called Γ_1, born from the bifurcation of the $\Sigma-$graph Γ of the previous case and the other one, called Γ_2, born from the bifurcation of the non generic tangential singularity presented in the previous case. Both of them are canard cycles of kind I. Using the software *Mathematica* we obtain that Γ_1 is a hyperbolic repeller canard cycle and Γ_2 is a hyperbolic attractor canard cycle. Note that, as λ increases, Γ_1 becomes smaller and Γ_2 becomes bigger. When λ assumes the limit value L_3, one of them collides to the other. See Figure 4.20.

$\diamond$ *Case* 14_1. $\lambda = L_3$*:* The distribution of the connected components of Σ and the behavior of H are the same of Case 13_1. Since $\lambda = L_3$, as described in the previous case, there exists a non hyperbolic canard cycle Γ of kind I which is an attractor for the trajectories inside it and is a repeller for the trajectories outside it. See Figure 4.20.

$\diamond$ *Case* 15_1. $L_3 < \lambda < L_2$*, Case* 16_1. $\lambda = L_2$*, Case* 17_1. $L_2 < \lambda < \beta$*, Case* 18_1. $\lambda = \beta$ *and Case* 19_1. $\lambda > \beta$*:* The points of Σ outside the interval (i_1, d_1) belong to Σ_1 and the points inside this interval belong to Σ_2. The direction function H assumes positive values in a neighborhood of d_1, negative values in a neighborhood of i_1 and there exists a unique value $\widetilde{P}$ such that $H(\widetilde{P}) = 0$. So, by (1.1), the $\Sigma-$repeller $P = (\widetilde{P}, 0)$, nearby $(0, 0)$, is the unique pseudo equilibrium of Z. In these cases canard cycles do not arise. See Figure 4.21.

The bifurcation diagram is illustrated in Figure 4.22. □

Remark 6. *In Cases* 11_1 *and* 15_1 *the ST-bifurcations (as described in [24]) arise. In fact, note that the trajectory passing through h can make more and more turns around P. This fact characterizes a global bifurcation also reached in other cases as shown in this section.*

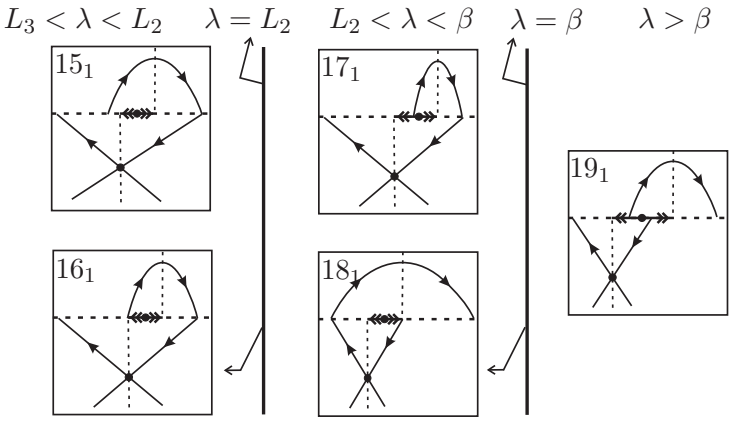

Figure 4.21: Cases $15_1 - 19_1$.

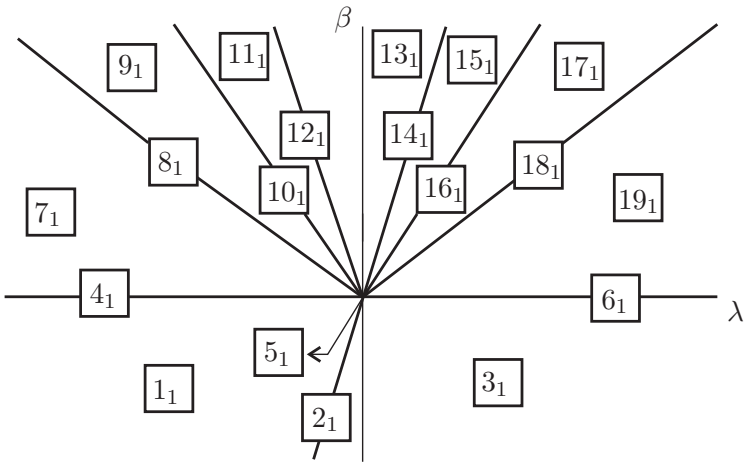

Figure 4.22: Bifurcation Diagram of Theorem 4.1.

4.2.4 Proof of Theorem 4.2

Proof of Theorem 4.2. In Cases 1_2, 2_2 and 3_2 we assume that Y presents the behavior Y^-. In Cases 4_2, 5_2 and 6_2 we assume that Y presents the behavior Y^0. In Cases $7_2 - 21_2$ we assume that Y presents the behavior Y^+.

$\diamond$ *Case* 1_2. $d_1 < e_1$, *Case* 2_2. $d_1 = e_1$, *Case* 3_2. $d_1 > e_1$, *Case* 4_2. $d_1 < s_1$, *Case* 5_2. $d_1 = s_1$ *and Case* 6_2. $d_1 > s_1$*:* The analysis of these cases are done in a similar way as the cases 1_1, 2_1, 3_1, 4_1, 5_1 and 6_1.

In what follows we call $M_0 = (-3 - 3\alpha(-2 + \alpha + 2(-1 + \alpha)\beta) + \sqrt{9(-1+\alpha)^4 - 12(-1+\alpha)^2\beta^2})/(6(-1 + \alpha)^2)$, $M_1 = -1/2 + \sqrt{9 - 12\beta^2}/6$ and $M_2 = (-3 + 6\beta - 3\alpha(-2 + \alpha + 2\beta) + \sqrt{9(-1+\alpha)^4 - 12(-1+\alpha)^2\alpha^2\beta^2})/(6(-1 + \alpha)^2)$. Observe that when $\lambda = M_0$ there exists an arc of trajectory of X connecting h and i. When $\lambda = M_1$ there exists an arc of

trajectory of X connecting h and j. When $\lambda = M_2$ there exists an arc of trajectory of X connecting i and j.

$\diamond$ *Case* 7_2. $\lambda < -\beta$, *Case* 8_2. $\lambda = -\beta$, *Case* 9_2. $-\beta < \lambda < M_0$, *Case* 10_2. $\lambda = M_0$ *and Case* 11_2. $M_0 < \lambda < M_1$: Analogous to Cases $7_1 - 11_1$ changing L_0 by M_0 and L_1 by M_1.

$\diamond$ *Case* 12_2. $\lambda = M_1$: The points of Σ outside the interval (d_1, i_1) belong to Σ_1 and the points inside this interval belong to Σ_3. The direction function H assumes positive values in a neighborhood of d_1, negative values in a neighborhood of i_1 and there exists a unique value $\widetilde{P} = \widetilde{P}_{\lambda,\alpha,\beta}$ such that $H(\widetilde{P}) = 0$. So $P = (\widetilde{P}, 0)$ is a $\Sigma-$attractor. Since $\lambda = M_1$, there is an arc γ_1^X of X connecting the points h and j. It generates a $\Sigma-$graph $\Gamma = \gamma_1^X \cup \sigma_2 \cup S \cup \sigma_1$ of kind I. Since $\alpha > \alpha_0$, where α_0 is given by (4.9), it is straight forward to show that the *First Return Map* defined in the interval $(h_1, d_1) \subset \Sigma$ do not has fixed points. By consequence, Γ is a repeller for the trajectories inside it and canard cycles do not arise. See Figure 4.23.

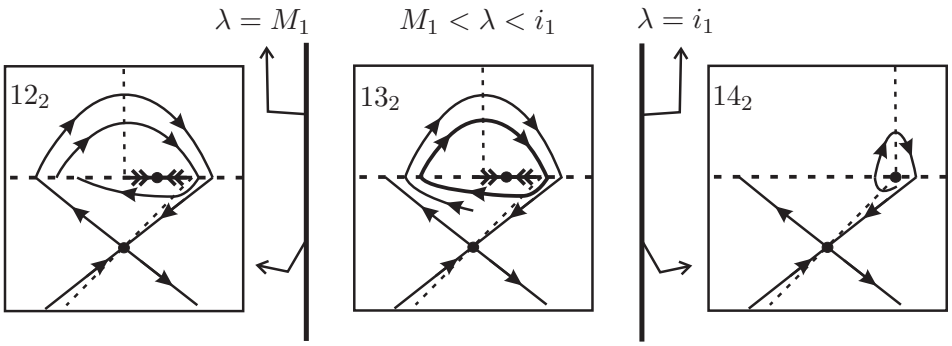

Figure 4.23: Cases 12_2, 13_2 and 14_2.

$\diamond$ *Case* 13_2. $M_1 < \lambda < i_1$: The distribution of the connected components of Σ and the behavior of H are the same of Case 12_2. Since $M_1 < \lambda < i_1$, there is an arc γ_1^X of X connecting j to a point $k = (k_1, 0) \in \Sigma$, where $k_1 \in (h_1, d_1)$, for negative time. Also there is an arc γ_1^Y of Y connecting k to a point $l = (l_1, 0) \in \Sigma$, where $l_1 \in (i_1, j_1)$, for negative time. Repeating this argument, we can find an increasing sequence $(k_i)_{i\in\mathbb{N}}$. We can prove that there is an interval $I \subset (k, d)$ such that $\eta' = (\varphi_Y \circ \varphi_X)' < 1$ on I. As P is a $\Sigma-$attractor, there is an interval $J \subset (k, d)$ such that $\eta' > 1$ on J. Moreover, using the software *Mathematica*, we can prove that η has a unique fixed point $Q \in (k, d)$. As consequence, by Q passes a repeller canard cycle Γ of kind I. See Figure 4.23. This canard cycle born from the bifurcation of the $\Sigma-$graph present in Case 12_2. The expression of η is too large, so the general case will be omitted. For the particular case when $\alpha = -1$, $\beta = 1/2$ and $\lambda = -1/2 + 11\sqrt{6}/60$, the application η is given by

$$\begin{aligned}\eta \;=\; & \tfrac{3}{4} + \tfrac{3}{2}\Big(-\tfrac{1}{2} + \tfrac{11}{10\sqrt{6}}\Big) + \tfrac{x}{2} + \\ & -\tfrac{1}{4}\sqrt{3}\sqrt{\Big(1 - 2\Big(-\tfrac{1}{2} + \tfrac{11}{10\sqrt{6}}\Big) - 2x\Big)\Big(3 + 2\Big(-\tfrac{1}{2} + \tfrac{11}{10\sqrt{6}}\Big) + 2x\Big)}\,.\end{aligned}$$

A straight forward calculus shows that the unique fixed point of this particular η occurs when $x = -\sqrt{29/2}/10$.

$\diamond$ *Case* 14_2. $\lambda = i_1$*:* Every point of Σ belongs to Σ_1 except the point $d = i$. The canard cycle present in the previous case is persistent for this case (remember that this canard cycle born from the bifurcation of the $\Sigma-$graph of Case 12_2. So, it radius do not tends to zero when λ tends to i_1). So the non generic tangential singularity $d = i$ behavior itself like a weak attractor focus. See Figure 4.23.

$\diamond$ *Case* 15_2. $i_1 < \lambda < M_3$ *and Case* 16_2. $\lambda = M_3$*:* Analogous to Cases $13_1 - 14_1$ changing L_1 by i_1 and L_3 by M_3, where M_3 is the limit value for with Γ_1 collides to Γ_2.

$\diamond$ *Case* 17_2. $M_3 < \lambda < M_2$, *Case* 18_2. $\lambda = M_2$, *Case* 19_2. $M_2 < \lambda < \beta$, *Case* 20_2. $\lambda = \beta$ *and Case* 21_2. $\lambda > \beta$*:* Analogous to Cases $15_1 - 19_1$ changing L_2 by M_2 and L_3 by M_3.

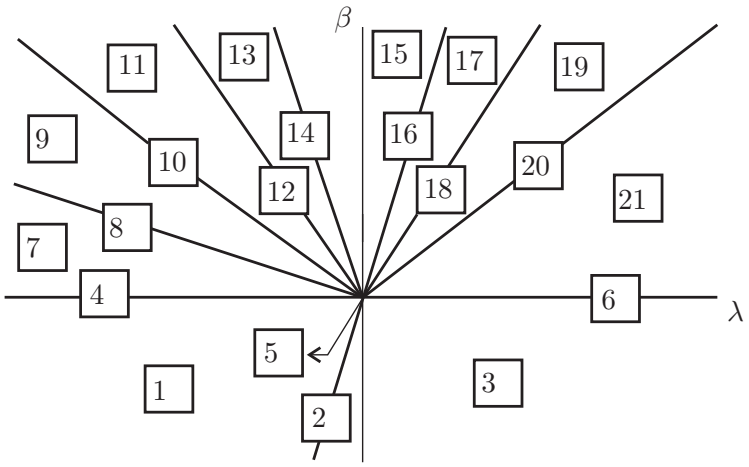

Figure 4.24: Bifurcation Diagram of Theorems 4.2 and 4.3.

The bifurcation diagram is illustrated in Figure 4.24. □

4.2.5 Proof of Theorem 4.3

Proof of Theorem 4.3. In Cases 1_3, 2_3 and 3_3 we assume that Y presents the behavior Y^-. In Cases 4_3, 5_3 and 6_3 we assume that Y presents the behavior Y^0. In Cases $7_3 - 21_3$ we assume that Y presents the behavior Y^+.

$\diamond$ *Case* 1_3. $d_1 < e_1$, *Case* 2_3. $d_1 = e_1$, *Case* 3_3. $d_1 > e_1$, *Case* 4_3. $d_1 < s_1$, *Case* 5_3. $d_1 = s_1$ *and Case* 6_3. $d_1 > s_1$*:* Analogous to Cases 1_1, 2_1, 3_1, 4_1, 5_1 and 6_1.

In what follows we consider M_0, M_1, M_2 and M_3 like in the previous theorem.

$\diamond$ *Case* 7_3. $\lambda < -\beta$, *Case* 8_3. $\lambda = -\beta$, *Case* 9_3. $-\beta < \lambda < M_0$, *Case* 10_3. $\lambda = M_0$ *and Case* 11_3. $M_0 < \lambda < i_1$*:* Analogous to Cases $7_2 - 11_2$ changing M_1 by i_1.

$\diamond$ *Case* 12_3. $\lambda = i_1$*:* Every point of $\Sigma/\{d\}$ belongs to Σ_1. In a similar way as Case 13_2, we can construct sequences $(k_i)_{i\in\mathbb{N}}$ and $(l_i)_{i\in\mathbb{N}}$. Since $d = i$ we have that $k_i \to d$ and $l_i \to d$.

So d is a non generic tangential singularity that behavior itself like an attractor. See Figure 4.25.

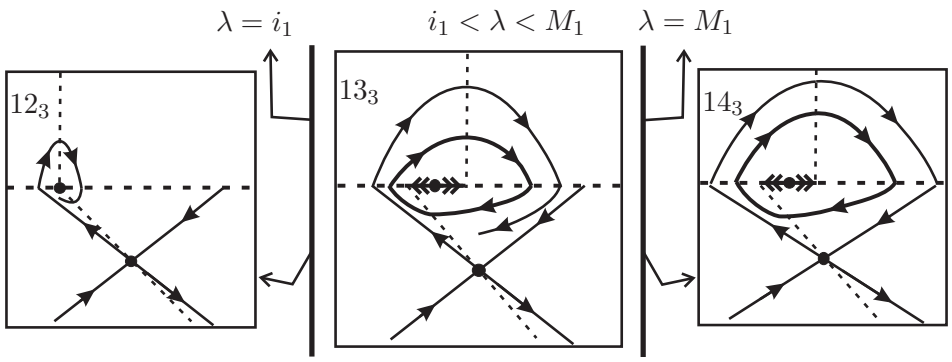

Figure 4.25: Cases 12_3, 13_3 and 14_3.

$\diamond$ *Case* 13_3. $i_1 < \lambda < M_1$*:* Analogous to Case 13_2 except that there is a change of stability on $P = (\widetilde{P}, 0)$, which is a $\Sigma-$repeller, and on Γ, which is an attractor canard cycle of kind I. This canard cycle born from the bifurcation of the attractor non generic tangential singularity present in Case 12_3. See Figure 4.25.

$\diamond$ *Case* 14_3. $\lambda = M_1$*:* Analogous to Case 12_2 except that occurs a change of stability on $P = (\widetilde{P}, 0)$, which is a $\Sigma-$repeller. This fact generates a bifurcation like Hopf near P and it appears a hyperbolic attractor canard cycle Γ_1, of kind I, between P and the $\Sigma-$graph Γ_2. See Figure 4.25.

$\diamond$ *Case* 15_3. $M_1 < \lambda < M_3$ *and Case* 16_3. $\lambda = M_3$*:* Analogous to Cases $15_2 - 16_2$, changing i_1 by M_1.

$\diamond$ *Case* 17_3. $M_3 < \lambda < M_2$, *Case* 18_3. $\lambda = M_2$, *Case* 19_3. $M_2 < \lambda < \beta$, *Case* 20_3. $\lambda = \beta$ *and Case* 21_2. $\lambda > \beta$*:* Analogous to Cases $17_2 - 21_2$.

The bifurcation diagram is illustrated in Figure 4.24. □

4.2.6 Proof of Theorem 4.7

Proof of Theorem 4.7. Since in Equation (4.8) we can take α in the interval $(-\infty, 0)$, from Theorems 4.1, 4.2 and 4.3 we derive that this equation, with $\tau = inv$, unfolds generically the (Invisible) Fold−Saddle singularity.

Observe that the bifurcation diagram contains all the 61 cases described in Theorems 4.1, 4.2 and 4.3. But some of them are $\Sigma-$equivalent and the number of distinct topological behaviors is 25. Moreover, each topological behavior can be represented respectively by the Cases 1_1, 2_1, 3_1, 4_1, 5_1, 6_1, 7_1, 8_1, 9_1, 10_1, 11_1, 12_1, 13_1, 14_1, 15_1, 16_1, 17_1, 18_1, 19_1, 12_2, 13_2, 14_2, 12_3, 13_3 and 14_3.

The full behavior of the three−parameter family of non−smooth vector fields expressed by Equation (4.8), with $\tau = inv$, is illustrated in Figure 4.26 where we consider a sphere

around the point $(\lambda, \mu, \beta) = (0, 0, 0)$ with a small radius and so we make a stereographic projection defined on the entire sphere, except the south pole. Still in relation with this figure, the pictured numbers correspond to the occurrence of the cases described in the previous theorems. As expected, the cases 5_1 and 5_2 are not represented in this figure because they are, respectively, the center and the south pole of the sphere. □

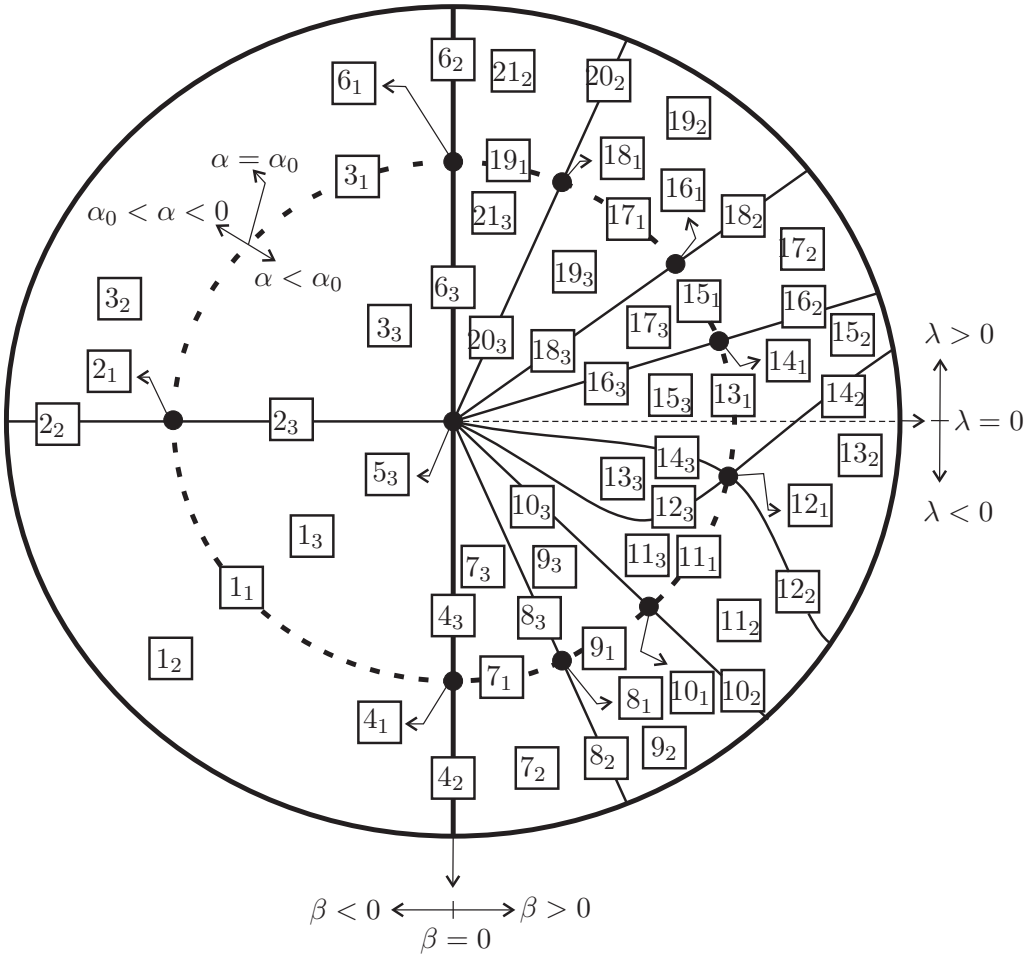

Figure 4.26: Bifurcation diagram of the (Invisible) Fold–Saddle singularity.

4.2.7 Proof of Theorem 4.4

Proof of Theorem 4.4. Since X has a unique Σ–fold point which is visible we conclude that canard cycles do not arise.

In Cases 1_4, 2_4 and 3_4 we assume that Y presents the behavior Y^-. In Cases 4_4, 5_4 and 6_4 we assume that Y presents the behavior Y^0. In these cases, when it is well defined, the direction function H assumes positive values.

$\diamond$ *Case* 1_4. $d_1 < e_1$*:* The points of Σ inside the interval (d_1, e_1) belong to Σ_1. The points on the left of d_1 belong to Σ_3 and the points on the right of e_1 belong to Σ_2. See Figure 4.27.

◇ *Case* 2_4. $d_1 = e_1$*:* Here $\Sigma_1 = \emptyset$. The vector fields X and Y are linearly dependent on $d_1 = e_1$ which is a tangential singularity. Moreover, it is an attractor for the trajectories of Z crossing Σ_3 and a repeller for the trajectories of Z crossing Σ_2. See Figure 4.27.

◇ *Case* 3_4. $d_1 > e_1$*:* The points of Σ inside the interval (e_1, d_1) belong to Σ_1. The points on the left of e_1 belong to Σ_3 and the points on the right of d_1 belong to Σ_2. See Figure 4.27.

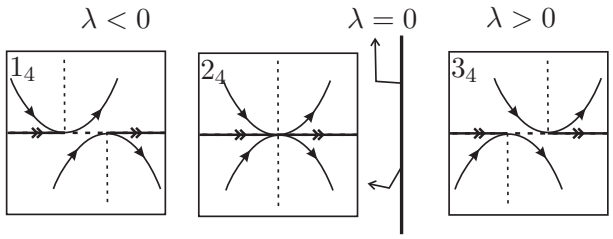

Figure 4.27: Cases 1_4, 2_4 and 3_4.

◇ *Case* 4_4. $d_1 < s_1$*:* The points of Σ inside the interval (d_1, s_1) belong to Σ_1. The points on the left of d_1 belong to Σ_3 and the points on the right of s_1 belong to Σ_2. See Figure 4.28.

◇ *Case* 5_4. $d_1 = s_1$*:* Here $\Sigma_1 = \emptyset$ and S is an attractor for the trajectories of Z crossing Σ_3 and it is a repeller for the trajectories of Z crossing Σ_2. See Figure 4.28.

◇ *Case* 6_4. $d_1 > s_1$*:* The points of Σ inside the interval (d_1, s_1) belong to Σ_1. The points on the left of s_1 belong to Σ_3 and the points on the right of d_1 belong to Σ_2. See Figure 4.28.

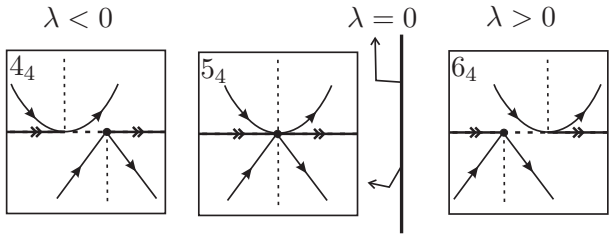

Figure 4.28: Cases 4_4, 5_4 and 6_4.

In Cases $7_4 - 13_4$ we assume that Y presents the behavior Y^+.

◇ *Case* 7_4. $d_1 < h_1$*, Case* 8_4. $d_1 = h_1$ *and Case* 9_4. $h_1 < d_1 < i_1$*:* The points of Σ inside the interval (d_1, i_1) belong to Σ_1. The points on the left of d_1 belong to Σ_3 and the points on the right of i_1 belong to Σ_2. The direction function H assumes positive values on Σ_3 and negative values in a neighborhood of i_1. Moreover, $H(\beta\lambda/(-1+\beta)) = 0$ and the $\Sigma-$repeller $P = (\beta\lambda/(-1+\beta), 0)$ is the unique pseudo equilibrium. See Figure 4.29.

◇ *Case* 10_4. $d_1 = i_1$*:* Here $\Sigma_1 = \emptyset$. The vector fields X and Y are linearly dependent on the tangential singularity $d_1 = i_1$. A straightforward calculation shows that $H(z) = (1-\beta)/2 \neq 0$ for all $z \in \Sigma/\{d\}$. So $d_1 = i_1$ is an attractor for the trajectories of Z crossing Σ_3 and a repeller for the trajectories of Z crossing Σ_2. Moreover, $\Delta = \{d\} \cup \overline{dj} \cup \sigma_2 \cup \{S\} \cup \sigma_1 \cup \overline{hd}$ is a $\Sigma-$graph

of kind III in such a way that each Q in its interior belongs to another $\Sigma-$graph of kind III passing through d. See Figure 4.29.

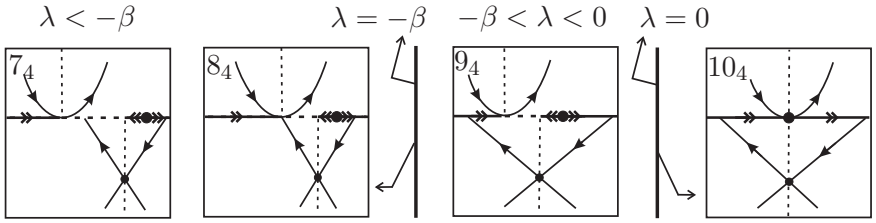

Figure 4.29: Cases $7_4 - 10_4$.

$\diamond$ *Case* 11_4. $i_1 < d_1 < j_1$, *Case* 12_4. $d_1 = j_1$ *and Case* 13_4. $j_1 < d_1$*:* The points of Σ inside the interval (i_1, d_1) belong to Σ_1. The points on the left of i_1 belong to Σ_3 and the points on the right of d_1 belong to Σ_2. The direction function H assumes positive values on Σ_2 and negative values in a neighborhood of i_1. Moreover, $H(\beta\lambda/(-1+\beta)) = 0$ and the $\Sigma-$attractor $P = (\beta\lambda/(-1+\beta), 0)$ is the unique pseudo equilibrium. See Figure 4.30.

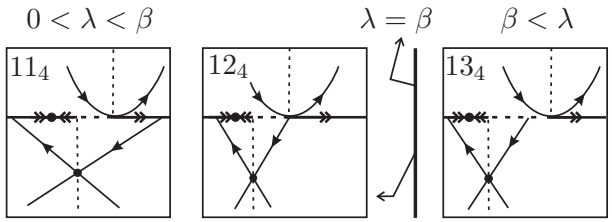

Figure 4.30: Cases $11_4 - 13_4$.

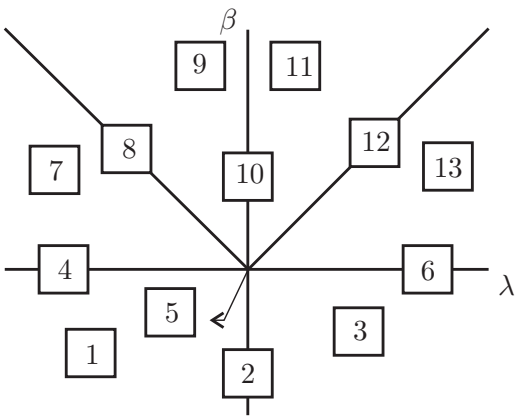

Figure 4.31: Bifurcation Diagram of Theorems 4.4, 4.5 and 4.6.

The bifurcation diagram is illustrated in Figure 4.31. □

4.2.8 Proof of Theorem 4.5

Proof of Theorem 4.5. The direction function H has a root $Q=(q,0)$ where

$$q = \frac{1}{2(\alpha+1)}((-1+\alpha)(1-\beta)-\lambda(1+\alpha)+ \\ +\sqrt{((-1+\alpha)(1-\beta)-\lambda(1+\alpha))^2+4\beta(1+\alpha)(1+\alpha+\lambda(-1+\alpha))}). \tag{4.10}$$

Moreover, H assumes positive values on the right of Q and negative values on the left of Q. Note that when $\alpha\to-1$ so $Q\to-\infty$ under the line $\{y=0\}$ and it occurs the configurations showed in Theorem 4.

In Cases 1_5, 2_5 and 3_5 we assume that Y presents the behavior Y^-. In Cases 4_5, 5_5 and 6_5 we assume that Y presents the behavior Y^0. In Cases 7_5-13_5 we assume that Y presents the behavior Y^+.

$\diamond$ *Case* 1_5. $d_1<e_1$, *Case* 2_5. $d_1=e_1$, *Case* 3_5. $d_1>e_1$, *Case* 4_5. $d_1<s_1$, *Case* 5_5. $d_1=s_1$ *and Case* 6_5. $d_1>s_1$: Analogous to Cases 1_4, 2_4, 3_4, 4_4, 5_4 and 6_4 respectively, except that here it appears the $\Sigma-$saddle Q on the left of d and e or S. See Figure 4.32.

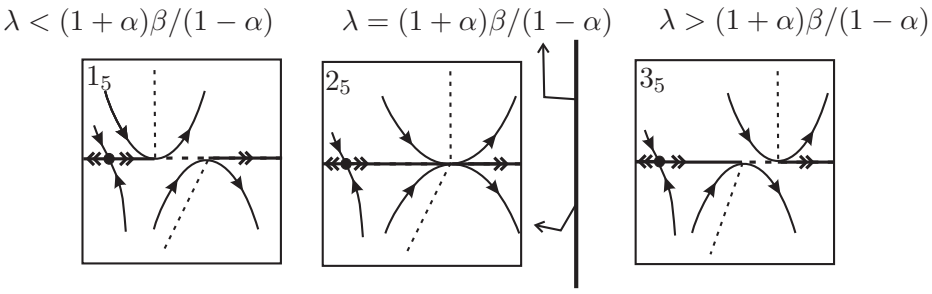

Figure 4.32: Cases 1_5, 2_5 and 3_5.

$\diamond$ *Case* 7_5. $d_1<h_1$, *Case* 8_5. $d_1=h_1$, *Case* 9_5. $h_1<d_1<i_1$: Analogous to Cases 7_4-9_4, except that here the $\Sigma-$saddle Q appears on the left of d_1 and i_1. Here $P=(p,0)$ where

$$p = \frac{1}{2(\alpha+1)}((-1+\alpha)(1-\beta)-\lambda(1+\alpha)+ \\ -\sqrt{((-1+\alpha)(1-\beta)-\lambda(1+\alpha))^2+4\beta(1+\alpha)(1+\alpha+\lambda(-1+\alpha))}). \tag{4.11}$$

$\diamond$ *Case* 10_5. $d_1=i_1$: Analogous to Case 10_4, except that here appear the $\Sigma-$saddle Q on the left of $d_1=i_1$.

$\diamond$ *Case* 11_5. $i_1<d_1<j_1$, *Case* 12_5. $d_1=j_1$ *and Case* 13_5. $j_1<d_1$: Analogous to Cases 11_4-13_4, except that here the $\Sigma-$saddle Q appears on the left of d_1 and i_1.

The bifurcation diagram is illustrated in Figure 4.31. □

4.2.9 Proof of Theorem 4.6

Proof of Theorem 4.6. The direction function H has a root $Q=(q,0)$ where q is given by (4.10). Moreover, H assumes positive values on the left of Q and negative values on the right

of Q. Note that when $\alpha \to -1$ so $Q \to \infty$ under the line $\{y = 0\}$ and the configurations shown in Theorem 4.4 occur.

In Cases 1_6, 2_6 and 3_6 we assume that Y presents the behavior Y^-. In Cases 4_6, 5_6 and 6_6 we assume that Y presents the behavior Y^0. In Cases $7_6 - 13_6$ we assume that Y presents the behavior Y^+.

$\diamond$ *Case* 1_6. $d_1 < e_1$, *Case* 2_6. $d_1 = e_1$, *Case* 3_6. $d_1 > e_1$, *Case* 4_6. $d_1 < s_1$, *Case* 5_6. $d_1 = s_1$ *and Case* 6_6. $d_1 > s_1$, *Case* 7_6. $d_1 < h_1$, *Case* 8_6. $d_1 = h_1$, *Case* 9_6. $h_1 < d_1 < i_1$, *Case* 10_6. $d_1 = i_1$, *Case* 11_6. $i_1 < d_1 < j_1$, *Case* 12_6. $d_1 = j_1$ *and Case* 13_6. $j_1 < d_1$*:* Analogous to Cases 1_5, 2_5, 3_5, 4_5, 5_5, 6_5, 7_5, 8_5, 9_5, 10_5, 11_5, 12_5 and 13_5 respectively, except that here the $\Sigma-$saddle Q takes place on the right of d_1, e_1, s_1 and i_1 when these points appear.

The bifurcation diagram is illustrated in Figure 4.31. □

4.2.10 Proof of Theorem 4.8

Proof of Theorem 4.8. Since in Equation (4.8) we can take α in the interval $(-1-\varepsilon_0, -1+\varepsilon_0)$ we conclude that Theorems 4.4, 4.5 and 4.6 prove that this equation, with $\tau = vis$, unfolds generically the (Visible) Fold−Saddle singularity. Its bifurcation diagram contains all distinct topological behaviors described in Theorems 4.4, 4.5 and 4.6. So, the number of distinct topological behaviors is 39.

The full behavior of the three−parameter family of non−smooth vector fields expressed by Equation (4.8), with $\tau = vis$, is illustrated in Figure 4.33 where we consider a sphere around the point $(\lambda, \mu, \beta) = (0, 0, 0)$ with a small ray and so we make a stereographic projection defined on the entire sphere, except the south pole. Still in relation with this figure, the numbers pictured correspond to the occurrence of the cases described in the previous theorems. As expected, the cases 5_4 and 5_5 are not represented in this figure because they are, respectively, the center and the south pole of the sphere. □

4.3 The Fold−Cusp Singularity

The specific topic addressed in this section is the characterization of the *Fold−Cusp bifurcation diagram.*

4.3.1 Setting the problem

Let X_0 be a smooth vector field defined in Σ_+. Assume that X_0 has a $\Sigma-$fold point p_0. We denote the set of all vector fields defined in Σ_+ presenting a $\Sigma-$fold point by $\Gamma^F_{\Sigma_+}$. We endow $\Gamma^F_{\Sigma_+}$ with the C^r-topology. In this universe a $\Sigma-$fold point has codimension zero. It is possible to consider $f(x, y) = y$ and the following generic normal forms $X_0(x, y) = (\alpha_1, \beta_1 x)$ with $\alpha_1 = \pm 1$ and $\beta_1 = \pm 1$ (see [43], Theorem 2).

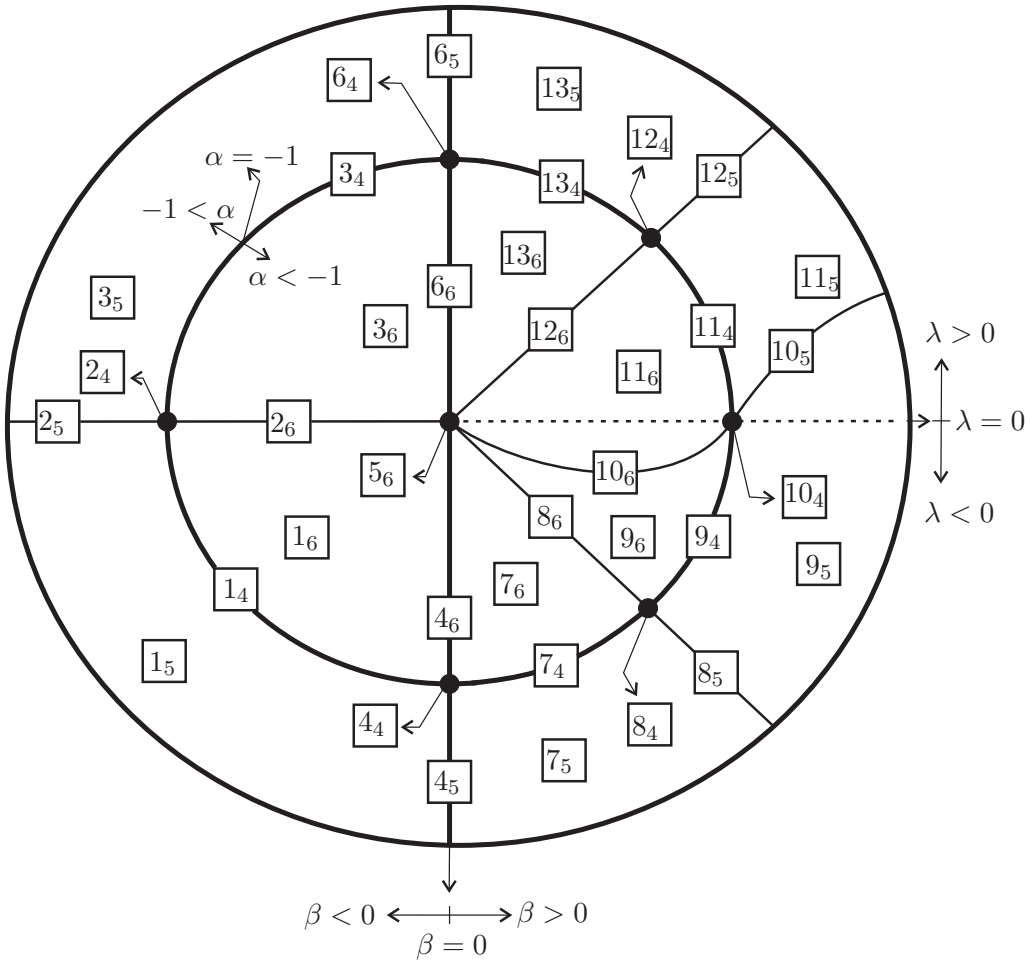

Figure 4.33: Bifurcation diagram of the (Visible) Fold−Saddle singularity.

Let Y_0 be a smooth vector field defined in Σ_-. Assume that Y_0 has an isolated $\Sigma-$cusp point q_0. We denote the set of all vector fields in Σ_- presenting an isolated $\Sigma-$cusp point by $\Gamma^C_{\Sigma_-}$. We endow $\Gamma^C_{\Sigma_-}$ with the C^r-topology. In this universe a $\Sigma-$cusp point q_0 has codimension one. Since $f(x,y) = y$ we derive the following generic normal forms $Y_0(x,y) = (\alpha_2, \omega_2 x^2)$ with $\alpha_2 = \pm 1$, and $\omega_2 = \pm 1$. Its generic unfolding is $Y_\beta(x,y) = (\alpha_2, \omega_2(x^2 + \beta))$ where $\beta \in \mathbb{R}$. Let U be a small neighborhood of Y_0 in $\Gamma^C_{\Sigma_-}$. Then:
(a) There exists a smooth function $L : U \to \mathbb{R}$, such that DL_{Y_0} is surjective;
(b) If $L(Y) > 0$ then $Y.f(q) \neq 0$ for every $q \in \Sigma$ nearby q_0.
(c) If $L(Y) = 0$ then there exists a point $q_Y \in \Sigma$, nearby q_0, such that it is a $\Sigma-$cusp point of Y. Moreover, the correspondence $Y \to q_Y$ is smooth.
(d) If $L(Y) < 0$ then there exist two $\Sigma-$fold points in Σ, m_Y and M_Y, such that $Y^2 f(m_Y) > 0$ and $Y^2 f(M_Y) < 0$. Moreover, the correspondences $Y \to m_Y$ and $Y \to M_Y$ are smooth.

In this section we are concerned with the bifurcation diagram of systems $Z_0 = (X_0, Y_0)$ in Ω^r such that $p_0 = q_0 \in \Sigma$. This singularity will be called **Fold − Cusp** singularity (see Figures 4.34 and 4.35).

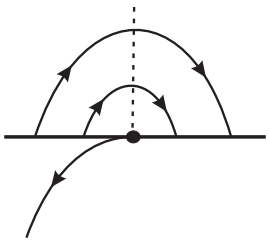

Figure 4.34: (Invisible) Fold − Cusp (of kind 1) Singularity.

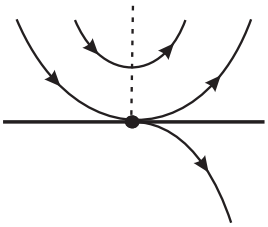

Figure 4.35: (Visible) Fold − Cusp (of kind 2) Singularity.

Let $p = (0,0)$ be a fold−cusp singularity of $Z = (X,Y)$. We denote the set of all non−smooth vector fields $Z = (X,Y)$ such that $X \in \Gamma^F_{\Sigma_+}$ and $Y \in \Gamma^C_{\Sigma_-}$ by Γ^{F-C}. We endow Γ^{F-C} with the product topology.

We depart from $Z_0^{ivb,k1}, Z_0^{vis,k2} \in \Omega^r$ written in the following forms:

$$Z_0^{ivb,k1} = \begin{cases} X_0^{ivb} = \begin{pmatrix} 1 \\ -x \end{pmatrix} & \text{if } y \geq 0, \\ Y_0^{k1} = \begin{pmatrix} -1 \\ -x^2 \end{pmatrix} & \text{if } y \leq 0, \text{ and} \end{cases} \tag{4.12}$$

$$Z_0^{vis,k2} = \begin{cases} X_0^{vis} = \begin{pmatrix} 1 \\ x \end{pmatrix} & \text{if } y \geq 0, \\ Y_0^{k2} = \begin{pmatrix} 1 \\ -x^2 \end{pmatrix} & \text{if } y \leq 0. \end{cases} \tag{4.13}$$

Note that X_0^{ivb} presents an invisible Σ−fold point on its phase portrait, X_0^{vis} presents a visible Σ−fold point, Y_0^{k1} presents a Σ−cusp point of kind 1 and Y_0^{k2} presents a Σ−cusp point of kind 2.

The main question is to exhibit the bifurcation diagram of $Z_0^{\tau,\rho}$, where either $\tau = ivb$ or $\tau = vis$ and either $\rho = k1$ or $\rho = k2$.

Consider $Z_0^{\tau,\rho} = (X_0^\tau, Y_0^\rho)$. Following basically the same steps of the previous section we obtain that:

I- There is a canonical imbedding $F_0^{\tau,\rho} : \mathbb{R}^2, 0 \to \chi^r, Z_0^{\tau,\rho}$ such that $F_0^{\tau,\rho}(\lambda,\beta) = Z_{\lambda,\beta}^{\tau,\rho}$ expressed by:

$$Z_{\lambda,\beta}^{\tau,\rho} = \begin{cases} X_\lambda^\tau = \begin{pmatrix} 1 \\ \omega_1(\tau)(x-\lambda) \end{pmatrix} & \text{if } y \geq 0, \\ Y_\beta^\rho = \begin{pmatrix} \alpha_2(\rho) \\ \omega_2(\rho)(x^2-\beta) \end{pmatrix} & \text{if } y \leq 0, \end{cases} \tag{4.14}$$

where $(\lambda,\beta) \in (-1/8,1/8)\times(-1/8,1/8)$, $\omega_1(vis) = 1$, $\omega_1(ivb) = -1$, $\omega_2(\rho) = \pm 1$ and $\alpha_2(\rho) = \pm 1$. Fix $\omega_2(\rho) = -1$ and consider $(\tau,\rho) = (ivb,k1)$ and $\alpha_2(k1) = -1$ or $(\tau,\rho) = (vis,k2)$ and $\alpha_2(k2) = 1$. The bifurcation diagrams of $Z_{\lambda,\beta}^{\tau,\rho}$ are exhibited (see Figures 4.52 and 4.58). We observe that there are some typical topological types nearby $Z_0^{\tau,\rho}$ that do not appear in the

bifurcation diagram of $Z^{\tau,\rho}_{\lambda,\beta}$. For example, when $(\tau,\rho)=(ivb,k1)$ and $\alpha_2(k1)=-1$ the stable configuration in Figure 4.36 is excluded.

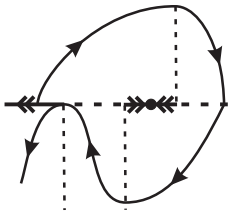

Figure 4.36:

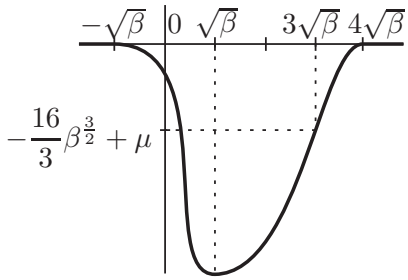

Figure 4.37: Graphic of B^{k1}.

II- We add an auxiliary parameter $\mu\in(-\mu_0,\mu_0)$, where μ_0 is sufficiently small, in the following way:

Consider $B^\rho(x,\beta,\mu)$ a $C^\infty-$bump function such that, for $\beta\geq 0$ and for $\rho=k1$,

$$B^{k1}(x,\beta,\mu)=\begin{cases}0, & \text{if } x\leq-\sqrt{\beta} \text{ or if } x\geq 4\sqrt{\beta};\\ G^{k1}(x,\beta,\mu), & \text{if } -\sqrt{\beta}<x<4\sqrt{\beta}.\end{cases}$$

Note that the function G^{k1} is not well defined if $\beta<0$. In order to deal with this situation, consider $B^{k1}(x,\beta,\mu)\equiv 0$ if $\beta<0$. So B^{k1} is well defined for all $\beta\in(-1/8,1/8)$. When $\beta\geq 0$, the non−positive function G^{k1} is chosen in such a way that F, given by

$$F(x)=\int g_2(x,\beta)dx+B^{k1}(x,\beta,\mu)=\frac{x^3}{3}-\beta x+B^{k1}(x,\beta,\mu)+c \tag{4.15}$$

(where $c\in\mathbb{R}$ is an arbitrary constant), has exactly one point of local minimum at the interval $(-\sqrt{\beta},4\sqrt{\beta})$. This point is located at $x_0=\sqrt{\beta}$. Moreover, we impose that $B^{k1}(3\sqrt{\beta},\beta,\mu)=-((16\beta^{3/2})/3)+\mu$, or equivalently, $F(3\sqrt{\beta})=\mu$. See Figure 4.37.

When $\rho=k2$ we consider B^{k2} with the same properties.

Let $Z^{\tau,\rho}_{\lambda,\beta,\mu}$ given by:

$$Z^{\tau,\rho}_{\lambda,\beta,\mu}=\begin{cases}X^\tau_\lambda=\begin{pmatrix}1\\ \omega_1(\tau)(x-\lambda)\end{pmatrix} & \text{if } y\geq 0,\\ Y^\rho_{\mu,\beta}=\begin{pmatrix}\alpha_2(\rho)\\ -x^2+\beta-\frac{\partial B^\rho}{\partial x}(x,\beta,\mu))\end{pmatrix} & \text{if } y\leq 0,\end{cases} \tag{4.16}$$

where $(\lambda,\beta)\in(-1/8,1/8)\times(-1/8,1/8)$, $\mu\in(-\mu_0,\mu_0)$, $(\tau,\rho)=(ivb,k1)$ and $\alpha_2(k1)=-1$ or $(\tau,\rho)=(vis,k2)$ and $\alpha_2(k2)=1$. Here we need to impose an extra generic assumption to get low codimension bifurcation. That is, we need to choose, appropriately, the bump function B such that the First Return Map η associated to $Z^{\tau,\rho}_{\lambda,\beta,\mu}$ has derivative bigger than 1 in the interval $(a,b)\in\Sigma$ when $\tau=inv$, $\beta>0$, $\mu=0$ and $\lambda=\sqrt{\beta}$. By means of this late unfolding its bifurcation diagram cover all topological types near $Z^{\tau,\rho}_{0,0,0}$.

It is worth to say that the parameter μ breaks the strong proportionality between the roots of g_2. The limit value $\mu_0 = 0$ is such that $Z^{\tau,\rho}_{\lambda,\beta,\mu}$ has distinct topological behaviors for $\mu < \mu_0$ or $\mu > \mu_0$.

Of course, we can take another values of (τ, ρ). Here we consider just the cases described in Equations (4.12) and (4.13). For the other cases a similar approach can be done.

It is worth mentioning that we detect branches of "*canard cycles*" in the bifurcation diagram of (4.12).

4.3.2 Statement of the Results

Our results concerning the Fold−Cusp singularity are now stated. Note that Theorems 4.9, 4.10 and 4.11 are intermediate steps towards Theorem 4.12. Here we follow Definition 1.1 to say when two non−smooth vector fields represent a same topological behavior.

Theorem 4.9. *Take* $(\tau, \rho) = (ivb, k1)$, $\alpha_2(k1) = -1$ *and* $\mu = 0$ *in Equation* (4.16). *Its bifurcation diagram in the* (λ, β)*−plane contains essentially* 17 *distinct topological behaviors (see Figure 4.48).*

It is easy to see that the cases covered by Theorem 4.9 do not represent the full unfolding of the (Invisible) Fold−Cusp singularity. Because of this, the next two theorems are necessary. Each one of them describes a distinct generic codimension two singularity.

Theorem 4.10. *Take* $(\tau, \rho) = (ivb, k1)$, $\alpha_2(k1) = -1$ *and* $0 < \mu < \mu_0$ *in Equation* (4.16). *Its bifurcation diagram in the* (λ, β)*−plane contains essentially* 19 *distinct topological behaviors (see Figure 4.50).*

Theorem 4.11. *Take* $(\tau, \rho) = (ivb, k1)$, $\alpha_2(k1) = -1$ *and* $-\mu_0 < \mu < 0$ *in Equation* (4.16). *Its bifurcation diagram in the* (λ, β)*−plane contains essentially* 19 *distinct topological behaviors (see Figure 4.50).*

Finally, we are able to state the main results of the section.

Theorem 4.12. *Equation* (4.16)*, with* $(\tau, \rho) = (ivb, k1)$ *and* $\alpha_2(k1) = -1$*, generically unfolds the (Invisible) Fold−Cusp singularity. Moreover, its bifurcation diagram exhibits* 55 *cases representing* 23 *distinct topological behaviors (see Figure 4.52).*

Theorem 4.13. *Equation* (4.16)*, with* $(\tau,\rho)=(vis,k2)$ *and* $\alpha_2(k2)=1$*, generically unfolds the (Visible) Fold−Cusp singularity. Moreover, its bifurcation diagram exhibits* 11 *distinct topological behaviors (see Figure 4.58).*

When it does not produce confusion, in order to simplify the notation we use $Z=(X,Y)$ instead $Z^{\tau,\rho}_{\lambda,\beta,\mu}=(X^{\tau}_{\lambda},Y^{\rho}_{\beta,\mu})$.

Given $Z=(X,Y)$, we describe some properties of both $X=X^{\tau}_{\lambda}$ and $Y=Y^{\rho}_{\beta,\mu}$. These properties are reached using $(\tau,\rho)=(ivb,k1)$ and $\alpha_2(k1)=-1$. Analogous properties are true for another choices of (τ,ρ) and $\alpha_2(\rho)$.

The parameter λ measures how the $\Sigma-$fold point $d=(\lambda,0)$ of X is translated away from the origin. More specifically, if $\lambda<0$ then d is translated to the left hand side and if $\lambda>0$ then d is translated to the right hand side.

The parameter β distinguishes the order of the contact between the trajectories of Y and Σ. In this way, it can happen one, and only one, of the following situations:

- $\mathbf{Y^{+}}$: In this case $\beta>0$. So Y has two $\Sigma-$fold points being one of them invisible and the other one visible. These points are expressed by $a=a_{\beta}=(-\sqrt{\beta},0)$ and $b=b_{\beta}=(\sqrt{\beta},0)$. Moreover, a third point $c=c_{\beta,\mu}$ plays an important role in this analysis. This point is the locus where the arc γ_1 of Y passing through a intersects transversally the set Σ for negative time (see Figure 4.38). Using the "bump function" B^{ρ} the distance between c and b is bigger or smaller than the distance between a and b according with the parameter μ. This fact will be important to change from Theorem 4.9 to Theorems 4.10 and 4.11.

- $\mathbf{Y^{0}}$: In this case $\beta=0$. So Y has a $\Sigma-$cusp point $e=(0,0)$ (see Figure 4.34).

- $\mathbf{Y^{-}}$: In this case $\beta<0$. So Y does not have $\Sigma-$fold points. In this way, $Y.f\neq 0$ and Y is transversal to Σ (see Figure 4.39).

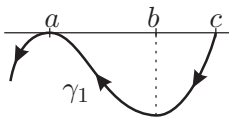

Figure 4.38: Case Y^{+}.

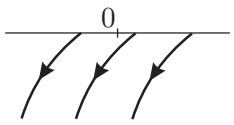

Figure 4.39: Case Y^{-}.

4.3.3 Proof of Theorem 4.9

Proof of Theorem 4.9. In Case 1_1 we assume that Y presents the behavior Y^{-}. In Cases 2_1, 3_1 and 4_1 we assume that Y presents the behavior Y^{0}. In these cases canard cycles are not allowed (for a proof, see [8]).

$\diamond$ *Case* 1_1. $\beta < 0$*:* The points of Σ on the left of d belong to Σ_2 and the points on the right of d belong to Σ_1. See Figure 4.40. The graphic of H is illustrated in H-3 of Figure 4.41. Since $p_i = (-1 + (-1)^i\sqrt{1 + 4\beta + 4\lambda})/2, 0) \in \Sigma_2$, $i = 1, 2$, p_1 is a $\Sigma-$saddle and p_2 is a $\Sigma-$repeller. The virtual pseudo equilibria $r_i = (1 + (-1)^i\sqrt{1 + 4\beta - 4\lambda})/2, 0) \in \Sigma_1$, $i = 1, 2$, correspond to the roots of the denominator of H where this function presents discontinuities.

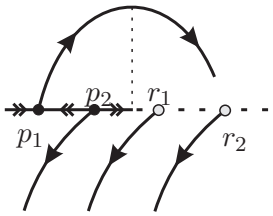

Figure 4.40: Case 1_1.

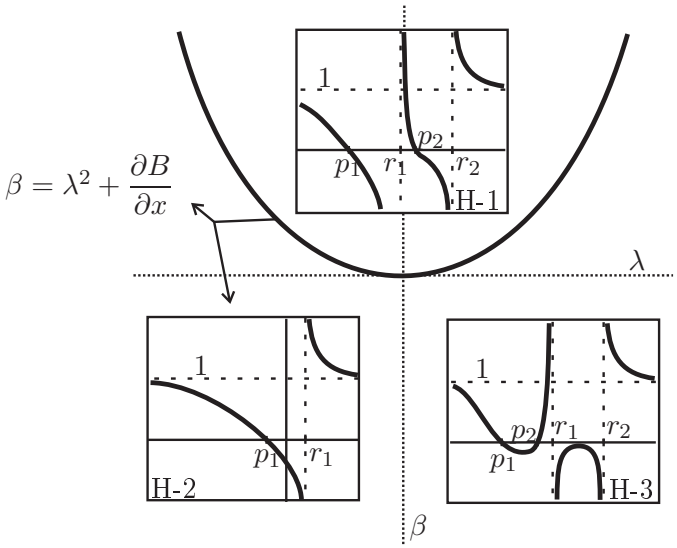

Figure 4.41: Variation of H with respect to λ and β. The dark lines in the boxes H-1, H-2 and H-3 correspond to the graphic of H.

$\diamond$ *Case* 2_1. $\lambda < 0$*, Case* 3_1. $\lambda = 0$ *and Case* 4_1. $\lambda > 0$*:* The configuration of the connected components of Σ is the same as Case 1_1. Since $\beta = 0$, the graphic of H, when $\lambda \neq 0$, is given by H-3 of Figure 4.41. When $\lambda = 0$ (Case 3_1), the graphic of H is given by H-2 of Figure 4.41. These cases are illustrated in Figure 4.42.

In Cases $5_1 - 17_1$ we assume that Y presents the behavior Y^+.

$\diamond$ *Case* 5_1. $\lambda < -\sqrt{\beta}$*:* The points of Σ on the left of d belong to Σ_2, the points inside the interval (a, b) belong to Σ_3 and the points on (d, a) and on the right of b belong to Σ_1. The graphic of H is like H-3 of Figure 4.41. We can prove that p_1 and r_1 are pseudo equilibria, both on the left of d. In fact, $p_2 \in (d, a)$ and r_2 on the right of b are virtual pseudo equilibria. Moreover, p_1 is a $\Sigma-$saddle and r_1 is a $\Sigma-$repeller.

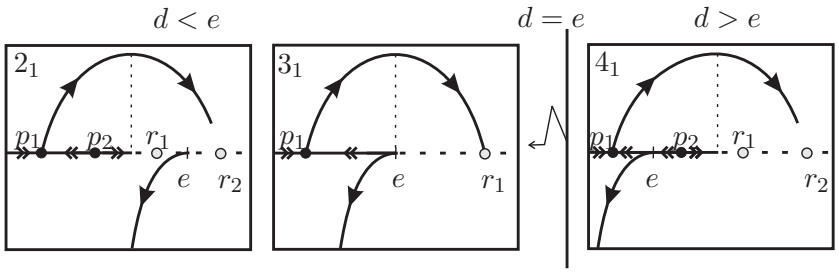

Figure 4.42: Cases 2_1, 3_1 and 4_1.

Easy calculations shown that $p_i = (-1 + (-1)^i\sqrt{1 - 4\partial B/\partial x + 4\beta + 4\lambda})/2, 0)$, $i = 1, 2$ and $r_i = (1 + (-1)^i\sqrt{1 - 4\partial B/\partial x + 4\beta - 4\lambda})/2, 0)$, $i = 1, 2$. Canard cycles are not allowed. See Figure 4.43.

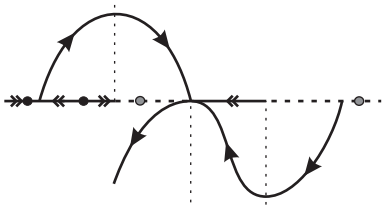

Figure 4.43: Case 5_1.

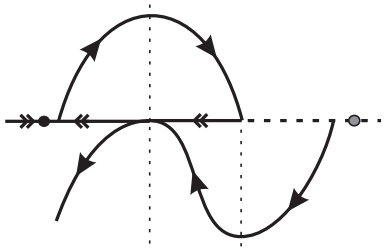

Figure 4.44: Case 6_1.

◇ *Case* 6_1. $\lambda = -\sqrt{\beta}$*:* In this case the points on the right of b belong to Σ_1, the points on $(a = d, b)$ belong to Σ_3 and the points on the left of $a = d$ belong to Σ_2. Since $\beta = \lambda^2$, H is like H-2 of Figure 4.41. There is an unique pseudo equilibrium p_1 (situated on the left of $d = a$) and an unique virtual pseudo equilibrium r_1 (situated on the right of b). When $p_1 < -4\sqrt{\beta}$ there exists a non hyperbolic canard cycle Γ of kind III passing through a and c. See Figure 4.44.

◇ *Case* 7_1. $-\sqrt{\beta} < \lambda < 0$*, Case* 8_1. $\lambda = 0$ *and Case* 9_1. $0 < \lambda < \sqrt{\beta}$*:* The configuration of the connected components of Σ is like Case 5_1 changing a by d and vice-versa. The graphic of H is like H-1 of Figure 4.41. We can prove that p_1, on the left of a, is a $\Sigma-$saddle and $p_2 \in (d, b)$ is a $\Sigma-$attractor. Moreover, the virtual pseudo equilibria $r_1 \in (a, d)$ and r_2 is on the right of b. When $p_1 < (\gamma_X^-(c) \cap \Sigma)$ (where $\gamma_X^-(c)$ is the arc of X passing through c oriented by negative time) there exists a hyperbolic repeller canard cycle Γ of kind III passing through a and c. See Figure 4.45.

◇ *Case* 10_1. $\lambda = \sqrt{\beta}$*:* Since $\lambda = \sqrt{\beta}$ there is an arc γ_1^X of X connecting the points a and c. It generates a non hyperbolic canard cycle $\Gamma = \gamma_1^X \cup \gamma_1^Y$, where γ_1^Y is an arc of Y connecting a and c. Moreover, since $\mu = 0$, there exists a non generic tangential singularity at the point $d = b$. So, the points of $\Sigma/\{d\}$ belong to Σ_1. Remember that we choose the bump function B such that the First Return Map $\eta : (a, d) \to (d, c)$ has derivative bigger

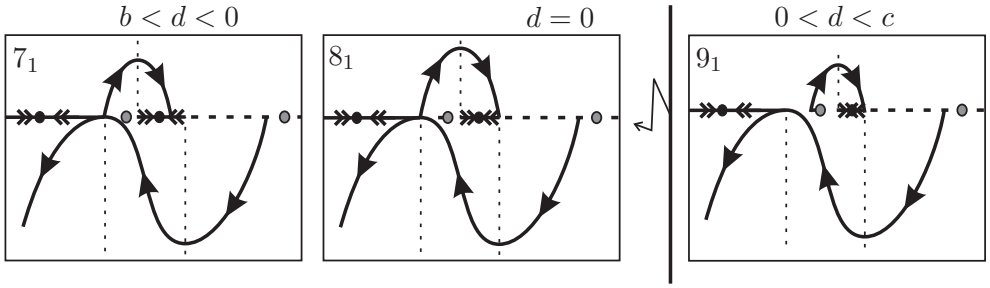

Figure 4.45: Cases $7_1 - 9_1$.

than 1. As consequence, Γ is a repeller for the trajectories inside it, $d = b$ behavior itself like an attractor weak focus. See Figure 4.46.

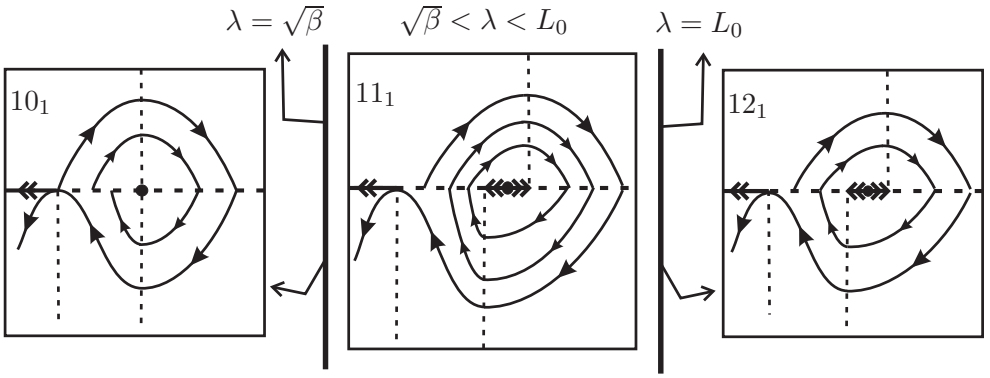

Figure 4.46: Cases 10_1, 11_1 and 12_1.

$\diamond$ *Case* 11_1. $\sqrt{\beta} < \lambda < L_0$*:* The meanning of L_0 will be given below in this case. The points of Σ outside the interval $(\sqrt{\beta}, \lambda)$ belong to Σ_1 and the points inside this interval belong to Σ_2. The graphic of H is like H-3 of Figure 4.41. We can prove that p_1, on the left of a, is a $\Sigma-$saddle and $p_2 \in (b, d)$ is a $\Sigma-$repeller. Moreover, the virtual pseudo equilibria r_1 and r_2 are on the right of d. When λ is a bit bigger than $\sqrt{\beta}$, the First Return Map η has two fixed points, i.e., Z has two canard cycles. One of them, called Γ_1, born from the bifurcation of the non hyperbolic canard cycle Γ of the previous case and the other one, called Γ_2, born from the bifurcation of the non generic tangential singularity presented in the previous case. Both of them are canard cycles of kind I. Moreover, Γ_1 is a hyperbolic repeller canard cycle and Γ_2 is a hyperbolic attractor canard cycle. Note that, as λ increases, Γ_1 becomes smaller and Γ_2 becomes bigger. When λ assumes the limit value L_0, one of them collides to the other. See Figure 4.46.

$\diamond$ *Case* 12_1. $\lambda = L_0$*:* The distribution of the connected components of Σ and the behavior of H are the same of Case 11_1. Since $\lambda = L_0$, as described in the previous case, there exists

a non hyperbolic canard cycle Γ of kind I which is an attractor for the trajectories inside it and is a repeller for the trajectories outside it. See Figure 4.46.

$\diamond$ *Case* 13_1. $L_0 < \lambda < 2\sqrt{\beta}$, *Case* 14_1. $\lambda = 2\sqrt{\beta}$, *Case* 15_1. $2\sqrt{\beta} < \lambda < 3\sqrt{\beta}$, *Case* 16_1. $\lambda = 3\sqrt{\beta}$ *and Case* 17_1. $\lambda > 3\sqrt{\beta}$*:* The distribution of the connected components of Σ and the behavior of H are the same of Case 11_1. Observe that canard cycles do not arise. See Figure 4.47.

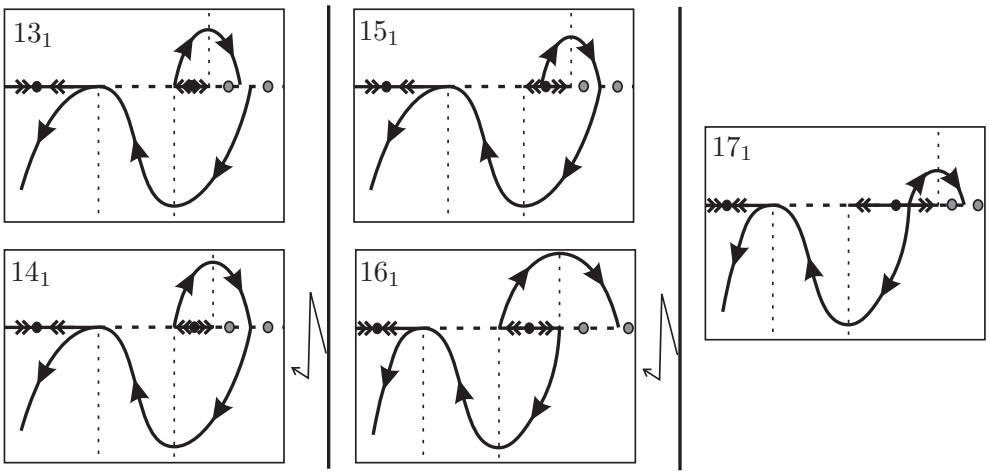

Figure 4.47: Cases $13_1 - 17_1$.

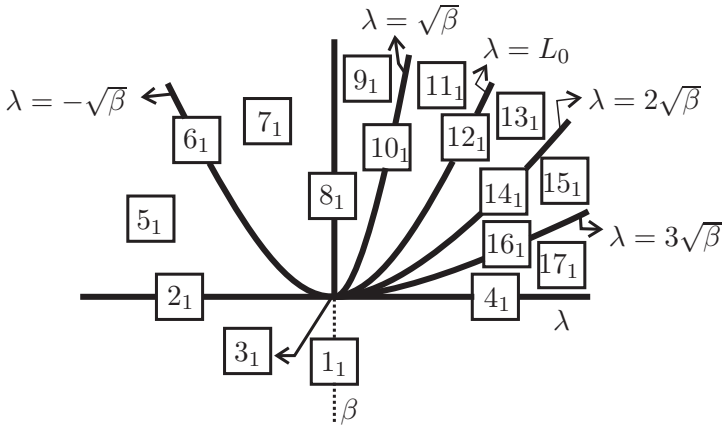

Figure 4.48: Bifurcation Diagram of Theorem 4.9.

The bifurcation diagram is illustrated in Figure 4.48. □

Remark 7. *In Cases* 9_1 *and* 13_1 *the ST−bifurcations (as described in [24]) arise. In fact, note that the trajectory passing through a, in Case* 9_1*, and passing through c, in Case* 13_1*, can make more and more turns around* p_2*. This fact characterizes a global bifurcation also reached in other cases as shown in this chapter.*

4.3.4 Proof of Theorem 4.10

Proof of Theorem 4.10. In Case 1_2 we assume that Y presents the behavior Y^-. In Cases 2_2, 3_2 and 4_2 we assume that Y presents the behavior Y^0. In Cases $5_2 - 19_2$ we assume that Y presents the behavior Y^+.

$\diamond$ *Case* 1_2. $\beta < 0$, *Case* 2_2. $\lambda < 0$, *Case* 3_2. $\lambda = 0$, *Case* 4_2. $\lambda > 0$. *Case* 5_2. $\lambda < -\sqrt{\beta}$. *Case* 6_2. $\lambda = -\sqrt{\beta}$. *Case* 7_2. $-\sqrt{\beta} < \lambda < 0$ *and Case* 8_2. $\lambda = 0$: By the choice of the bump function B, these cases are analogous to Cases 1_1, 2_1, 3_1, 4_1, 5_1, 6_1, 7_1 and 8_1.

Let $m \in (2\sqrt{\beta}, 4\sqrt{\beta})$ be the point such that $F_0(m) = 0$, where F_0 is obtained from the function F given by (4.15) taking $c = c_0 = -2\beta\sqrt{\beta}/2$. Since $0 < \mu < \mu_0$ we conclude that $m < 3\sqrt{\beta}$. Note that in Theorem 4.9 we have that $m = 3\sqrt{\beta}$. So it appears distinct topological behaviors.

$\diamond$ *Case* 9_2. $0 < \lambda < \sqrt{\beta} - dist(m, 3\sqrt{\beta})/2$: The analysis of this case is done in a similar way as the Case 9_1.

$\diamond$ *Case* 10_2. $\lambda = \sqrt{\beta} - dist(m, 3\sqrt{\beta})/2$: The points of Σ on the left of a belong to Σ_2 and the points on (d, b) belong to Σ_3. The points on (a, d) and on the right of b belong to Σ_1. The graphic of H is like H-3 of Figure 4.41. We can prove that p_1, on the left of a, is a $\Sigma-$saddle and $p_2 \in (d, b)$ is a $\Sigma-$attractor. Moreover, the virtual pseudo equilibria r_1 and r_2 are on the right of b. In this case the arc $\gamma_X(a)$ of X passing through a returns to Σ at the point c. So it appears a non hyperbolic canard cycle $\Gamma = \gamma_X(a) \cup \gamma_Y(c)$. Inside Γ the First Return Map $\eta : (a, \gamma_X^-(\gamma_Y^-(b))) \to (a, d)$ has derivative bigger than 1, where $\gamma_W^-(x)$ is an arc of the vector field W, oriented by negative time, that passes through x. See Figure 4.49.

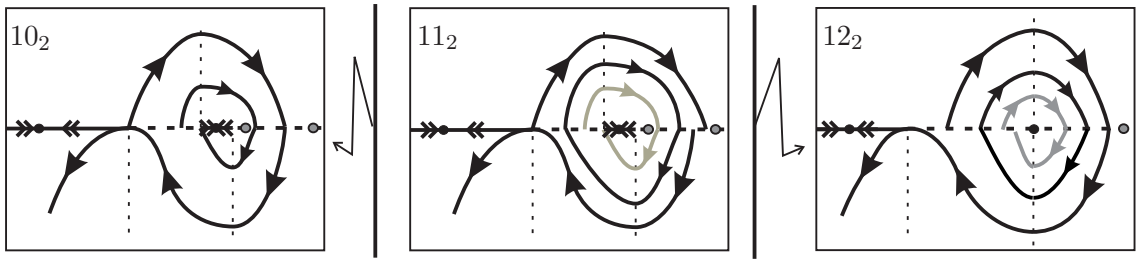

Figure 4.49: Cases $10_2 - 12_2$.

$\diamond$ *Case* 11_2. $\sqrt{\beta} - dist(m, 3\sqrt{\beta})/2 < \lambda < \sqrt{\beta}$: The configuration on Σ and the graphic of H are the same as Case 10_2. Since $\gamma_X^-(c) \in (a, d)$ there exists a point $Q \in (\gamma_X^-(c), \gamma_X^-(\gamma_Y^-(b)))$ such that $\eta'(Q) = 1$. So there exists a hyperbolic repeller canard cycle Γ, of kind I, passing through Q. Observe that Γ born from the bifurcation of the non hyperbolic canard cycle of the previous case. See Figure 4.49.

$\diamond$ *Case* 12_2. $\lambda = \sqrt{\beta}$: The points of Σ on the left of a belong to Σ_2 and the points on the right of a belong to Σ_1, except by the non generic tangential singularity $b = d$. The graphic of H is like H-2 of Figure 4.41. The canard cycle Γ present in the previous case is persistent for this case (remember that Γ born from the bifurcation of the non hyperbolic canard cycle

of Case 10_2. So, it radius do not tends to zero when λ tends to $\sqrt{\beta}$). So, the non generic tangential singularity $b = d$ behavior itself like a weak attractor focus. See Figure 4.49.

$\diamond$ *Case* 13_2. $\sqrt{\beta} < \lambda < M_0$ *and Case* 14_2. $\lambda = M_0$*:* Analogous to Cases 11_1 and 12_1, respectively, changing L_0 by M_0, where M_0 is the limit value for with Γ_1 collides to Γ_2.

$\diamond$ *Case* 15_2. $M_0 < \lambda < \sqrt{\beta} + dist(\sqrt{\beta}, m)/2$, *Case* 16_2. $\lambda = \sqrt{\beta} + dist(\sqrt{\beta}, m)/2$, *Case* 17_2. $\sqrt{\beta} + dist(\sqrt{\beta}, m)/2 < \lambda < m$, *Case* 18_2. $\lambda = m$ *and Case* 19_2. $\lambda > m$*:* The analysis of these cases is done in a similar way as Cases 13_1, 14_1, 15_1, 16_1 and 17_1.

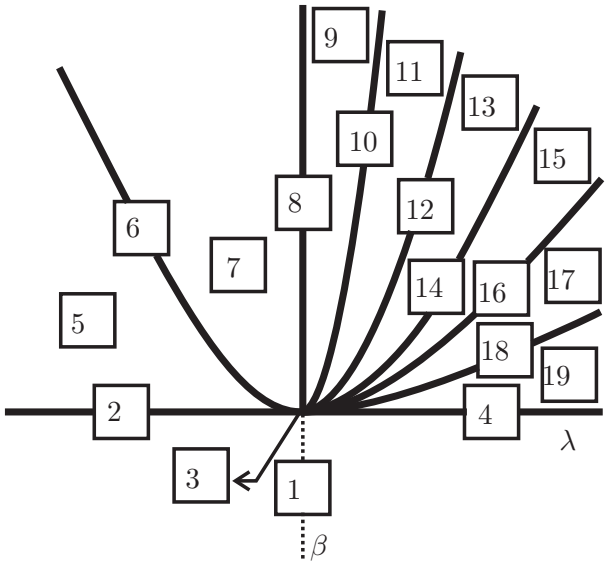

Figure 4.50: Bifurcation Diagram of Theorems 4.10 and 4.11.

The bifurcation diagram is illustrated in Figure 4.50. □

4.3.5 Proof of Theorem 4.11

Proof of Theorem 4.11. In Case 1_3 we assume that Y presents the behavior Y^-. In Cases 2_3, 3_3 and 4_3 we assume that Y presents the behavior Y^0. In Cases $5_3 - 19_3$ we assume that Y presents the behavior Y^+.

$\diamond$ *Case* 1_3. $\beta < 0$, *Case* 2_3. $\lambda < 0$, *Case* 3_3. $\lambda = 0$, *Case* 4_3. $\lambda > 0$, *Case* 5_3. $\lambda < -\sqrt{\beta}$, *Case* 6_3. $\lambda = -\sqrt{\beta}$, *Case* 7_3. $-\sqrt{\beta} < \lambda < 0$, *Case* 8_3. $\lambda = 0$ *and Case* 9_3. $0 < \lambda < \sqrt{\beta}$*:* By the choice of the bump function B, these cases are analogous to Cases 1_1, 2_1, 3_1, 4_1, 5_1, 6_1, 7_1, 8_1 and 9_1.

Let $m \in (2\sqrt{\beta}, 4\sqrt{\beta})$ be the point such that $F_0(m) = 0$, where F_0 is obtained from the function F given by (4.15) taking $c = c_0 = -2\beta\sqrt{\beta}/2$. Since $-\mu_0 < \mu < 0$ we conclude that $m > 3\sqrt{\beta}$. Note that in Theorem 4.9 we have that $m = 3\sqrt{\beta}$ and in Theorem 4.10 we have that $m < 3\sqrt{\beta}$. So it appears distinct topological behaviors.

$\diamond$ *Case* 10_3. $\lambda = \sqrt{\beta}$*:* The points of Σ on the left of a belong to Σ_2 and the points on the right of a belong to Σ_1, except by the non generic tangential singularity $b = d$. The graphic

of H is like H-2 of Figure 4.41. Observe that the First return Map has derivative bigger than 1 in the interval $(a, b = d) \subset \Sigma$. So, the non generic tangential singularity $b = d$ behavior itself like a weak attractor focus. See Figure 4.51.

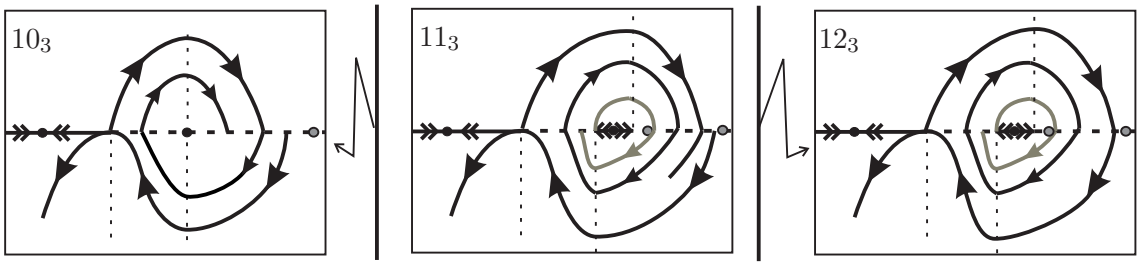

Figure 4.51: Cases $10_3 - 12_3$.

$\diamond$ *Case* 11_3. $\sqrt{\beta} < \lambda < \sqrt{\beta} + dist(m, 3\sqrt{\beta})/2$*:* The points of Σ on the left of a and on (b, d) belong to Σ_2. The points on (a, b) and on the right of d belong to Σ_1. The graphic of H is like H-3 of Figure 4.41. We can prove that p_1, on the left of a, is a $\Sigma-$saddle and $p_2 \in (b, d)$ is a $\Sigma-$repeller. Moreover, the virtual pseudo equilibria r_1 and r_2 are on the right of d. Since $\gamma_Y(\gamma_X(a)) \in (a, b)$ there exists a point $Q \in (\gamma_Y(\gamma_X(a)), \gamma_Y(d))$ such that $\eta'(Q) = 1$. So there exists a hyperbolic attractor canard cycle Γ, of kind I, passing through Q. This canard cycle born from the bifurcation of the attractor non generic tangential singularity present in the previous case. See Figure 4.51.

$\diamond$ *Case* 12_3. $\lambda = \sqrt{\beta} + dist(m, 3\sqrt{\beta})/2$*:* The configuration on Σ and the graphic of H are the same as Case 11_3. In this case the arc $\gamma_X(a)$ of X passing through a returns to Σ at the point c. So it appears a non hyperbolic canard cycle $\Gamma_1 = \gamma_X(a) \cup \gamma_Y(c)$. The canard cycle Γ present in the previous case is persistent for this case (remember that Γ born from the bifurcation of the non generic tangential singularity of Case 10_3. So, it radius do not tends to zero when λ tends to $\sqrt{\beta} + dist(m, 3\sqrt{\beta})/2)$. See Figure 4.51.

$\diamond$ *Case* 13_3. $\sqrt{\beta} + dist(m, 3\sqrt{\beta})/2 < \lambda < M_0$ *and Case* 14_3. $\lambda = M_0$*:* Analogous to Cases 13_2 and 14_2.

$\diamond$ *Case* 15_3. $M_0 < \lambda < \sqrt{\beta} + dist(\sqrt{\beta}, m)/2$*, Case* 16_3. $\lambda = \sqrt{\beta} + dist(\sqrt{\beta}, m)/2$*, Case* 17_3. $\sqrt{\beta} + dist(\sqrt{\beta}, m)/2 < \lambda < m$*, Case* 18_3. $\lambda = m$ *and Case* 19_3. $\lambda > m$*:* The analysis of these cases is done in a similar way as Cases 11_1, 12_1, 13_1, 14_1 and 15_1.

The bifurcation diagram is illustrated in Figure 4.50. □

4.3.6 Proof of Theorem 4.12

Proof of Theorem 4.12. Since in Equation (4.16) we can take $\mu \in (-\mu_0, \mu_0)$, from Theorems 4.9, 4.10 and 4.11 we derive that this equation, with $(\tau, \rho) = (ivb, k1)$ and $\alpha_2(k1) = -1$, unfolds generically the (Invisible) Fold−Cusp singularity.

Observe that the bifurcation diagram contain all 55 cases described in Theorems 4.9, 4.10 and 4.11. But some of them are $\Sigma-$equivalent and the number of distinct topological

behaviors is 23. Moreover, each topological behavior can be represented respectively by the Cases 1_1, 2_1, 3_1, 4_1, 5_1, 6_1 7_1, 8_1, 9_1, 10_1, 11_1, 12_1, 13_1, 14_1, 15_1, 16_1, 17_1, 10_2, 11_2, 12_2, 10_3, 11_3 and 12_3.

The full behavior of the three−parameter family of non−smooth vector fields expressed by Equation (4.16), with $(\tau, \rho) = (ivb, k1)$ and $\alpha_2(k1) = -1$, is illustrated in Figure 4.52 where we consider a sphere around the point $(\lambda, \beta, \mu) = (0, 0, 0)$ with a small ray and so we make a stereographic projection defined on the entire sphere, except the south pole. Still in relation to this figure, the numbers pictured correspond to the occurrence of the cases described in the previous theorems. As expected, the cases 3_1 and 3_2 are not represented in this figure because they are, respectively, the center and the south pole of the sphere. □

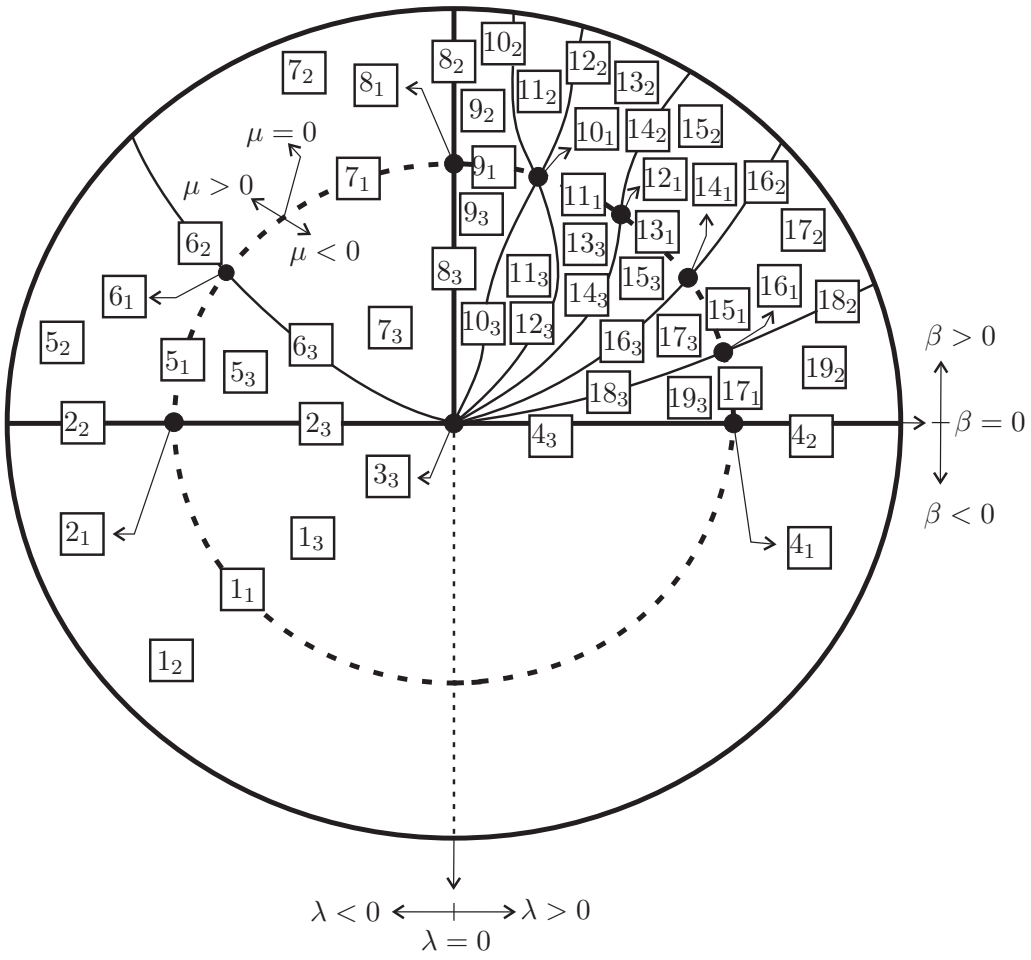

Figure 4.52: Bifurcation diagram of the (Invisible) Fold−Cusp singularity.

4.3.7 Proof of Theorem 4.13

When we consider (4.16), with $(\tau, \rho) = (vis, k2)$ and $\alpha_2(k2) = 1$, the function H, given by (1.1), is constant and equal to 1 independently of the value of μ. Moreover, distinct values

of the bump function B^{k2} do not produce any topological change in the bifurcation diagram of the singularity. In another words, two parameters are enough to describe the full behavior of this singularity. So, instead of (4.16) we will prefer to use (4.14), with $(\tau, \rho) = (vis, k2)$ and $\alpha_2(k2) = 1$ (remind that $\omega_2(\rho) = -1$ is fixed). Observe that, by Proposition 1.1, we have $\Sigma^f = \emptyset$ and it does not have virtual pseudo equilibria.

Proof of Theorem 4.13. Since X has an unique $\Sigma-$fold point which is visible we conclude that canard cycles are not allowed. In Case 1_B we assume that Y presents the behavior Y^-. In Cases 2_B, 3_B and 4_B we assume that Y presents the behavior Y^0. In Cases $5_B - 11_B$ we assume that Y presents the behavior Y^+.

$\diamond$ *Case* 1_B. $\beta < 0$*:* The points of Σ on the left of d belong to Σ_1 and the points on the right of d belong to Σ_2. See Figure 4.53.

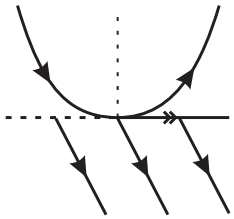

Figure 4.53: Case 1_B.

$\diamond$ *Case* 2_B. $\lambda < 0$*, Case* 3_B. $\lambda = 0$ *and Case* 4_B. $\lambda > 0$*:* The configuration of the connected components of Σ is the same as Case 1_B. Note that, when $\lambda < 0$ (Case 2_B), it appears a tangential singularity $P = (\lambda, 0) \in \Sigma_2$ but Z^Σ is always oriented from the left to the right. These cases are illustrated in Figure 4.54.

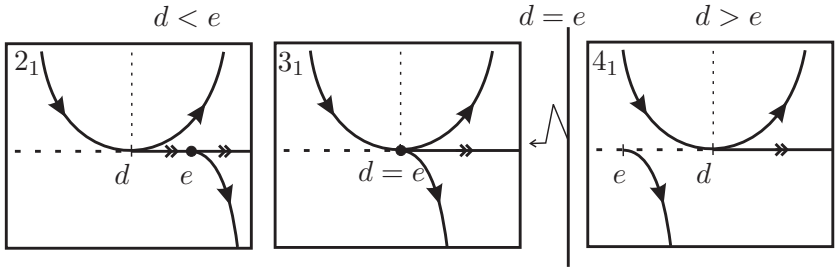

Figure 4.54: Cases $2_B - 4_B$.

$\diamond$ *Case* 5_B. $\lambda < -2\sqrt{\beta}$*, Case* 6_B. $\lambda = -2\sqrt{\beta}$ *and Case* 7_B. $-2\sqrt{\beta} < \lambda < -\sqrt{\beta}$*:* The points of Σ on the right of b and inside the interval (d, a) belong to Σ_2. The points on (a, b) and on the left of d belong to Σ_1. See Figure 4.55.

$\diamond$ *Case* 8_B. $\lambda = -\sqrt{\beta}$*:* The configuration of the connected components of Σ is like Case 5_B except that the interval (d, a) is degenerated. See Figure 4.56.

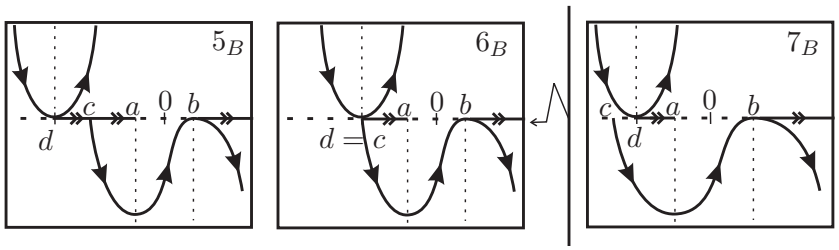

Figure 4.55: Cases $5_B - 7_B$.

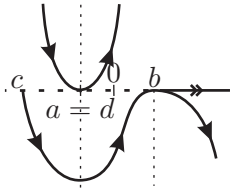

Figure 4.56: Case 8_B.

◇ *Case* 9_B. $-\sqrt{\beta} < \lambda < \sqrt{\beta}$*:* The points of Σ on the right side of b belong to Σ_2 and the points inside the interval (a, d) belong to Σ_3. The points on (d, b) and on the left of a belong to Σ_1. See Figure 4.57.

◇ *Case* 10_B. $\lambda = \sqrt{\beta}$*:* The configuration of the connected components of Σ is like Case 9_B except that the interval (d, b) is degenerated. See Figure 4.57.

◇ *Case* 11_B. $\lambda > \sqrt{\beta}$*:* The points of Σ on the right of d belong to Σ_2 and the points inside the interval (a, b) belong to Σ_3. The points on (b, d) and on the left of a belong to Σ_1. See Figure 4.57.

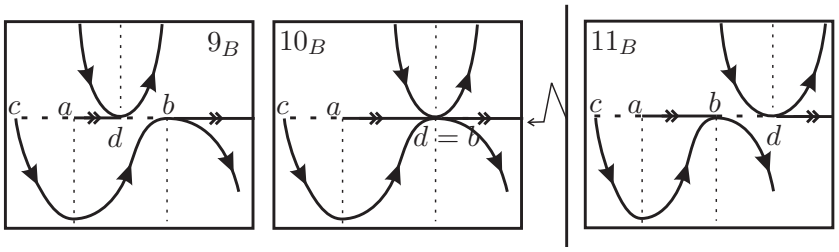

Figure 4.57: Cases $9_B - 11_B$.

Each topological behavior can be represented respectively by the Cases 1_B, 2_B, 3_B, 4_B, 5_B, 6_B, 7_B, 8_B, 9_B, 10_B and 11_B. The bifurcation diagram is illustrated in Figure 4.58. □

4.3.8 Conclusion

Observe that in [24] a codimension two Fold−Cusp singularity was studied. In that paper some constraints are considered in such a way that some topological behaviors do not appear

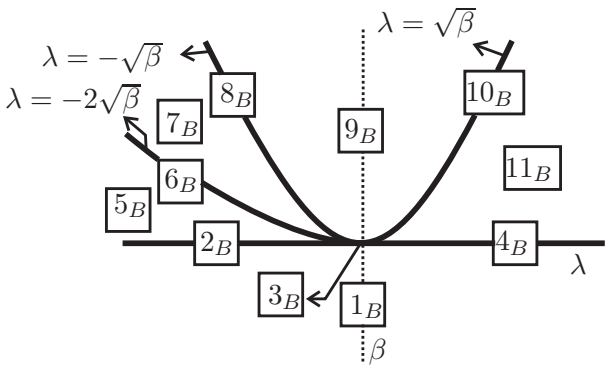

Figure 4.58: Bifurcation Diagram of Theorem 4.8.

in the bifurcation diagram. To break such constraints we introduce the bump function B^ρ. Now, with the variation of the parameter μ we obtain several scenarios, including those ones described in [24]. For example, around the case 10_1, in Figure 4.52, there exist cases without canard cycles, cases with canard cycles of kind I, cases with canard cycles of kind III, cases with a $\Sigma-$attractor or cases with a $\Sigma-$repeller. Most of these cases are not observed in [24]. However, as shown in Theorem 4.13, only two parameters are enough to describe a Fold$-$Cusp singularity when $(\tau, \rho) = (vis, k2)$. Using other choices of τ, ρ and $\omega_2(\rho)$ we can produce more cases of Fold$-$Cusp singularities. But our approach, established in Theorem 4.12 and in Theorem 4.13, is sufficient to characterize all these singularities.

Chapter

5

Averaging Method and the Number of Periodic Limit Sets

Piecewise linear differential systems appear in a natural way in control theory, and in the study of electrical circuits. These systems can present complicated dynamical phenomena such as those exhibited by general nonlinear differential systems. One of the main ingredients in the qualitative description of the dynamical behavior of a differential system is the number and the distribution of its limit cycles.

In this chapter we describe the *Averaging Method* and we apply this method in order to find the number of limit periodic sets of some piecewise linear differential systems. In what follows, limit periodic sets will means limit cycles or canard cycles in the terms of the previous definitions.

In [28] the authors studied the bifurcation of limit cycles from a two−dimensional center inside $\mathbb{R}^n$. In this case they proved that the maximum number of limit cycles that can bifurcate from the periodic orbits of the linear differential center is 1, up to first−order expansion of the displacement function of the perturbed system with respect to the small parameter ε.

The main result of [6] states that for $n = 4$ at most three limit cycles of the piecewise linear differential system (5.4) bifurcate from the periodic orbits of system (5.6), up to first−order expansion of the displacement function of (5.4) with respect to the small parameter ε. Moreover, this upper bound is reached.

We study the bifurcation of limit cycles from the periodic orbits of 2−dimensional, 4−dimensional or n−dimensional (with n even) linear centers in $\mathbb{R}^n$ perturbed inside a class of

discontinuous piecewise linear differential systems. Our main results shows that at most 1 (respectively 3) limit cycle can bifurcate up to first−order expansion of the displacement function with respect to the small parameter in the case of the 2−dimensional (respectively 4−dimensional) linear center. This upper bound is reached. For a linear center $n-$dimensional at most $(4n-6)^{n/2-1}$ limit cycles can bifurcate up to first−order expansion of the displacement function with respect to the small parameter. For proving these results we use the averaging theory in a form where the differentiability of the system is not needed.

The goal of this chapter is to study the existence of limit cycles of the control system of the form

$$\dot{x} = A_0 x + \varepsilon F(x), \tag{5.1}$$

with $|\varepsilon| \neq 0$ a sufficiently small real parameter, where A_0 is equal to

$$A_0^1 = \begin{pmatrix} 0 & -1 & 0 & \dots & 0 \\ 1 & 0 & 0 & \dots & 0 \\ 0 & 0 & 0 & \dots & 0 \\ \vdots & \vdots & \vdots & \ddots & \vdots \\ 0 & 0 & 0 & \dots & 0 \end{pmatrix}, A_0^2 = \begin{pmatrix} 0 & -1 & 0 & 0 & 0 & \dots & 0 \\ 1 & 0 & 0 & 0 & 0 & \dots & 0 \\ 0 & 0 & 0 & -1 & 0 & \dots & 0 \\ 0 & 0 & 1 & 0 & 0 & \dots & 0 \\ 0 & 0 & 0 & 0 & 0 & \dots & 0 \\ \vdots & \vdots & \vdots & \vdots & \vdots & \ddots & \vdots \\ 0 & 0 & 0 & 0 & 0 & \dots & 0 \end{pmatrix}, \text{ or}$$

$$A_0^3 = \begin{pmatrix} 0 & -1 & 0 & 0 & \dots & 0 & 0 \\ 1 & 0 & 0 & 0 & \dots & 0 & 0 \\ 0 & 0 & 0 & -1 & \dots & 0 & 0 \\ 0 & 0 & 1 & 0 & \dots & 0 & 0 \\ \vdots & \vdots & \vdots & \vdots & \ddots & \vdots & \vdots \\ 0 & 0 & 0 & 0 & \dots & 0 & -1 \\ 0 & 0 & 0 & 0 & \dots & 1 & 0 \end{pmatrix}.$$

For $A_0 = A_0^1$ or $A_0 = A_0^2$, the function $F : \mathbb{R}^n \longrightarrow \mathbb{R}^n$ is given by $F(x) = Ax + \varphi_0(k^T x)b$ and for $A_0 = A_0^3$, the function F is given by $F(x) = Ax + \varphi(k^T x)b$, with $A \in \mathcal{M}_n(\mathbb{R})$, $k, b \in \mathbb{R}^n \backslash \{0\}$ in any case. Moreover, $\varphi_0 : \mathbb{R} \longrightarrow \mathbb{R}$ is the discontinuous function

$$\varphi_0(x_1) = \begin{cases} -1 & \text{if } x_1 \in (-\infty, 0), \\ 1 & \text{if } x_1 \in (0, \infty), \end{cases} \tag{5.2}$$

and $\varphi : \mathbb{R} \longrightarrow \mathbb{R}$ is the piecewise linear function

$$\varphi(x_1) = \begin{cases} -1 & \text{if } x_1 \in (-\infty, -1), \\ x_1 & \text{if } x_1 \in [-1, 1], \\ 1 & \text{if } x_1 \in (1, \infty), \end{cases} \tag{5.3}$$

where $x = (x_1, \dots, x_n)^T$. The independent variable is denoted by t, vectors of $\mathbb{R}^n$ are column vectors, and k^T denotes a transposed vector.

For $A_0 = A_0^1$ or $A_0 = A_0^2$, first we will study the problem

$$\dot{x} = A_0 x + \varepsilon F_\alpha(x), \tag{5.4}$$

where F_α is equal to F replacing φ_0 by the piecewise linear function $\varphi_\alpha : \mathbb{R} \longrightarrow \mathbb{R}$ given by

$$\varphi_\alpha(x_1) = \begin{cases} -1 & \text{if } x_1 \in (-\infty, -\alpha), \\ \dfrac{x_1}{\alpha} & \text{if } x_1 \in [-\alpha, \alpha], \\ 1 & \text{if } x_1 \in (\alpha, \infty), \end{cases} \tag{5.5}$$

where $\alpha > 0$, and after we will tend α to 0. The graphics of φ_0 and φ_α are illustrated in Figures 5.1 and 5.2, respectively.

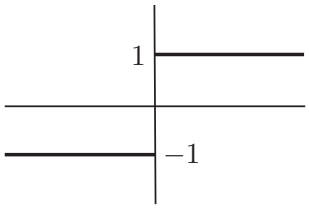

Figure 5.1: Graphic of φ_0.

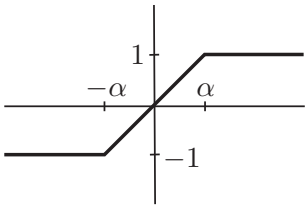

Figure 5.2: Graphic of φ_α.

For $\varepsilon = 0$ and $A_0 = A_0^1$, system (5.4) becomes

$$\dot{x}_1 = -x_2,\ \dot{x}_2 = x_1,\ \dot{x}_i = 0 \text{ for } i = 3, \ldots, n, \tag{5.6}$$

for $\varepsilon = 0$ and $A_0 = A_0^2$, system (5.4) becomes

$$\dot{x}_1 = -x_2,\ \dot{x}_2 = x_1,\ \dot{x}_3 = -x_4,\ \dot{x}_4 = x_3,\ \dot{x}_i = 0 \text{ for } i = 5, \ldots, n \tag{5.7}$$

and for $\varepsilon = 0$ and $A_0 = A_0^3$, system (5.1) becomes

$$\dot{x}_1 = -x_2, \quad \dot{x}_2 = x_1, \quad \ldots \quad , \dot{x}_{n-1} = -x_n, \quad \dot{x}_n = x_{n-1}. \tag{5.8}$$

We note that the origin of every plane $x_k = \text{constant}$ for $k = 3, \ldots, n$ in the first case, of every hyperplane $k = 5, \ldots, n$ in the second case, and of $\mathbb{R}^n$ in the third case is a *global isochronous center* of (5.6), (5.7) and (5.8), respectively, i.e. all the orbits contained in such a plane, hyperplane or $\mathbb{R}^n$ distinct from the origin are periodic with the same period 2π.

A *limit cycle* of a differential system is an isolated periodic orbit in the set of all periodic orbits of the system. The *Poincaré map* (or equivalently, the *displacement map*) is a suitable tool for studying limit cycles of autonomous systems (detailed explanations can be found in [17] or [23]; see also section 5.1). We recall that a limit cycle of a system corresponds to an isolated zero of the displacement function.

The main results of this chapter are the following.

Theorem 5.1. *Consider $A_0 = A_0^1$. For $n \geq 2$ at most one limit cycle of the piecewise linear differential system* (5.4) *bifurcates from the periodic orbits of system* (5.6)*, up to first−order*

expansion of the displacement function of (5.4) *with respect to the small parameter* ε. *Moreover there are systems* (5.4) *having exactly one limit cycle bifurcating from a circle centered at the origin of the plane* $x_3 = \ldots = x_n = 0$.

Corollary 5.1. *Consider* $A_0 = A_0^1$. *For* $n \geq 2$ *at most one limit cycle of the discontinuous piecewise linear differential system* (5.1) *bifurcates from the periodic orbits of system* (5.6), *up to first−order expansion of the displacement function of* (5.1) *with respect to the small parameter* ε. *Moreover there are systems* (5.1) *having exactly one limit cycle.*

Theorem 5.2. *Consider* $A_0 = A_0^2$. *For* $n \geq 4$ *at most three limit cycles of the piecewise linear differential system* (5.4) *bifurcate from the periodic orbits of system* (5.7), *up to first−order expansion of the displacement function of* (5.4) *with respect to the small parameter* ε. *Moreover there are systems* (5.4) *having exactly three limit cycles bifurcating from circles centered at the origin of the plane* $x_5 = \ldots = x_n = 0$.

Corollary 5.2. *Consider* $A_0 = A_0^2$. *For* $n \geq 4$ *at most three limit cycles of the discontinuous piecewise linear differential system* (5.1) *bifurcates from the periodic orbits of system* (5.7), *up to first−order expansion of the displacement function of* (5.1) *with respect to the small parameter* ε. *Moreover there are systems* (5.1) *having exactly three limit cycles.*

Theorem 5.3. *Consider* $A_0 = A_0^3$. *For all* $n \geq 6$ *even and from each periodic orbit of the differential system* (5.8), *which corresponds to a simple zero in* D_m *of the function* $h = (h_1, \ldots, h_{n-1})$ *given in* (5.44), *at most* $(4n-6)^{n/2-1}$ *branches of limit cycles bifurcate for the differential system* (5.1), *up to first−order expansion of the displacement function of* (5.1) *with respect to the small parameter* ε.

Theorems 5.1 and 5.2 are extensions of the main results of [28] and [6] respectively, where is done the case $\alpha = 1$.

We emphasize that the bifurcation from $\varepsilon = 0$ to $\varepsilon \neq 0$ in Theorems 5.1, 5.2 and 5.3 takes place for $\varepsilon > 0$ and for $\varepsilon < 0$ sufficiently small, i.e. on both sides of the value $\varepsilon = 0$. We remark that in a Hopf bifurcation the limit cycle only appears on one side of the bifurcation value of the parameter, but in our case in which the limit cycles bifurcate from periodic orbits of the period annulus of a center they appear on both sides of the parameter.

If we consider $n \geq 6$ it is very difficult to obtain the exact number of limit cycles of system (5.1) that bifurcate from the periodic orbits of system (5.8). The jump for the case $n = 6$ offers already a much larger mathematical difficulty than for instance in the case $n = 4$. So for $n \geq 6$ everything that we can do is to give an upper bound of the number of limit cycles that can bifurcate.

The proofs of Theorems 5.1, 5.2 and 5.3 are based on the first−order averaging method. We will present this method in Section 5.1, in the form obtained in [5]. The advantage of this result is that the smoothness assumptions for the vector field of the differential system are minimal. In particular, it can be applied to piecewise linear differential systems, which are not C^2 (not even C^1), as required in its classical version, see for instance, Theorem 11.5

of [42]. This non−differential application of the averaging method to control systems was used for the first time in [6]. This method has been used frequently for computing periodic orbits; see for instance [11]. From the paper [7] we can study the stability of the limit cycles of Theorems 5.1, 5.2 and 5.3; for more details see remarks 11, 12 and 13.

The proofs of Theorems 5.1, 5.2 and 5.3 will be the subject of Sections 5.2, 5.3 and 5.4 respectively. The first step in the study of system (5.1), Lemmas 5.1, 5.4 and 5.12, is to reduce the number of parameters by a linear change of variables. The next objective is to transform the system into one which is in the standard form for applying the averaging theory. This is accomplished in Lemmas 5.2, 5.5 and 5.13 through a change of variables related on the first integrals of systems (5.6), (5.7) and (5.8). The computation of the averaged function (see equation (5.10)) will be also a special task. After that we must determine the number of its isolated zeros. The relation between the averaging method and the displacement function will be also discussed.

Reference [25] can be seen for a theoretical discussion about suitable transformations of high dimensional differential systems which are small perturbations of a center, into the standard form for averaging. The general idea is to relate this change of variables with the first integral of the unperturbed center.

We would like to add some comments related to our approach to the problem of counting the limit cycles of piecewise linear differential systems. We have chosen here to study bifurcation with respect to a small parameter from the periodic orbits of a center, up to first−order expansion of the displacement map. For some values of the coefficients, this order is sufficient for finding the exact number of limit cycles. But in some cases the first−order expansion of the displacement map can be identically zero, then a higher order averaging theory is needed. The study can be done by using second−, third−, ... order averaging theory. A key point in these studies is the relation between the averaging theory and the displacement map due to the fact that the displacement map of a piecewise linear differential system is analytic in a neighborhood of a limit cycle.

5.1 First−Order Averaging Method

The aim of this section is to present the first−order averaging method as obtained in [5]. Differentiability of the vector field is not needed. The specific conditions for the existence of a simple isolated zero of the averaged function are given in terms of the Brouwer degree. In fact, the Brouwer degree theory is the key point in the proof of this theorem. We remind here that continuity of some finite dimensional function is a sufficient condition for the existence of its Brouwer degree (see [30] for precise definitions).

Theorem 5.4. *We consider the following differential system*

$$\dot{x}(t) = \varepsilon H(t,x) + \varepsilon^2 R(t,x,\varepsilon), \tag{5.9}$$

where $H : \mathbb{R} \times D \longrightarrow \mathbb{R}^n$, $R : \mathbb{R} \times D \times (-\varepsilon_f, \varepsilon_f) \longrightarrow \mathbb{R}^n$ are continuous functions, $T-$periodic in the first variable, and D is an open subset of $\mathbb{R}^n$. We define $h : D \longrightarrow \mathbb{R}^n$ as

$$h(z) = \int_0^T H(s, z)ds, \tag{5.10}$$

and assume that:

(i) H and R are locally Lipschitz with respect to x;

(ii) for $a \in D$ with $h(a) = 0$, there exists a neighborhood V of a such that $h(z) \neq 0$ for all $z \in \overline{V} \backslash \{a\}$ and $d_B(h, V, 0) \neq 0$ (here $d_B(h, V, 0)$ denote the Brouwer degree of h at 0).

Then, for $|\varepsilon| > 0$ sufficiently small, there exists an isolated $T-$periodic solution $\psi(., \varepsilon)$ of system (5.9) such that $\psi(0, \varepsilon) \to a$ as $\varepsilon \to 0$.

Here we will need some facts from the proof of Theorem 5.4. Hypothesis (i) assures the existence and uniqueness of the solution of each initial value problem on the interval $[0, T]$. Hence, for each $z \in D$, it is possible to denote by $x(., z, \varepsilon)$ the solution of (5.9) with the initial value $x(0, z, \varepsilon) = z$. We consider also the displacement function $\zeta : D \times (-\varepsilon_f, \varepsilon_f) \longrightarrow \mathbb{R}^n$ defined by

$$\zeta(z, \varepsilon) = \int_0^T [\varepsilon H(t, x(t, z, \varepsilon)) + \varepsilon^2 R(t, x(t, z, \varepsilon), \varepsilon)]dt. \tag{5.11}$$

From the proof of Theorem 5.4 we extract the following facts.

Remark 8. *For every $z \in D$ the following relation holds*

$$x(T, z, \varepsilon) - x(0, z, \varepsilon) = \zeta(z, \varepsilon).$$

The function ζ can be written in the form

$$\zeta(z, \varepsilon) = \varepsilon h(z) + \varepsilon^2 O(1),$$

where h is given by (5.10) and the symbol $O(1)$ denotes a bounded function on every compact subset of $D \times (-\varepsilon_f, \varepsilon_f)$. Moreover, for $|\varepsilon|$ sufficiently small, $z = \psi(0, \varepsilon)$ is an isolated zero of $\zeta(., \varepsilon)$.

Note that from Remark 8 it follows that a zero z of the *displacement function* $\zeta(z, \varepsilon)$ at time T provides initial conditions for a periodic orbit of the system of period T. We also remark that $h(z)$ is the displacement function up to terms of order ε. Consequently the zeros of $h(z)$, when $h(z)$ is not identically zero, also provides periodic orbits of period T.

Let $f : D \longrightarrow \mathbb{R}^n$ be a C^1 function, with $f(a) = 0$, where D is an open subset of $\mathbb{R}^n$ and $a \in D$. The point a is a *simple zero* of f if the Jacobian $J_f(a)$ of f at a is not zero.

For a given systems there is the possibility that the function ζ is not globally differentiable, but the function h is C^1 when $z > \alpha$, as we shall see in Sections 5.2, 5.3 and 5.4. In fact, only differentiability in some neighborhood of a fixed isolated zero of h could be enough. When this is the case, one can use the following remark in order to verify the hypothesis (ii) of Theorem 5.4.

Remark 9. *Let $h : D \longrightarrow \mathbb{R}^n$ be a C^1 function, with $h(a) = 0$, where D is an open subset of $\mathbb{R}^n$ and $a \in D$. Whenever a is a simple zero of h, then there exists a neighborhood V of a such that $h(z) \neq 0$ for all $z \in \overline{V}\backslash\{a\}$ and $d_B(h, V, 0) \in \{-1, 1\}$.*

5.2 Proof of Theorem 5.1

In this section we assume that $A_0 = A_0^1$. The next lemma shows that through a linear change of variables, it is possible to reduce the number of parameters of system (5.4).

Lemma 5.1. *Assume that $k_1^2 + k_2^2 \neq 0$ if $n = 2$, and $(k_1^2 + k_2^2)k_3 \neq 0$ if $n > 2$. Then by a linear change of variables system (5.4) can be transformed into the system*

$$\dot{x} = A_1 x + \varepsilon \overline{A} x + \varepsilon \varphi_\alpha(x_1)\overline{b}, \tag{5.12}$$

where $\overline{A} \in M_n(\mathbb{R})$ and $\overline{b} \in \mathbb{R}^n$ are convenient functions of A and b. Moreover

$$A_1 = \begin{pmatrix} 0 & -1 \\ 1 & 0 \end{pmatrix}$$

if $n = 2$, and

$$A_1 = \begin{pmatrix} 0 & -1 & \varepsilon & 0 & \dots & 0 \\ 1 & 0 & \varepsilon & 0 & \dots & 0 \\ 0 & 0 & 0 & 0 & \dots & 0 \\ \vdots & \vdots & \vdots & \vdots & \ddots & \vdots \\ 0 & 0 & 0 & 0 & \dots & 0 \end{pmatrix}$$

if $n > 2$.

For a proof see Lemma 1 of [28].

A system equivalent to system (5.12), which will be in the standard form for applying the averaging theory, will be obtained in the next lemma by a proper change of the variables.

Lemma 5.2. *Changing the variables $(x_1, x_2, x_3, \dots, x_n)$ to $(\theta, r, x_3, \dots, x_n)$ by using $x_1 = r\cos\theta$ and $x_2 = r\operatorname{sen}\theta$, system (5.12) is transformed into a system of the form*

$$\begin{aligned} \frac{dr}{d\theta} &= \varepsilon H_1(\theta, r, x_3, \dots, x_n) + O(\varepsilon^2), \\ \frac{dx_j}{d\theta} &= \varepsilon H_{j-1}(\theta, r, x_3, \dots, x_n) + O(\varepsilon^2), \end{aligned} \tag{5.13}$$

for $j = 3, \dots, n$ where

$$H_1 = \cos\theta F_1 + \operatorname{sen}\theta F_2,$$

$$H_j = a_{j1} r\cos\theta + a_{j2} r\operatorname{sen}\theta + b_j \varphi_\alpha(r\cos\theta) + \sum_{k=3}^{n} a_{jk} x_k,$$

and for $i = 1, 2$ we have that $F_i = a_{i1} r\cos\theta + a_{i2} r\operatorname{sen}\theta + \varphi_\alpha(r\cos\theta)b_i + \sum_{k=3}^{n} a_{ik}x_k$. We take ε_0 sufficiently small, m arbitrarily large and $D_m = (1/m, m)$. Then the vector field of system

(5.13) *is well defined and continuous on* $\mathbb{R} \times D_m \times \mathbb{R}^{n-2} \times (-\varepsilon_0, \varepsilon_0)$. *Moreover this system is* $2\pi-$*periodic with respect to the variable* θ *and locally Lipschitz with respect to the variable* $(r, x_3, \ldots, x_n)$.

Proof. System (5.12) in the variables (θ, r) becomes

$$\begin{aligned}
\dot{r} &= \varepsilon H_1(\theta, r, x_3, \ldots, x_n), \\
\dot{\theta} &= 1 + \frac{\varepsilon}{r}(\cos\theta F_2 - \operatorname{sen}\theta F_1), \\
\dot{x}_j &= \varepsilon H_{j-1}(\theta, r, x_3, \ldots, x_n) \quad \text{for } j = 3, \ldots, n.
\end{aligned}$$

We note that for $|\varepsilon|$ sufficiently small $\dot{\theta}(t) > 0$ for each t when $(\theta, r, x_3, \ldots, x_n) \in \mathbb{R} \times D_m \times \mathbb{R}^{n-2}$. Now we eliminate the variable t in the above system by considering θ as the new independent variable. It is easy to see that the right$-$hand side of the new system, for every fixed α, is well defined and continuous on $\mathbb{R} \times D_m \times \mathbb{R}^{n-2} \times (-\varepsilon_0, \varepsilon_0)$, it is $2\pi-$periodic with respect to the independent variable θ and locally Lipschitz with respect to $(r, x_3, \ldots, x_n)$. Form (5.13) is obtained after an expansion with respect to the small parameter ε. □

Here $\overline{A} = (a_{ij})$ if $n = 2$, and if $n > 2$ then a_{ij} is the element of the row i and column j of the $n \times n$ matrix

$$\overline{A} + \begin{pmatrix} 0 & 0 & 1 & 0 & \ldots & 0 \\ 0 & 0 & 1 & 0 & \ldots & 0 \\ 0 & 0 & 0 & 0 & \ldots & 0 \\ \vdots & \vdots & \vdots & \vdots & \ddots & \vdots \\ 0 & 0 & 0 & 0 & \ldots & 0 \end{pmatrix}.$$

Our next step is to find the corresponding function (5.10), so we must compute

$$h_j(r, x_3, \ldots, x_n) = \int_0^{2\pi} H_j(\theta, r, x_3, \ldots, x_n) d\theta, \tag{5.14}$$

for $j = 1, \ldots, n-1$.

In order to calculate the expression of h, we will use the following formulas

$$\int_0^{2\pi} \cos^2\theta d\theta = \pi, \quad \int_0^{2\pi} \operatorname{sen}^2\theta d\theta = \pi, \quad \int_0^{2\pi} \cos(\theta+s)\operatorname{sen}(\theta+s) d\theta = 0,$$

$$\int_0^{2\pi} \cos\theta\cos(\theta+s) d\theta = \pi\cos s, \quad \int_0^{2\pi} \cos\theta\operatorname{sen}(\theta+s) d\theta = \pi\operatorname{sen} s,$$

$$\int_0^{2\pi} \operatorname{sen}\theta\cos(\theta+s) d\theta = -\pi\operatorname{sen} s, \quad \int_0^{2\pi} \operatorname{sen}\theta\operatorname{sen}(\theta+s) d\theta = \pi\cos s,$$

$$\int_0^{2\pi} \cos^2(\theta+s) d\theta = \pi, \quad \int_0^{2\pi} \operatorname{sen}^2(\theta+s) d\theta = \pi, \quad \int_0^{2\pi} \cos\theta\operatorname{sen}\theta d\theta = 0.$$

For each $r > 0$ we define

$$\begin{aligned} I_0(r) &= \int_0^{2\pi} \varphi_\alpha(r\cos\theta)d\theta, \\ I_1(r) &= \int_0^{2\pi} \varphi_\alpha(r\cos\theta)\cos\theta d\theta, \\ I_2(r) &= \int_0^{2\pi} \varphi_\alpha(r\cos\theta)\operatorname{sen}\theta d\theta, \end{aligned}$$

where φ_α is the piecewise linear function given by (5.5).

Lemma 5.3. *The integrals I_0, I_1 and I_2 satisfy $I_0(r) = I_2(r) = 0$ for all $r > 0$, and*

$$I_1(r) = \begin{cases} \dfrac{\pi r}{\alpha} & \text{if } r \le \alpha, \\ \dfrac{\pi r}{\alpha} + \dfrac{2}{r}\sqrt{r^2-\alpha^2} - 2r\arctan\Big(\dfrac{\sqrt{r^2-\alpha^2}}{\alpha}\Big) & \text{if } r > \alpha. \end{cases} \tag{5.15}$$

Proof. Whenever $0 < r \le \alpha$ we have that $|r\cos\theta| \le \alpha$ and $|r\operatorname{sen}\theta| \le \alpha$ for all $\theta \in [0, 2\pi)$. Then $\varphi_\alpha(r\cos\theta) = (r\cos\theta)/\alpha$ for every θ. Thus

$$\begin{aligned} I_0(r) &= \frac{r}{\alpha}\int_0^{2\pi} \cos\theta d\theta &&= 0, \\ I_1(r) &= \frac{r}{\alpha}\int_0^{2\pi} \cos^2\theta d\theta &&= \frac{\pi r}{\alpha}, \\ I_2(r) &= \frac{r}{\alpha}\int_0^{2\pi} \operatorname{sen}\theta\cos\theta d\theta &&= 0. \end{aligned}$$

We fix now $r > \alpha$ and consider $\theta_c \in (0, \pi/2)$ such that $\cos\theta_c = \alpha/r$. Then we can write

$$\begin{aligned} I_0(r) &= \int_0^{\theta_c} d\theta + \frac{r}{\alpha}\int_{\theta_c}^{\pi-\theta_c} \cos\theta d\theta - \int_{\pi-\theta_c}^{\pi+\theta_c} d\theta + \\ &\quad \frac{r}{\alpha}\int_{\pi+\theta_c}^{2\pi-\theta_c} \cos\theta d\theta + \int_{2\pi-\theta_c}^{2\pi} d\theta, \\ I_1(r) &= \int_0^{\theta_c} \cos\theta d\theta + \frac{r}{\alpha}\int_{\theta_c}^{\pi-\theta_c} \cos^2\theta d\theta - \int_{\pi-\theta_c}^{\pi+\theta_c} \cos\theta d\theta + \\ &\quad \frac{r}{\alpha}\int_{\pi+\theta_c}^{2\pi-\theta_c} \cos^2\theta d\theta + \int_{2\pi-\theta_c}^{2\pi} \cos\theta d\theta, \\ I_2(r) &= \int_0^{\theta_c} \operatorname{sen}\theta d\theta + \frac{r}{\alpha}\int_{\theta_c}^{\pi-\theta_c} \operatorname{sen}\theta\cos\theta d\theta - \int_{\pi-\theta_c}^{\pi+\theta_c} \operatorname{sen}\theta d\theta + \\ &\quad \frac{r}{\alpha}\int_{\pi+\theta_c}^{2\pi-\theta_c} \operatorname{sen}\theta\cos\theta d\theta + \int_{2\pi-\theta_c}^{2\pi} \operatorname{sen}\theta d\theta. \end{aligned}$$

Straightforward computations lead to the following expressions:

$$\begin{aligned} I_0(r) &= 0, \\ I_1(r) &= \frac{\pi r}{\alpha} + \frac{2}{r}\sqrt{r^2-\alpha^2} - 2r\arctan\Big(\frac{\sqrt{r^2-\alpha^2}}{\alpha}\Big), \\ I_2(r) &= 0, \end{aligned}$$

where we use that $\operatorname{sen}\theta_c = \sqrt{r^2-\alpha^2}/r$ and $\theta_c = \arctan(\sqrt{r^2-\alpha^2}/\alpha)$. □

In short, from (5.47) we get that

$$\begin{aligned} h_1(r, x_3, \ldots, x_n) &= \pi r a_{11} + b_1 I_1(r) + \pi r a_{22}, \\ h_{j-1}(r, x_3, \ldots, x_n) &= 2\pi(a_{j3}x_3 + \ldots + a_{jn}x_n), \end{aligned} \tag{5.16}$$

for $j = 3, \ldots, n$.

Proposition 5.1. *Suppose that*

(i) the determinant of the minor of the matrix $\overline{A} = (a_{ij})$ erasing the first two rows and the first two columns is not zero (of course this condition is only required if $n > 2$), and

(ii) $\dfrac{(a_{11} + a_{22} + (b_1/\alpha))}{b_1} \in (K_\alpha, 1)$, *where* $K_\alpha = 0$ *when* $M_\alpha = \max\left\{\alpha, \alpha\sqrt{\dfrac{2}{1+\alpha}}\right\}$ *is* α, *or* $K_\alpha = \dfrac{2}{\pi}\arctan\left(\sqrt{\dfrac{1-\alpha}{1+\alpha}}\right)$ *when* $M_\alpha = \alpha\sqrt{\dfrac{2}{1+\alpha}}$.

Then system (5.12) for $|\varepsilon| \neq 0$ sufficiently small has exactly one limit cycle bifurcating from the circle of radius $\overline{r}_\alpha$ centered at the origin of the plane $x_3 = \ldots = x_n = 0$, where $\overline{r}_\alpha$ is the unique solution in the interval (M_α, ∞) of the equation

$$\arctan\left(\frac{\sqrt{r^2-\alpha^2}}{\alpha}\right) - \frac{\sqrt{r^2-\alpha^2}}{r^2} = \frac{\pi(a_{11} + a_{22} + (b_1/\alpha))}{2b_1}.$$

Proof. In order to have that the system $h_i(r, x_3, \ldots, x_n) = 0$ for $i = 1, \ldots, n-1$ has isolated solutions − otherwise the Jacobian on them becomes zero and we cannot apply Theorem 5.4 for studying the limit cycles of system (5.12) for $|\varepsilon| \neq 0$ sufficiently small − it is required for $n > 2$ that the determinant of the matrix B obtained from the minor of the matrix $\overline{A}$ by erasing the first two rows and the first two columns is not zero. Then from the equations $h_i(r, x_3, \ldots, x_n) = 0$ for $i = 2, \ldots, n-1$ we get that $x_3 = \ldots = x_n = 0$. For $r > \alpha$, from equation $h_1(r, x_3, \ldots, x_n) = 0$ we obtain

$$f_\alpha(r) = \arctan\left(\frac{\sqrt{r^2-\alpha^2}}{\alpha}\right) - \frac{\sqrt{r^2-\alpha^2}}{r^2} = \frac{\pi(a_{11} + a_{22} + (b_1/\alpha))}{2b_1}.$$

Note that with the previous hypotheses,

$$\det\left(\frac{\partial(h_1, \ldots, h_{n-1})}{\partial(r, x_3, \ldots, x_n)}\right) = 0 \tag{5.17}$$

if and only if $h_1'(r, x_3, \ldots, x_n).\det(B) = 0$, or equivalently $r = r_\alpha^0 = \alpha\sqrt{\dfrac{2}{1+\alpha}}$.

Also $f_\alpha'(r) = 0$ if and only if $r = r_\alpha^0$.

Take $\alpha < 1$. So the function

$$f_\alpha : (r_\alpha^0, \infty) \to \left(\arctan\left(\sqrt{\frac{1-\alpha}{1+\alpha}}\right) - \frac{\sqrt{1-\alpha^2}}{2\alpha}, \frac{\pi}{2}\right)$$

is a diffeomorphism and there exist a unique solution $\overline{r}_\alpha > r_\alpha^0$ such that

$$f_\alpha(\overline{r}_\alpha) = \frac{\pi(a_{11} + a_{22} + (b_1/\alpha))}{2b_1}.$$

For $\alpha \geq 1$ we have $f_\alpha : (\alpha, \infty) \to (0, \pi/2)$ and the result follows as above. □

Therefore Theorem 5.1 follows directly from Theorem 5.4 and Proposition 5.1.

Remark 10. *Note that for $r \leq \alpha$ we have $h_1(r, x_3, \ldots, x_n) = 0$ if and only if $a_{11} + a_{22} + (b_1/\alpha) = 0$. Since in the hypothesis (ii) of Proposition 5.1 we exclude this possibility then there is not limit cycles for $r \leq \alpha$.*

5.2.1 Proof of Corollary 5.1

Proof of Corollary 5.1. Using the previous notations let α tends to 0. So we have

$$\lim_{\alpha \to 0} \overline{r}_\alpha \geq \lim_{\alpha \to 0} r_\alpha^0 = 0. \tag{5.18}$$

But $\lim_{\alpha \to 0} \overline{r}_\alpha \neq 0$. In fact, consider the function

$$g_\alpha(r) = f_\alpha(r) - \frac{\pi(a_{11} + a_{22} + (b_1/\alpha))}{2b_1}.$$

Remember that $\overline{r}_\alpha$ is a zero of this function. So

$$\lim_{\alpha \to 0} \overline{r}_\alpha = 0 = \lim_{\alpha \to 0} r_\alpha^0 \Rightarrow 0 = \lim_{\alpha \to 0} g_\alpha(\overline{r}_\alpha) = \lim_{\alpha \to 0} g_\alpha(r_\alpha^0),$$

but a straightforward calculus shows that

$$\lim_{\alpha \to 0} g_\alpha(r_\alpha^0) = -\infty,$$

which is a contradiction, and so $\lim_{\alpha \to 0} \overline{r}_\alpha \neq 0$.

We can conclude that there exists a unique limit cycle of radius $\overline{r}_0 = \lim_{\alpha \to 0} \overline{r}_\alpha > 0$ for the discontinuous system (5.1) with $A_0 = A_0^1$ and $\varphi_0 = \lim_{\alpha \to 0} \varphi_\alpha$. □

Remark 11. *Using the main result of [7] the stability of the limit cycles associated with the solution $(\overline{r}_\alpha, 0, \ldots, 0)$ is given by the eigenvalues of the matrix*

$$\frac{\partial(h_1, \ldots, h_{n-1})}{\partial(r, x_3, \ldots, x_n)}\Big|_{(r, x_3, \ldots, x_n) = (\overline{r}_\alpha, 0, \ldots, 0)}.$$

5.3 Proof of Theorem 5.2

In this section we assume that $A_0 = A_0^2$. As in Section 5.2, the next lemma shows that through a linear change of variables, it is possible to reduce the number of parameters of system (5.4).

Lemma 5.4. *Assume that for $n > 4$, $(k_1^2 + k_2^2)k_5 \neq 0$ or $(k_3^2 + k_4^2)k_5 \neq 0$, and vector $b = (b_1, \ldots, b_n)$ is such that $b_1^2 + b_2^2 + b_3^2 + b_4^2 \neq 0$. Then by a linear change of variables system (5.4) can be transformed into the system*

$$\dot{x} = A_1 x + \varepsilon \overline{A} x + \varepsilon \varphi_\alpha(x_1)\overline{b}, \tag{5.19}$$

where $\overline{A} \in M_n(\mathbb{R})$ is an convenient matrix of A and $\overline{b} = e_1$ or $\overline{b} = e_3$. Moreover

$$A_1 = \begin{pmatrix} 0 & -1 & 0 & 0 \\ 1 & 0 & 0 & 0 \\ 0 & 0 & 0 & -1 \\ 0 & 0 & 1 & 0 \end{pmatrix}$$

if $n = 4$, and

$$A_1 = \begin{pmatrix} 0 & -1 & 0 & 0 & \varepsilon & 0 & \ldots & 0 \\ 1 & 0 & 0 & 0 & \varepsilon & 0 & \ldots & 0 \\ 0 & 0 & 0 & -1 & \varepsilon & 0 & \ldots & 0 \\ 0 & 0 & 1 & 0 & \varepsilon & 0 & \ldots & 0 \\ 0 & 0 & 0 & 0 & 0 & 0 & \ldots & 0 \\ \vdots & \vdots & \vdots & \vdots & \vdots & \vdots & \ddots & \vdots \\ 0 & 0 & 0 & 0 & 0 & 0 & \ldots & 0 \end{pmatrix}$$

if $n > 4$.

Proof. For the case $n = 4$ see the proof of Lemma 3.1 of [6]. So, we consider $n > 4$. Since the linear change of variables $x = Jy$, with J an invertible matrix, transforms system (5.4) into

$$\dot{y} = J^{-1}A_0 Jy + \varepsilon J^{-1} A J y + \varepsilon \varphi_\alpha(k^T J y) J^{-1} b,$$

we have to find J such that

$$J^{-1}A_0 J = A_1, \tag{5.20}$$

$$k^T = e_1^T J^{-1}, \tag{5.21}$$

$$J^{-1}b = \overline{b}. \tag{5.22}$$

We denote by z_{ij}, for $i, j = 1, \ldots, n$ the elements of the matrix J^{-1}. Using equations (5.40) and (5.41), easy computations show that J^{-1} is given by

$$\begin{pmatrix} k_1 & k_2 & k_3 & k_4 & k_5 & k_6 & k_7 & \ldots & k_n \\ -k_2 & k_1 & -k_4 & k_3 & -k_5 & -k_6 & -k_7 & \ldots & -k_n \\ z_{31} & z_{32} & z_{33} & z_{34} & k_5 & k_6 & k_7 & \ldots & k_n \\ -z_{32} & z_{31} & -z_{34} & z_{33} & -k_5 & -k_6 & -k_7 & \ldots & -k_n \\ 0 & 0 & 0 & 0 & -k_5\varepsilon^{-1} & -k_6\varepsilon^{-1} & -k_7\varepsilon^{-1} & \ldots & -k_n\varepsilon^{-1} \\ 0 & 0 & 0 & 0 & z_{65} & z_{66} & z_{67} & \ldots & z_{6n} \\ 0 & 0 & 0 & 0 & z_{75} & z_{76} & z_{77} & \ldots & z_{7n} \\ \vdots & \vdots & \vdots & \vdots & \vdots & \vdots & \vdots & \ddots & \vdots \\ 0 & 0 & 0 & 0 & z_{n5} & z_{n6} & z_{n7} & \ldots & z_{nn} \end{pmatrix}.$$

If we take $z_{31} = z_{32} = z_{34} = 0$, $z_{33} = z_{66} = \cdots = z_{nn} = 1$, $z_{ij} = 0$ for $i = 6, \ldots, n$, $j = 5, \ldots, n$ (except for $z_{66}, \ldots, z_{nn}$), $k_1 = b_1/(b_1^2 + b_2^2)$ and $k_2 = b_2/(b_1^2 + b_2^2)$ in the expression of J^{-1}, then equation (5.42) is satisfied with $\overline{b} = e_1$. In this case we obtain a matrix J^{-1} whose determinant is $-(k_1^2 + k_2^2)k_5/\varepsilon$.

On the other hand, if we take $z_{32} = z_{33} = z_{34} = 0$, $z_{31} = z_{66} = \cdots = z_{nn} = 1$, $z_{ij} = 0$ for $i = 6, \ldots, n$, $j = 5, \ldots, n$ (except for $z_{66}, \ldots, z_{nn}$), $k_3 = b_3/(b_3^2 + b_4^2)$ and $k_4 = b_4/(b_3^2 + b_4^2)$ in the expression of J^{-1}, then equation (5.42) is satisfied with $\overline{b} = e_3$. In this case we obtain a matrix J^{-1} whose determinant is $-(k_3^2 + k_4^2)k_5/\varepsilon$.

By hypothesis at least one of the above expressions for the determinant of J^{-1} is nonzero. Hence there exists the change of variables $x = Jy$. This completes the proof of Lemma 5.4. □

An equivalent system in the standard form for applying the averaging theory, will be found in the next lemma doing a convenient change of variables.

Lemma 5.5. *Changing the variables $(x_1, x_2, \ldots, x_n)$ to $(\theta, r, \rho, s, x_5, \ldots, x_n)$ by using*

$$x_1 = r\cos\theta, \quad x_2 = r\operatorname{sen}\theta, \quad x_3 = \rho\cos(\theta + s), \quad x_4 = \rho\operatorname{sen}(\theta + s),$$

system (5.19) is transformed into a system of the form

$$\begin{aligned} \frac{dr}{d\theta} &= \varepsilon H_1(\theta, r, \rho, s, x_5, \ldots, x_n) + O(\varepsilon^2), \\ \frac{d\rho}{d\theta} &= \varepsilon H_2(\theta, r, \rho, s, x_5, \ldots, x_n) + O(\varepsilon^2), \\ \frac{ds}{d\theta} &= \varepsilon H_3(\theta, r, \rho, s, x_5, \ldots, x_n) + O(\varepsilon^2), \\ \frac{dx_j}{d\theta} &= \varepsilon H_{j-1}(\theta, r, , \rho, s, x_5, \ldots, x_n) + O(\varepsilon^2), \end{aligned} \tag{5.23}$$

for $j = 5, \ldots, n$ where

$$H_1 = \cos\theta F_1 + \operatorname{sen}\theta F_2,$$

$$H_2 = \cos(\theta + s)F_3 + \operatorname{sen}(\theta + s)F_4,$$

$$H_3 = \frac{1}{r}\cos\theta F_2 - \frac{1}{r}\operatorname{sen}\theta F_1 - \frac{1}{\rho}\cos(\theta + s)F_4 + \frac{1}{\rho}\operatorname{sen}(\theta + s)F_3,$$

$$H_{j-1} = a_{j1}r\cos\theta + a_{j2}r\operatorname{sen}\theta + a_{j3}\rho\cos(\theta + s) + a_{j4}\rho\operatorname{sen}(\theta + s) +$$

$$+ b_j\varphi_\alpha(r\cos\theta) + \sum_{k=5}^{n} a_{jk}x_k,$$

and for $i = 1, \ldots, 4$ we have that $F_i = a_{i1}r\cos\theta + a_{i2}r\operatorname{sen}\theta + a_{i3}\rho\cos(\theta + s) + a_{i4}\rho\operatorname{sen}(\theta + s) + \varphi_\alpha(r\cos\theta)b_i + \sum_{k=5}^{n} a_{ik}x_k$. We take ε_0 sufficiently small, m arbitrarily large and $D_m = (1/m, m)\times(1/m, m)\times\mathbb{R}$. Then the vector field of system (5.23) is well defined and continuous on $\mathbb{R}\times D_m\times\mathbb{R}^{n-4}\times(-\varepsilon_0, \varepsilon_0)$. Moreover this system is $2\pi-$periodic with respect to the variable θ and locally Lipschitz with respect to the variable $(r, \rho, s, x_5, \ldots, x_n)$.

Proof. System (5.19) in the variables $(\theta, r, \rho, s, x_5, \ldots, x_n)$ becomes

$$\begin{aligned}
\dot{\theta} &= 1 + \frac{\varepsilon}{r}(\cos\theta F_2 - \operatorname{sen}\theta F_1),\\
\dot{r} &= \varepsilon H_1(\theta, r, \rho, s, x_5, \ldots, x_n),\\
\dot{\rho} &= \varepsilon H_2(\theta, r, \rho, s, x_5, \ldots, x_n),\\
\dot{s} &= \varepsilon H_3(\theta, r, \rho, s, x_5, \ldots, x_n),\\
\dot{x}_j &= \varepsilon H_{j-1}(\theta, r, \rho, s, x_5, \ldots, x_n) \text{ for } j = 5, \ldots, n.
\end{aligned}$$

We note that for $|\varepsilon|$ sufficiently small $\dot{\theta}(t) > 0$ for each t when $(\theta, r, \rho, s, x_5, \ldots, x_n) \in \mathbb{R} \times D_m \times \mathbb{R}^{n-4}$. Now we eliminate the variable t in the above system by considering θ as the new independent variable. It is easy to see that the right−hand side of the new system, for every fixed α, is well defined and continuous on $\mathbb{R} \times D_m \times \mathbb{R}^{n-4} \times (-\varepsilon_0, \varepsilon_0)$, it is $2\pi-$periodic with respect to the independent variable θ and locally Lipschitz with respect to $(r, \rho, s, x_5, \ldots, x_n)$. Form (5.23) is obtained after an expansion with respect to the small parameter ε. □

Here $\overline{A} = (a_{ij})$ if $n = 4$, and if $n > 4$ then a_{ij} is the element of the row i and column j of the $n \times n$ matrix

$$\overline{A} + \begin{pmatrix}
0 & 0 & 0 & 0 & 1 & 0 & \ldots & 0\\
0 & 0 & 0 & 0 & 1 & 0 & \ldots & 0\\
0 & 0 & 0 & 0 & 1 & 0 & \ldots & 0\\
0 & 0 & 0 & 0 & 1 & 0 & \ldots & 0\\
0 & 0 & 0 & 0 & 0 & 0 & \ldots & 0\\
\vdots & \vdots & \vdots & \vdots & \vdots & \vdots & \ddots & \vdots\\
0 & 0 & 0 & 0 & 0 & 0 & \ldots & 0
\end{pmatrix}.$$

We will apply Theorem 5.4 to system (5.23). Now we will find the corresponding function (5.10). We will denote it by $h : D_n \times \mathbb{R}^{n-4} \to \mathbb{R}^{n-1}$, $h = (h_1, h_2, \ldots, h_{n-1})^T$. For each $i = 1, \ldots, n-1$ the component h_i is defined by the formula

$$h_i(r, \rho, s, x_5, \ldots, x_n) = \int_0^{2\pi} H_i(\theta, r, \rho, s, x_5, \ldots, x_n) d\theta$$

where H_i are like in Lemma 5.5.

For each $r > 0$ we consider the functions I_0, I_1 and I_2 defined in section 5.2. Their expressions were obtained in Lemma 5.3. Thus we obtain the following expressions for the components of h

$$\begin{aligned}
h_1 &= c_1 r + (c_2 \cos s + c_3 \operatorname{sen} s)\rho + b_1 I_1(r),\\
h_2 &= (c_5 \cos s + c_6 \operatorname{sen} s) r + c_7 \rho + b_3 \cos s I_1(r),\\
h_3 &= c_4 + (c_2 \operatorname{sen} s - c_3 \cos s)\frac{\rho}{r} + (c_5 \operatorname{sen} s - c_6 \cos s)\frac{r}{\rho} +\\
&\quad + b_3 \operatorname{sen} s \frac{I_1(r)}{\rho},\\
h_{j-1} &= 2\pi(a_{j5} x_5 + \ldots + a_{jn} x_n),
\end{aligned} \tag{5.24}$$

for $j = 5, \ldots, n$, where the coefficients c_i are given by $c_1 = (a_{11} + a_{22})\pi$, $c_2 = (a_{13} + a_{24})\pi$, $c_3 = (a_{14} - a_{23})\pi$, $c_4 = (a_{21} - a_{12} - a_{43} + a_{34})\pi$, $c_5 = (a_{31} + a_{42})\pi$, $c_6 = (a_{41} - a_{32})\pi$ and $c_7 = (a_{33} + a_{44})\pi$.

In order to have that the system $h_i(\theta, r, \rho, s, x_5, \ldots, x_n) = 0$ for $i = 1, \ldots, n-1$ has isolated solutions it is required for $n > 4$ that the determinant of the matrix B obtained from the minor of the matrix $\overline{A}$ by erasing the first four rows and the first four columns is not zero. Then from the equations $h_i = 0$ for $i = 4, \ldots, n-1$ we get that $x_5 = \ldots = x_n = 0$.

Our next step is to study the solvability of the system

$$\begin{aligned} h_1(r, \rho, s, x_5, \ldots, x_n) &= 0, \\ h_2(r, \rho, s, x_5, \ldots, x_n) &= 0, \\ h_3(r, \rho, s, x_5, \ldots, x_n) &= 0. \end{aligned} \tag{5.25}$$

Of course any isolated $2\pi-$periodic solution of (5.23) with $|\varepsilon| \neq 0$ sufficiently small, corresponds to a limit cycle of (5.19).

Lemma 5.5 states that the hypotheses of Theorem 5.4 are fulfilled for system (5.23), where the function h is given by (5.24). Using also Remark 9 we conclude that, for $|\varepsilon|$ sufficiently small, and for each simple zero $(r^*, \rho^*, s^*, 0, \ldots, 0) \in D_m \times \mathbb{R}^{n-4}$ of h, there exists an isolated $2\pi-$periodic solution $\varphi(., \varepsilon)$ of system (5.23) such that $\varphi(0, \varepsilon) \to (r^*, \rho^*, s^*, 0, \ldots, 0)$ as $\varepsilon \to 0$. In short we have proved the next result.

Proposition 5.2. *From each periodic orbit of system* (5.7)*, which corresponds to a simple zero of h in $D_m \times \mathbb{R}^{n-4}$, a branch of limit cycles bifurcates from system* (5.19)*.*

For a proof of the next result see Lemma 3.4 of [6].

Lemma 5.6. *The displacement function of system* (5.19) *for the transversal section $x_2 = 0$, written in the coordinates of Lemma 5.5, has the form*

$$\varepsilon h(r, \rho, s, x_5, \ldots, x_n) + O(\varepsilon^2).$$

The proof of the following result will be the subject of the next section. We note that, in order to find the zeros of h in $D_m \times \mathbb{R}^{n-4}$ (or equivalently, to find the zeros $(r^*, \rho^*, s^*) \in D_m$ of system (5.25), because $x_5 = \cdots = x_n = 0$), it is sufficient to look for them in $(0, \infty) \times (0, \infty) \times [0, 2\pi)$. This is due to the fact that m can be chosen arbitrarily large, and h, as well as the transformation of Lemma 5.5 are $2\pi-$periodic with respect to the variable s.

Proposition 5.3. *Let $\tilde{h} : (M_\alpha, \infty) \times (0, \infty) \times \mathbb{R} \to \mathbb{R}^3$ be the function $\tilde{h} = (h_1, h_2, h_3)$ whose components are given by* (5.24)*, where* $M_\alpha = \max\left\{\alpha, \alpha\sqrt{\dfrac{2}{1+\alpha}}\right\}$*, c_i, for $i = 1, \ldots, 7$ are arbitrary real parameters, $b_1, b_3 \in \{0, 1\}$ with $b_1 b_3 = 0$ and $b_1^2 + b_3^2 \neq 0$. Then*

(i) $\tilde{h}$ is of class C^1;

(ii) the maximum number of isolated zeros of $\tilde{h}$ *in* $(M_\alpha, \infty) \times (0, \infty) \times \mathbb{R}$ *is three.*

(iii) Suppose that $0 < \alpha < 1$. *For*

$$c_1 = -2 + \frac{8(-1+\alpha)\pi}{9\alpha}, \quad c_2 = c_1, \quad c_3 = 0, \quad c_4 = -\frac{21c_1}{20}, \quad c_5 = 0,$$
$$c_6 = -\frac{c_1}{2}, \quad c_7 = \frac{c_1}{2}, \quad b_1 = 1, \quad b_2 = b_3 = b_4 = 0,$$

the function $\tilde{h}$ *has exactly three simple zeros.*

(iv) Suppose that $\alpha \in [1, 3) \cup (3, \infty)$. *For*

$$c_1 = 1 - \frac{3}{\alpha}, \quad c_2 = c_1, \quad c_3 = 0, \quad c_4 = -\frac{21c_1}{20}, \quad c_5 = 0,$$
$$c_6 = -\frac{c_1}{2}, \quad c_7 = \frac{c_1}{2}, \quad b_1 = 1, \quad b_2 = b_3 = b_4 = 0,$$

the function $\tilde{h}$ *has exactly three simple zeros.*

(v) Suppose that $\alpha = 3$. *For*

$$c_1 = -\frac{1}{2}, \quad c_2 = c_1, \quad c_3 = 0, \quad c_4 = -\frac{21c_1}{20}, \quad c_5 = 0,$$
$$c_6 = -\frac{c_1}{2}, \quad c_7 = \frac{c_1}{2}, \quad b_1 = 1, \quad b_2 = b_3 = b_4 = 0,$$

the function $\tilde{h}$ *has exactly three simple zeros.*

The conclusion of Theorem 5.2 follows from Lemmas 5.4 and 5.16 and Propositions 5.2 and 5.3.

5.3.1 Proof of Proposition 5.3

Function $\widetilde{h}$ is a composition of some elementary functions and function I_1. A direct study of I_1 shows that it is of class C^1 on (α, ∞). Thus, since $M_\alpha \geq \alpha$, statement (i) holds. We will divide the proof of the statement (ii) into several lemmas. Two auxiliary results will be given at the beginning, followed by a discussion with respect to different values of the coefficients.

The following notations will be used

$$d(s) = b_3 \cos s(c_2 \cos s + c_3 \operatorname{sen} s) - b_1 c_7,$$
$$k_1(s) = (c_5 b_1 - c_1 b_3) \cos s + c_6 b_1 \operatorname{sen} s,$$
$$k_2(s) = -c_2 c_5 \cos^2 s - (c_2 c_6 + c_3 c_5) \cos s \operatorname{sen} s - c_3 c_6 \operatorname{sen}^2 s + c_1 c_7,$$
$$\begin{aligned} f(s) &= c_4 d(s) k_1(s) + (c_2 \operatorname{sen} s - c_3 \cos s) k_1^2(s) + \\ &\quad (c_5 \operatorname{sen} s - c_6 \cos s) d^2(s) + b_3 d(s) k_2(s) \operatorname{sen} s. \end{aligned}$$

For studying the zeros of $\widetilde{h}$ it will be necessary to study the zeros of f.

Lemma 5.7. *The function $f : [0, 2\pi) \to \mathbb{R}$ can have at most six isolated zeros. Moreover they appear in pairs of the form s^* together with $\xi^* = s^* + \pi (\mathrm{mod}\ 2\pi)$ and when $b_1 = 0$ and $b_3 = 1$ two of them are $s^* = \pi/2$ and $\xi^* = 3\pi/2$.*

For a proof see Lemma 4.1 of [6].

The following result will be needed in the sequel.

Lemma 5.8. *We consider the equation*

$$I_1(r) = \frac{c}{\alpha} r, \quad r > 0, \tag{5.26}$$

where $I_1(r)$ is like before and c is a real parameter. Then we have the following situations.

(I) Assume that $\alpha \geq 1$.

(I-i) If $\pi(1 - \alpha) < c < \pi$, then (5.26) has a unique solution $r^* > \alpha$.

(I-ii) If $c = \pi$, then (5.26) has the interval $(0, \alpha]$ as the set of solutions.

(I-iii) If $c > \pi$ or $c \leq \pi(1 - \alpha)$, then (5.26) has no solution.

(II) Assume that $\alpha < 1$ and denote by $Q(\alpha)$ the number

$$Q(\alpha) = \pi + (1 + \alpha)\sqrt{\frac{1 - \alpha}{(1 + \alpha)}} - 2\alpha \arctan \sqrt{\frac{1 - \alpha}{(1 + \alpha)}}.$$

(II-i) If $\pi(1 - \alpha) < c < \pi$, then (5.26) has a unique solution $r^* > \alpha\sqrt{2/(1 + \alpha)}$.

(II-ii) If $c = \pi$, then (5.26) has $(0, \alpha] \cup \{r^*\}$, where $r^* > \alpha\sqrt{2/(1 + \alpha)}$, as the set of solutions.

(II-iii) If $\pi < c < Q(\alpha)$, then (5.26) has exactly two solutions $r_1^* < \alpha\sqrt{2/(1 + \alpha)}$ and $r_2^* > \alpha\sqrt{2/(1 + \alpha)}$.

(II-iv) If $c = Q(\alpha)$, then (5.26) has a unique solution $r^* = \alpha\sqrt{2/(1 + \alpha)}$.

(II-v) If $c > Q(\alpha)$ or $c \leq \pi(1 - \alpha)$, then (5.26) has no solution.

Proof. It is easy to see that the result holds for $r \in (0, \alpha]$, since in this case $I_1(r) = \dfrac{\pi}{\alpha} r$. For $r > \alpha$ equation (5.26) becomes

$$\frac{\pi r}{\alpha} + \frac{2}{r}\sqrt{r^2 - \alpha^2} - 2r \arctan\left(\frac{\sqrt{r^2 - \alpha^2}}{\alpha}\right) = \frac{c}{\alpha} r.$$

Introducing the new variable $u = \sqrt{r^2 - \alpha^2}/\alpha$, we obtain the equivalent equation

$$\alpha \arctan u - \frac{(\pi - c)}{2} - \frac{u}{1 + u^2} = 0, \quad u > 0.$$

We study the graphic of this function on the interval $(0, \infty)$. Then we can see:

(I) If $\alpha \geq 1$ then the equation has solution if and only if $\pi(1-\alpha) < c < \pi$. In this case the solution $u^* > 0$ is unique.

(II) If $\alpha < 1$ then the equation has solution if and only if $\pi(1-\alpha) < c \leq Q(\alpha)$. Moreover, if $\pi(1-\alpha) < c \leq \pi$, then the solution $u^* > \sqrt{(1-\alpha)}/(1+\alpha)$ is unique. If $\pi < c < Q(\alpha)$, then there exists two solutions $u_1^* < \sqrt{(1-\alpha)}/(1+\alpha)$ and $u_2^* > \sqrt{(1-\alpha)}/(1+\alpha)$. If $c = Q(\alpha)$ then the solution $u^* = \sqrt{(1-\alpha)}/(1+\alpha)$ is unique.

This completes the proof of the lemma. □

The next three lemmas study the zeros of $\tilde{h}$.

Lemma 5.9. *The function $\tilde{h}$ can have at most three isolated zeros $(r^*, \rho^*, s^*) \in (M_\alpha, \infty) \times (0, \infty) \times \mathbb{R}$, where M_α is like in Proposition 5.3, with $d(s^*) \neq 0$. When $b_1 = 0$, $b_3 = 1$ and $c_1 = 0$, then $\tilde{h}$ has at most two such zeros. If $b_1 = 0$, $b_3 = 1$ and $c_1 = 0$, then $\tilde{h}$ has no such zeros.*

Proof. We have that the two first equations of system (5.25) are equivalent to

$$\rho = \frac{k_1(s)}{d(s)} r, \tag{5.27}$$

$$I_1(r) = \frac{k_2(s)}{d(s)} r, \tag{5.28}$$

where d, k_1 and k_2 are defined at the beginning of this section. Replacing (5.27) and (5.28) in h_3 we obtain that $h_3 = 0$ is equivalent to $f(s) = 0$, where f also was defined at the beginning of this section.

Fix a zero s^* of f. We wish to study the solvability of (5.28) with respect to $r > M_\alpha$.

By Lemma 5.8 there exists an isolated solution $r > M_\alpha$ of (5.28) if and only if

$$\frac{\pi}{\alpha} - \pi < \frac{k_2(s^*)}{d(s^*)} < \frac{\pi}{\alpha} \text{ when } \alpha \geq 1, \text{ or} \tag{5.29}$$

$$\frac{\pi}{\alpha} - \pi < \frac{k_2(s^*)}{d(s^*)} < \frac{Q(\alpha)}{\alpha} \text{ when } \alpha < 1, \tag{5.30}$$

and in these cases it is unique. Note that we are excluding the case $c = Q(\alpha)$. Also, for a fixed r^*, corresponding to some s^*, whenever

$$\frac{k_1(s^*)}{d(s^*)} > 0, \tag{5.31}$$

we can uniquely find ρ^* satisfying (5.27). We will verify that condition (5.31) is satisfied only for at most half of the zeros of f. In order to do this, we note that $k_1(s+\pi) = -k_1(s)$, $d(s+\pi) = d(s)$, and we remind that the zeros of f appear in pairs, s^* together with $s^* + \pi$. Thus, condition (5.31) is satisfied either for s^*, or for $s^* + \pi$, unless $k_1(s^*) = 0$. Hence, function $\tilde{h}$ can have at most three isolated zeros $(r^*, \rho^*, s^*) \in (M_\alpha, \infty) \times (0, \infty) \times \mathbb{R}$ with $d(s^*) \neq 0$.

If $b_1 = 0$, $b_3 = 1$ and $c_1 = 0$ then $k_1 = 0$, so (5.31) cannot be satisfied for any s. If $b_1 = 0$, $b_3 = 1$ and $c_1 \neq 0$, then $k_1(s) = -c_1 \cos s$. By Lemma (5.7) two of the zeros of f are $s^* = \pi/2$ and $s^* = 3\pi/2$, which cannot provide any solution since (5.31) does not hold. □

Lemma 5.10. *When $b_1 = 1$, $b_3 = 0$, $c_7 = 0$, the function $\tilde{h}$ can have at most two isolated zeros in $(M_\alpha, \infty) \times (0, \infty) \times \mathbb{R}$.*

Proof. In this case $d = 0$, so we cannot apply Lemma 5.9. We can prove that system (5.25) is equivalent to

$$I_1(r) = \Big(-c_1 - q(s)\frac{\rho}{r}\Big)r, \tag{5.32}$$

$$k_1(s) = 0, \tag{5.33}$$

$$p_1(s)\Big(\frac{\rho}{r}\Big)^2 + c_4\frac{\rho}{r} + p_2(s) = 0, \tag{5.34}$$

where $q(s) = c_2 \cos s + c_3 \text{sen}\, s$, $p_1(s) = c_2 \text{sen}\, s - c_3 \cos s$ and $p_2(s) = c_5 \text{sen}\, s - c_6 \cos s$. For a fixed s, equation (5.34) provides at most two isolated values of ρ/r. By Lemma 5.8 for fixed s and fixed ρ/r, if $r > M_\alpha$ then equation (5.32) gives at most one isolated value for r. If $k_1 = 0$ then system (5.32)–(5.34) has no isolated solution. If $k_1 \neq 0$, then we denote by s^* and $\xi^* = s^* + \pi$, the zeros of k_1. Substituting s^* and ξ^* in (5.34) we obtain

$$p_1(s^*)\Big(\frac{\rho}{r}\Big)^2 + c_4\frac{\rho}{r} + p_2(s^*) = 0$$

and

$$p_1(s^*)\Big(\frac{\rho}{r}\Big)^2 - c_4\frac{\rho}{r} + p_2(s^*) = 0,$$

respectively. These two equations can have together at most two positive solutions ρ/r. We conclude that $\tilde{h}$ can have at most two isolated zeros. □

Lemma 5.11. *When $b_1 = 0$, $b_3 = 1$ and $c_7 \neq 0$ the function $\tilde{h}$ can have at most two isolated zeros $(r^*, \rho^*, s^*) \in (M_\alpha, \infty) \times (0, \infty) \times \mathbb{R}$ with $d(s^*) = 0$. Moreover either $c_1 = 0$, or $\tilde{h}$ has at most one isolated zero.*

Proof. Whenever $b_1 = 0$, system (5.25) is equivalent to

$$q(s)\frac{\rho}{r} = -c_1, \tag{5.35}$$

$$\cos s\frac{I_1(r)}{r} = -\tilde{q}(s) - c_7\frac{\rho}{r}, \tag{5.36}$$

$$p_2(s)\frac{r}{\rho} + \text{sen}\, s\frac{I_1(r)}{\rho} = 0,$$

where $\tilde{q}(s) = c_5 \cos s + c_6 \text{sen}\, s$ and q, p_1 and p_2 are like in the proof of Lemma 5.10. In this case $d(s) = q(s)\cos s$. We study the cases when $d(s^*) = 0$, i.e. either $q(s^*) = 0$ and equation (5.35) is degenerate, or $\cos s^* = 0$ and equation (5.36) is degenerate. If (5.35) is degenerate, but (5.36) is not, then we can write $I_1(r)/r$ as a function of s and ρ/r. Discussion is similar now to the one done in the proof of Lemma 5.10. The conclusion will be that $\tilde{h}$ can have at

most two isolated solutions (r^*, ρ^*, s^*) with $r^* > M_\alpha$ and $d(s^*) = 0$, and they can be found knowing that

$$c_2 \cos s^* + c_3 \operatorname{sen} s^* = 0, \tag{5.37}$$

$$\cos s^* p_1(s^*) \Big(\frac{\rho}{r}\Big)^2 + p_3(s^*)\frac{\rho}{r} - c_6 = 0,$$

$$\frac{I_1(r)}{r} = -\frac{\tilde{q}(s^*)}{\cos s^*} - \frac{c_7}{\cos s^*}\frac{\rho}{r},$$

where $p_3(s) = c_4 \cos s - c_7 \operatorname{sen} s$. In this case, equations (5.35) and (5.37) say that necessary conditions for the existence of isolated solutions are $c_1 = 0$ and $c_2^2 + c_3^2 \neq 0$, respectively.

It remains to study when equation (5.36) is degenerate, i.e. if $s^* = \pi/2$ or $s^* = 3\pi/2$. When we replace these values in (5.35) and (5.36) we obtain

$$c_3\frac{\rho}{r} = -c_1, \quad c_7\frac{\rho}{r} = -c_6,$$

and

$$c_3\frac{\rho}{r} = c_1, \quad c_7\frac{\rho}{r} = c_6,$$

respectively. From each system we can obtain at most one isolated value of ρ/r, but it is easy to see that only one of them is positive. Thus, $\tilde{h}$ can have at most one zero with $s^* = \pi/2$ or $3\pi/2$, and $c_1 \neq 0$ is a necessary condition for the existence of such zero. □

In order to conclude that $\tilde{h}$ can have at most three zeros in D_m, three different cases will be considered.

(i) If $b_1 = 1$, $b_3 = 0$, $c_7 \neq 0$, then $d(s) = c_7 \neq 0$ for all $s \in [0, 2\pi)$. The conclusion follows by Lemma 5.9;

(ii) If $b_1 = 1$, $b_3 = 0$, $c_7 = 0$, then we apply Lemma 5.10;

(iii) If $b_1 = 0$, $b_3 = 1$, $c_7 \neq 0$ then the conclusion holds by Lemmas 5.9 and 5.11.

We will now prove statements (iii)−(v) of Proposition 5.3.

For the values of the coefficients given in statement (iii), the components of function $\tilde{h}$ are

$$h_1 = \Big(-2 + \frac{4(-1+\alpha)\pi}{5\alpha}\Big)(r + \rho\cos s) + I_1(r),$$

$$h_2 = \Big(-1 + \frac{2(-1+\alpha)\pi}{5\alpha}\Big)(\rho - r\operatorname{sen} s),$$

$$h_3 = \Big(-2 + \frac{4(-1+\alpha)\pi}{5\alpha}\Big)\Big(-\frac{21}{20} + \frac{r\cos s}{2\rho} + \frac{\rho \operatorname{sen} s}{r}\Big),$$

and the equation $f(s) = 0$ is equivalent to

$$21\operatorname{sen} s - 20\operatorname{sen}^3 s - 10\cos s = 0.$$

If we consider the notation $x = \cos s$ then $\operatorname{sen} s = \sqrt{1-x^2}$ or $\operatorname{sen} s = -\sqrt{1-x^2}$. In both cases equation $f(s) = 0$ becomes

$$1 - 61x^2 + 360x^4 - 400x^6 = 0.$$

This polynomial equation has six solutions $x_{1,2} = \pm\sqrt{5}/5$, $x_{3,4,5,6} = \pm\sqrt{(7 \pm 2\sqrt{11})/20}$, and all are in the interval $(-1, 1)$.

We obtain that f has the following zeros, $s_1 = \arccos(\sqrt{5}/5)$, $s_{2,3} = \arccos\Big(\sqrt{(7 \pm 2\sqrt{11})/20}\Big)$, $\xi_{1,2,3} = s_{1,2,3} + \pi$.

One can prove that condition (5.30) is satisfied for every zero of f, but condition (5.31) is satisfied only for the zeros s_1, s_2 and s_3 of f. Then, $\tilde{h}$ has exactly three zeros. Since $\rho^* = r^* \operatorname{sen} s^*$ and $r^* > \alpha$ is the unique solution of (5.28) we conclude, using the software *Mathematica*, that $J_{\tilde{h}}(r^*, \rho^*, s^*) = 0$ if and only if α is approximately 4.89655. But in the statement (iii) we have that $0 < \alpha < 1$ and so $J_{\tilde{h}}(r^*, \rho^*, s^*) \neq 0$.

For the values of the coefficients given in statement (iv), the components of function $\tilde{h}$ are

$$h_1 = \frac{\alpha - 3}{\alpha}\Big(r + \rho\cos s\Big) + I_1(r),$$

$$h_2 = \frac{3 - \alpha}{2\alpha}\Big(r\operatorname{sen} s - \rho\Big),$$

$$h_3 = \frac{3 - \alpha}{\alpha}\Big(\frac{21}{20} - \frac{\rho}{r}\operatorname{sen} s - \frac{r}{2\rho}\cos s\Big),$$

and the equation $f(s) = 0$ also is equivalent to

$$21\operatorname{sen} s - 20\operatorname{sen}^3 s - 10\cos s = 0.$$

The zeros of f were obtained above.

One can prove that condition (5.29) is satisfied for every zero of f, but condition (5.31) is satisfied only for the zeros s_1, s_2 and s_3 of f. Then, $\tilde{h}$ has exactly three zeros. Since $\rho^* = r^* \operatorname{sen} s^*$ and $r^* > \alpha$ is the unique solution of (5.28) we conclude, using the software *Mathematica*, that $J_{\tilde{h}}(r^*, \rho^*, s^*) = 0$ if and only if $\alpha = 3$. But in the statement (iv) we have that $\alpha \in [1, 3) \cup (3, \infty)$ so $J_{\tilde{h}}(r^*, \rho^*, s^*) \neq 0$.

For the values of the coefficients given in statement (v), the components of $\tilde{h}$ are given by

$$h_1 = -\frac{r}{2} - \frac{\rho\cos s}{2} + I_1(r),$$

$$h_2 = -\frac{\rho}{4} + \frac{r\operatorname{sen} s}{4},$$

$$h_3 = \frac{21}{40} - \frac{\rho\operatorname{sen} s}{2r} - \frac{r\cos s}{4\rho},$$

and the equation $f(s) = 0$ has the same zeros obtained above.

One can prove that conditions (5.29) (for $\alpha = 3$) is satisfied for every zero of f, but condition (5.31) is satisfied only for the zeros s_1, s_2 and s_3 of f. Then $\tilde{h}$ has exactly three zeros. Using the software *Mathematica* we conclude that $J_{\tilde{h}}(r^*, \rho^*, s^*) \neq 0$ with the hypothesis of the statement (v). This concludes the proof of Proposition 5.3.

□

Taking $x_i = 0$, for $i = 5, \ldots, n$, we conclude directly that the map h has exactly three zeros in $(M_\alpha, \infty) \times (0, \infty) \times \mathbb{R} \times \mathbb{R}^{n-4}$.

Remark 12. *Using the main result of [7] the stability of the limit cycles associated with the solution* $(r^*, \rho^*, s^*, 0, \ldots, 0)$ *is given by the eigenvalues of the matrix*

$$\frac{\partial(h_1, \ldots, h_{n-1})}{\partial(r, \rho, s, x_5, \ldots, x_n)}\Big|_{(r,\rho,s,x_5,\ldots,x_n)=(r^*,\rho^*,s^*,0,\ldots,0)}.$$

5.3.2 Proof of Corollary 5.2

Proof of Corollary 5.2. By Lemma 5.9 we have that $\overline{r}_i^\alpha > M_\alpha$ where $\overline{r}_i^\alpha$ for $i = 1, 2, 3$ is the radius of the limit cycles when $\varepsilon \to 0$. Now let α tends to 0. So we have

$$\lim_{\alpha\to 0} \overline{r}_i^\alpha \geq \lim_{\alpha\to 0} M_\alpha = 0. \tag{5.38}$$

But $\lim_{\alpha\to 0} \overline{r}_i^\alpha \neq 0$. In fact consider the function

$$g_\alpha(r) = \alpha \arctan\Big(\frac{\sqrt{r^2-\alpha^2}}{\alpha}\Big) - \frac{(\pi - c)}{2} - \frac{\alpha\sqrt{r^2-\alpha^2}}{r^2}$$

given in Lemma 5.8. Remember that $\overline{r}_i^\alpha$ for $i = 1, 2, 3$ are zeros of this function. So

$$\lim_{\alpha\to 0} \overline{r}_i^\alpha = 0 = \lim_{\alpha\to 0} M_\alpha \Rightarrow 0 = \lim_{\alpha\to 0} g_\alpha(\overline{r}_i^\alpha) = \lim_{\alpha\to 0} g_\alpha(M_\alpha) = \frac{-\pi + c - 1}{2},$$

and this last number is equal to zero if and only if $c = \pi + 1$. Looking again at Lemma 5.8 we can see that, when α tends to zero, we have $\pi < c \leq \pi + 1$, and $c = \pi + 1$ implies that $c = Q(0)$. But this case was excluded in the proof of Lemma 5.9. So $c \neq \pi + 1$ and $\lim_{\alpha\to 0} \overline{r}_i^\alpha \neq 0$.

We can conclude that, for each $i = 1, 2, 3$, there exists a limit cycle of radius $\overline{r}_i^0 = \lim_{\alpha\to 0} \overline{r}_i^\alpha > 0$ (when $\varepsilon \to 0$), for the discontinuous system (5.1) with $A_0 = A_0^2$ and $\varphi_0 = \lim_{\alpha\to 0} \varphi_\alpha$. □

5.4 Proof of Theorem 5.3

In this section we assume that $A_0 = A_0^3$. The next lemma shows that through a linear change of variables, it is possible to reduce the number of parameters of system (5.1).

Lemma 5.12. *By a linear change of variables system* (5.1) *can be transformed into the system*

$$\dot{x} = A_0 x + \varepsilon \overline{A} x + \varepsilon \varphi(x_1) \overline{b}, \tag{5.39}$$

where $\overline{A} \in M_n(\mathbb{R})$ *is an arbitrary matrix and* $\overline{b} = (b_1, \ldots, b_n) = e_l$ *for some* $l = 1, 3, \ldots, n-1$, *where* e_l *is the* $l-$*th vector of the canonical basis of* $\mathbb{R}^n$.

Proof. Since the linear change of variables $x = Jy$, with J an invertible matrix, transforms system (5.1) into

$$\dot{y} = J^{-1}A_0Jy + \varepsilon J^{-1}AJy + \varepsilon\varphi(k^TJy)J^{-1}b,$$

we have to find J such that

$$J^{-1}A_0J = A_1, \tag{5.40}$$

$$k^T = e_1^TJ^{-1}, \tag{5.41}$$

$$J^{-1}b = \overline{b}. \tag{5.42}$$

We denote by z_{ij}, for $i, j = 1, \ldots, n$ the elements of the matrix J^{-1}. Using equations (5.40) and (5.41), easy computations show that J^{-1} is given by

$$\begin{pmatrix} k_1 & k_2 & k_3 & k_4 & \cdots & k_{n-1} & k_n \\ -k_2 & k_1 & -k_4 & k_3 & \cdots & -k_n & k_{n-1} \\ z_{31} & z_{32} & z_{33} & z_{34} & \cdots & z_{3(n-1)} & z_{3n} \\ -z_{32} & z_{31} & -z_{34} & z_{33} & \cdots & -z_{3n} & z_{3(n-1)} \\ \vdots & \vdots & \vdots & \vdots & \ddots & \vdots & \vdots \\ z_{(n-1)1} & z_{(n-1)2} & z_{(n-1)3} & z_{(n-1)4} & \cdots & z_{(n-1)(n-1)} & z_{(n-1)n} \\ -z_{(n-1)2} & z_{(n-1)1} & -z_{(n-1)4} & z_{(n-1)3} & \cdots & -z_{(n-1)n} & z_{(n-1)(n-1)} \end{pmatrix}.$$

If we take $z_{rr} = 1$, for $r = 3, 5, \ldots, n-1$, $z_{ij} = 0$ (of course, except for the elements mentioned previously), $k_1 = b_1/(b_1^2 + b_2^2)$ and $k_2 = b_2/(b_1^2 + b_2^2)$ in the expression of J^{-1}, then equation (5.42) is satisfied with $\overline{b} = e_1$. In this case we obtain a matrix J^{-1} whose determinant is $k_1^2 + k_2^2$.

On the other hand, if we take $z_{31} = z_{53} = \cdots = z_{l(l-2)} = 1$, $z_{rr} = 1$, for $r = l+2, l+4, \ldots, n-1$, $z_{1(l-2)} = k_{(l-2)} = 1$, $z_{1(l-1)} = k_{(l-1)} = 0$, $k_l = -b_l/(b_l^2 + b_{(l+1)}^2)$, $k_{(l+1)} = -b_{(l+1)}/(b_l^2 + b_{(l+1)}^2)$ and $z_{ij} = 0$ for the remaining elements, in the expression of J^{-1}, then equation (5.42) is satisfied with $\overline{b} = e_l$, where $l = 3, 5, \ldots, n-1$. In this case we obtain for each $l = 3, 5, \ldots, n-1$ a matrix J^{-1} whose determinant is $-(k_l^2 + k_{(l+1)}^2)$.

We recall that we work in the hypotheses that neither k, nor b is the null vector. So at least one of the above statements (i.e. when $\overline{b} = e_l$ for some $l = 1, 3, \ldots, n-1$) is well defined. Moreover at least one of the above expressions for the determinant of J^{-1} is nonzero. Hence there exists the change of variables $x = Jy$. This completes the proof of Lemma 5.12. □

Lemma 5.13. *Changing the variables* $(x_1, x_2, \ldots, x_n)$ *to* $(\theta, r, \theta_1, r_1, \ldots, \theta_{(n/2-1)}, r_{(n/2-1)})$ *by using*

$$\begin{aligned} x_1 = r\cos\theta, \quad & x_2 = r\operatorname{sen}\theta, \\ x_3 = r_1\cos(\theta+\theta_1), \quad & x_4 = r_1\operatorname{sen}(\theta+\theta_1), \\ & \vdots \\ x_{n-1} = r_{(n/2-1)}\cos(\theta+\theta_{(n/2-1)}), \quad & x_n = r_{(n/2-1)}\operatorname{sen}(\theta+\theta_{(n/2-1)}), \end{aligned}$$

system (5.39) *is transformed into a system of the form*

$$\begin{aligned}
\frac{dr}{d\theta} &= \varepsilon H_1(\theta, r, \theta_1, r_1, \ldots, \theta_{(n/2-1)}, r_{(n/2-1)}) + O(\varepsilon^2),\\
\frac{dr_1}{d\theta} &= \varepsilon H_2(\theta, r, \theta_1, r_1, \ldots, \theta_{(n/2-1)}, r_{(n/2-1)}) + O(\varepsilon^2),\\
\frac{d\theta_1}{d\theta} &= \varepsilon H_3(\theta, r, \theta_1, r_1, \ldots, \theta_{(n/2-1)}, r_{(n/2-1)}) + O(\varepsilon^2),\\
&\vdots\\
\frac{dr_{(n/2-1)}}{d\theta} &= \varepsilon H_{n-2}(\theta, r, \theta_1, r_1, \ldots, \theta_{(n/2-1)}, r_{(n/2-1)}) + O(\varepsilon^2),\\
\frac{d\theta_{(n/2-1)}}{d\theta} &= \varepsilon H_{n-1}(\theta, r, \theta_1, r_1, \ldots, \theta_{(n/2-1)}, r_{(n/2-1)}) + O(\varepsilon^2).
\end{aligned} \tag{5.43}$$

where

$$H_1 = \cos\theta F_1 + \operatorname{sen}\theta F_2,$$

$$H_j = \cos(\theta + \theta_{\frac{j}{2}})F_{j+1} + \operatorname{sen}(\theta + \theta_{\frac{j}{2}})F_{j+2},$$

$$H_{j+1} = -\frac{1}{r}\cos\theta F_2 + \frac{1}{r}\operatorname{sen}\theta F_1 + \frac{1}{r_{\frac{j}{2}}}\cos(\theta + \theta_{\frac{j}{2}})F_{j+2} - \frac{1}{r_{\frac{j}{2}}}\operatorname{sen}(\theta + \theta_{\frac{j}{2}})F_{j+1},$$

for $j = 2, 4, \ldots, n-2$, *and for* $i = 1, 2, \ldots, n$ *we have that* $F_i = (a_{i1}\cos\theta + a_{i2}\operatorname{sen}\theta)r + \sum_{l=3}^{\frac{n}{2}+1}\Big(a_{i(2l-3)}\cos(\theta + \theta_{l-2}) + a_{i(2l-2)}\operatorname{sen}(\theta + \theta_{l-2})\Big)r_{l-2} + \varphi(r\cos\theta)b_i$.

We take ε_0 *sufficiently small,* m *arbitrarily large and*

$$D_m = \left\{(r, \theta_1, r_1, \ldots, \theta_{(n/2-1)}, r_{(n/2-1)}) \in \Big(\frac{1}{m}, m\Big) \times \Big[\mathcal{S}^1 \times \Big(\frac{1}{m}, m\Big)\Big]^{\frac{n}{2}-1}\right\}.$$

Then the vector field of system (5.43) *is well defined and continuous on* $\mathcal{S}^1 \times D_m \times (-\varepsilon_0, \varepsilon_0)$. *Moreover the system is* $2\pi-$*periodic with respect to variable* θ *and locally Lipschitz with respect to variables* $(r, \theta_1, r_1, \ldots, \theta_{(n/2-1)}, r_{(n/2-1)})$.

Proof. System (5.39) in the variables $(\theta, r, \theta_1, r_1, \ldots, \theta_{(n/2-1)}, r_{(n/2-1)})$ becomes

$$\begin{aligned}
\dot\theta &= 1 + \frac{\varepsilon}{r}(\cos\theta F_2 - \operatorname{sen}\theta F_1),\\
\dot r &= \varepsilon H_1(\theta, r, \theta_1, r_1, \ldots, \theta_{(n/2-1)}, r_{(n/2-1)}),\\
\dot{r_1} &= \varepsilon H_2(\theta, r, \theta_1, r_1, \ldots, \theta_{(n/2-1)}, r_{(n/2-1)}),\\
\dot{\theta_1} &= \varepsilon H_3(\theta, r, \theta_1, r_1, \ldots, \theta_{(n/2-1)}, r_{(n/2-1)}),\\
&\vdots\\
\dot r_{(n/2-1)} &= \varepsilon H_{n-2}(\theta, r, \theta_1, r_1, \ldots, \theta_{(n/2-1)}, r_{(n/2-1)}),\\
\dot\theta_{(n/2-1)} &= \varepsilon H_{n-1}(\theta, r, \theta_1, r_1, \ldots, \theta_{(n/2-1)}, r_{(n/2-1)}).
\end{aligned}$$

We note that for $|\varepsilon|$ sufficiently small $\dot{\theta}(t) > 0$ for each t when $(\theta, r, \theta_1, r_1, \ldots, \theta_{(n/2-1)}, r_{(n/2-1)}) \in \mathbb{R} \times D_m$. Now we eliminate the variable t in the above system by considering θ as the new independent variable. It is easy to see that the right−hand side of the new system is well defined and continuous on $\mathbb{R}\times D_m \times (-\varepsilon_0, \varepsilon_0)$, it is $2\pi-$periodic with respect to the independent variable θ and locally Lipschitz with respect to $(r, \theta_1, r_1, \ldots, \theta_{(n/2-1)}, r_{(n/2-1)})$. Form (5.13) is obtained after an expansion with respect to the small parameter ε. □

We will apply Theorem 5.4 (see Section 5.1) to system (5.43). Our next step is to find the corresponding function (5.10). We will denote it by $h : D_m \to \mathbb{R}^{n-1}$, $h = (h_1, \ldots, h_{n-1})^T$.

Lemma 5.14. *The components of the averaged function h are given by*

$$
\begin{aligned}
h_1 &= c_1 r + \sum_{l=3}^{\frac{n}{2}+1} \Big(c_{1,(2l-4)} \cos\theta_{l-2} + c_{1,(2l-3)} \operatorname{sen}\theta_{l-2} \Big) r_{l-2} + b_1 I_1(r), \\
h_j &= (c_j \cos\theta_{\frac{j}{2}} + c_{(j+1)} \operatorname{sen}\theta_{\frac{j}{2}}) r + \\
&\quad \sum_{l=3}^{\frac{n}{2}+1} \Big(c_{j,(2l-4)} \cos(\theta_{\frac{j}{2}} - \theta_{l-2}) + c_{j,(2l-3)} \operatorname{sen}(\theta_{\frac{j}{2}} - \theta_{l-2}) \Big) r_{l-2} + \\
&\quad b_{j+1} \cos\theta_{\frac{j}{2}} I_1(r), \\
h_{j+1} &= c + \sum_{l=3}^{\frac{n}{2}+1} \Big(c_{1,(2l-3)} \cos\theta_{l-2} - c_{1,(2l-4)} \operatorname{sen}\theta_{l-2} \Big) \frac{r_{l-2}}{r} + \\
&\quad \Big(c_{(j+1)} \cos\theta_{\frac{j}{2}} - c_j \operatorname{sen}\theta_{\frac{j}{2}} \Big) \frac{r}{r_{\frac{j}{2}}} + \\
&\quad \sum_{l=3}^{\frac{n}{2}+1} \Big(c_{j,(2l-3)} \cos(\theta_{\frac{j}{2}} - \theta_{l-2}) - c_{j,(2l-4)} \operatorname{sen}(\theta_{\frac{j}{2}} - \theta_{l-2}) \Big) \frac{r_{l-2}}{r_{\frac{j}{2}}} - \\
&\quad \frac{b_{j+1}}{r_{\frac{j}{2}}} \operatorname{sen}\theta_{\frac{j}{2}} I_1(r),
\end{aligned}
\tag{5.44}
$$

for $j = 2, 4, \ldots, n-2$, where the coefficients $c's$ are given by

$$
c = (a_{12} - a_{21})\pi, \quad c_1 = (a_{11} + a_{22})\pi,
$$

$$
c_j = (a_{(j+1)1} + a_{(j+2)2})\pi, \quad c_{(j+1)} = (a_{(j+2)1} - a_{(j+1)2})\pi,
$$

$$
c_{1,(2l-4)} = (a_{1(2l-3)} + a_{2(2l-2)})\pi, \quad c_{1,(2l-3)} = (a_{1(2l-2)} - a_{2(2l-3)})\pi,
$$

$$
c_{j,(2l-4)} = (a_{(j+1)(2l-3)} + a_{(j+2)(2l-2)})\pi,
$$

$$
c_{j,(2l-3)} = (a_{(j+2)(2l-3)} - a_{(j+1)(2l-2)})\pi,
$$

for $l = 3, \ldots, n/2+1$, and the coefficients a_{rs} are the elements of the matrix $\overline{A}$ of Lemma 5.12.

In order to calculate the expression of h given by (5.44), we will use the following formulas

$$\int_0^{2\pi} \cos(\theta+s_1)\text{sen}\,(\theta+s_2)d\theta = \pi\text{sen}\,(s_2-s_1),$$
$$\int_0^{2\pi} \text{sen}\,(\theta+s_1)\cos(\theta+s_2)d\theta = -\pi\text{sen}\,(s_2-s_1),$$
$$\int_0^{2\pi} \text{sen}\,(\theta+s_1)\text{sen}\,(\theta+s_2)d\theta = \int_0^{2\pi} \cos(\theta+s_1)\cos(\theta+s_2)d\theta \;=$$
$$= \;\pi\cos(s_2-s_1),$$

for all $s_1, s_2 \in \mathbb{R}$.

For each $r>0$ we define

$$I_1(r) = \int_0^{2\pi} \varphi(r\cos\theta)\cos\theta d\theta,$$
$$I_2(r) = \int_0^{2\pi} \varphi(r\cos\theta)\text{sen}\,\theta d\theta,$$

where φ is the piecewise linear function given by (5.3).

Lemma 5.15. *The integrals I_1 and I_2 satisfy*

$$I_2(r) = 0 \text{ for all } r>0, \tag{5.45}$$

and

$$I_1(r) = \begin{cases} \pi r & \text{if } 0<r\le 1, \\ \pi r + \dfrac{2}{r}\sqrt{r^2-1} - 2r\arctan\left(\sqrt{r^2-1}\right) & \text{if } r>1. \end{cases} \tag{5.46}$$

Proof. Whenever $0<r\le 1$ we have that $|r\cos\theta|\le 1$ and $|r\text{sen}\,\theta|\le 1$ for all $\theta\in[0,2\pi)$. Then $\varphi(r\cos\theta) = r\cos\theta$ for every θ. Thus

$$\begin{aligned} I_1(r) &= r\int_0^{2\pi}\cos^2\theta d\theta &&= \pi r, \\ I_2(r) &= r\int_0^{2\pi}\text{sen}\,\theta\cos\theta d\theta &&= 0. \end{aligned}$$

We fix now $r>1$ and consider $\theta_c\in(0,\pi/2)$ such that $\cos\theta_c = 1/r$. Then we can write

$$\begin{aligned} I_1(r) &= \int_0^{\theta_c}\cos\theta d\theta + r\int_{\theta_c}^{\pi-\theta_c}\cos^2\theta d\theta - \int_{\pi-\theta_c}^{\pi+\theta_c}\cos\theta d\theta + \\ &\quad r\int_{\pi+\theta_c}^{2\pi-\theta_c}\cos^2\theta d\theta + \int_{2\pi-\theta_c}^{2\pi}\cos\theta d\theta, \\ I_2(r) &= \int_0^{\theta_c}\text{sen}\,\theta d\theta + r\int_{\theta_c}^{\pi-\theta_c}\text{sen}\,\theta\cos\theta d\theta - \int_{\pi-\theta_c}^{\pi+\theta_c}\text{sen}\,\theta d\theta + \\ &\quad r\int_{\pi+\theta_c}^{2\pi-\theta_c}\text{sen}\,\theta\cos\theta d\theta + \int_{2\pi-\theta_c}^{2\pi}\text{sen}\,\theta d\theta. \end{aligned}$$

Straightforward computations lead to the following expressions:

$$\begin{aligned} I_1(r) &= \pi r + \frac{2}{r}\sqrt{r^2-1} - 2r\arctan\left(\sqrt{r^2-1}\right), \\ I_2(r) &= 0, \end{aligned}$$

where we use that $\operatorname{sen}\theta_c = \sqrt{r^2-1}/r$ and $\theta_c = \arctan\left(\sqrt{r^2-1}\right)$. □

Proof of Lemma 5.14. We must compute

$$h_j(r,\theta_1,r_1,\ldots,\theta_{(n/2-1)},r_{(n/2-1)}) = \int_0^{2\pi} H_j(\theta,r,\theta_1,r_1,\ldots,\theta_{(n/2-1)},r_{(n/2-1)})d\theta, \tag{5.47}$$

for $j = 1,\ldots,n-1$. Using Lemma 5.15, from (5.47) we can obtain the expressions given in (5.44) for the components of the function h. This ends the proof of Lemma 5.14. □

For each point $(r^*,\theta_1^*,r_1^*,\ldots,\theta_{(n/2-1)}^*,r_{(n/2-1)}^*) \in D_m$ of system (5.44) we have a periodic orbit of system (5.8), because

$$r = \sqrt{x_1^2+x_2^2}, \quad r_i = \sqrt{x_{(2i+1)}^2+x_{(2i+2)}^2}, \quad \theta_i = \arctan\frac{x_{(2i+2)}}{x_{(2i+1)}} - \arctan\frac{x_2}{x_1},$$

for $i = 1,\ldots,n/2-1$ are first integrals of system (5.8).

Of course any isolated $2\pi-$periodic solution of (5.43) with $|\varepsilon| \neq 0$ sufficiently small, corresponds to a limit cycle of (5.39).

Theorem 5.5. *From each periodic orbit of the differential system* (5.8)*, with $n \geq 2$ even, which corresponds to a simple zero in D_m of the function $h = (h_1,\ldots,h_{n-1})$ given in* (5.44)*, a branch of limit cycles bifurcates for the differential system* (5.39)*.*

Proof. Lemma 5.13 states that the hypotheses of Theorem 5.4 are fulfilled for system (5.43), where the function h is given by (5.44). Using also Remark 9 we conclude that for $|\varepsilon|$ sufficiently small and for each simple zero $(r^*,\theta_1^*,r_1^*,\ldots,\theta_{(n/2-1)}^*, r_{(n/2-1)}^*) \in D_m$ of h, there exists an isolated $2\pi-$periodic solution $\varphi(.,\varepsilon)$ of system (5.43) such that $\varphi(0,\varepsilon) \to (r^*,\theta_1^*,r_1^*,\ldots,\theta_{(n/2-1)}^*,r_{(n/2-1)}^*)$ as $\varepsilon \to 0$. In short we have proved the Theorem 5.5. □

For a proof of the next result see Lemma 3.4 of [6].

Lemma 5.16. *The displacement function of system* (5.39) *for the transversal section $x_2 = 0$, written in the coordinates of Lemma 5.13, has the form*

$$\varepsilon h(r,\theta_1,r_1,\ldots,\theta_{(n/2-1)},r_{(n/2-1)}) + O(\varepsilon^2).$$

We note that in order to find the zeros of h in D_m it is sufficient to look for them in $(0,\infty)\times\left[\mathcal{S}^1\times(0,\infty)\right]^{\frac{n}{2}-1}$. This is due to the fact that m can be chosen arbitrarily large, and h, as well as the transformation of Lemma 5.13 are $2\pi-$periodic with respect to the variables $\theta_1,\ldots,\theta_{(n/2-1)}$.

Before proving Theorem 5.3 for arbitrary $n \geq 6$, we shall provide a more detailed proof for the particular case $n = 6$.

Proposition 5.4. *Consider system* (5.44) *with* $n = 6$. *Let* $h : (0,\infty) \times [\mathcal{S}^1 \times (0,\infty)]^2 \to \mathbb{R}^5$ *be the function* $h = (h_1, h_2, h_3, h_4, h_5)$ *whose components are given by* (5.44). *Then*

(i) h *is of class* C^1;

(ii) the maximum number of isolated zeros of h *in* $(0,\infty) \times [\mathcal{S}^1 \times (0,\infty)]^2$ *is* 324.

Proof. Function h is a composition of some elementary functions and function I_1. A direct study of I_1 shows that it is of class C^1 on $(0,\infty)$. Thus statement (i) holds. We will divide the proof of the statement (ii) into Lemmas 5.18, 5.19 and 5.20.

The following result will be needed later on. For a proof see Lemma 4.2 of [6].

Lemma 5.17. *We consider the equation*

$$I_1(r) = \lambda r, \quad r > 0, \tag{5.48}$$

where $I_1(r)$ *is like before and* λ *is a real parameter. Then we have the following situations.*

(a) If $0 < \lambda < \pi$, *then* (5.48) *has a unique solution* $r^* > 1$.

(b) If $\lambda = \pi$, *then* (5.48) *has the interval* $(0,1]$ *as the set of solutions.*

(c) If $\lambda > \pi$ *or* $\lambda \leq 0$, *then* (5.48) *has no solution.*

Our next goal is to find zeros of $h = 0$. The components of h are given by

$$\begin{aligned}
h_1 &= c_1 r + (c_{1,2}\cos\theta_1 + c_{1,3}\mathrm{sen}\,\theta_1) r_1 + \\
&\quad + (c_{1,4}\cos\theta_2 + c_{1,5}\mathrm{sen}\,\theta_2) r_2 + b_1 I_1(r) \\
h_2 &= (c_2\cos\theta_1 + c_3\mathrm{sen}\,\theta_1) r + c_{2,2} r_1 + \\
&\quad (c_{2,4}\cos(\theta_1-\theta_2) + c_{2,5}\mathrm{sen}\,(\theta_1-\theta_2)) r_2 + b_3\cos\theta_1 I_1(r), \\
h_3 &= (c + c_{2,3}) + (c_{1,3}\cos\theta_1 - c_{1,2}\mathrm{sen}\,\theta_1)\frac{r_1}{r} + \\
&\quad (c_{1,5}\cos\theta_2 - c_{1,4}\mathrm{sen}\,\theta_2)\frac{r_2}{r} + (c_3\cos\theta_1 - c_2\mathrm{sen}\,\theta_1)\frac{r}{r_1} + \\
&\quad (c_{2,5}\cos(\theta_1-\theta_2) - c_{2,4}\mathrm{sen}\,(\theta_1-\theta_2))\frac{r_2}{r_1} - \frac{b_3}{r_1}\mathrm{sen}\,\theta_1 I_1(r), \\
h_4 &= (c_4\cos\theta_2 + c_5\mathrm{sen}\,\theta_2) r + (c_{4,2}\cos(\theta_2-\theta_1) + c_{4,3}\mathrm{sen}\,(\theta_2-\theta_1)) r_1 + \\
&\quad c_{4,4} r_2 + b_5\cos\theta_2 I_1(r), \\
h_5 &= (c + c_{4,5}) + (c_{1,3}\cos\theta_1 - c_{1,2}\mathrm{sen}\,\theta_1)\frac{r_1}{r} + \\
&\quad (c_{1,5}\cos\theta_2 - c_{1,4}\mathrm{sen}\,\theta_2)\frac{r_2}{r} + (c_5\cos\theta_2 - c_4\mathrm{sen}\,\theta_2)\frac{r}{r_2} + \\
&\quad (c_{4,3}\cos(\theta_2-\theta_1) - c_{4,2}\mathrm{sen}\,(\theta_2-\theta_1))\frac{r_1}{r_2} - \frac{b_5}{r_2}\mathrm{sen}\,\theta_2 I_1(r).
\end{aligned} \tag{5.49}$$

By Lemma 5.12, we get (b_1, b_3, b_5) equal to $(1,0,0)$ or $(0,1,0)$ or $(0,0,1)$. Each one of the three next lemmas make reference to one of these cases.

Lemma 5.18. *Consider* $(b_1, b_3, b_5) = (1, 0, 0)$. *So, system* (5.49) *can have at most 324 zeros.*

Proof. Using $h_2 = h_4 = 0$ we obtain

$$r_1 = \frac{f_1(\theta_1, \theta_2)}{g_1(\theta_1, \theta_2)} r \text{ and } r_2 = \frac{f_2(\theta_1, \theta_2)}{g_1(\theta_1, \theta_2)} r,$$

and we get $r \neq 0$. Consider $\widetilde{r}_1 = g_1(\theta_1, \theta_2)^2 r_1/r$ and $\widetilde{r}_2 = g_1(\theta_1, \theta_2)^2 r_2/r$.

With the notations $\cos\theta_1 = x$, $\operatorname{sen}\theta_1 = z$, $\cos\theta_2 = y$, $\operatorname{sen}\theta_2 = w$, multiplying $h_3 = 0$ by $\widetilde{r}_1$ and $h_5 = 0$ by $\widetilde{r}_2$, we obtain a system with four equations and four unknowns (x, y, z, w) given by

$$\begin{aligned} \widetilde{h}_3 &= 0 \\ \widetilde{h}_5 &= 0 \\ x^2 + x^2 - 1 &= 0 \\ y^2 + w^2 - 1 &= 0. \end{aligned} \tag{5.50}$$

Using the software *Mathematica* we get that the first and the second equations of (5.50) are polinomial function of degree 9. By Bezout's Theorem, (5.50) have at most 324 solutions. Using the first equation of (5.49) and Lemma 5.17, to each solution $(x^*, y^*, z^*, w^*) \in (-1, 1) \times (-1, 1) \times (-1, 1) \times (-1, 1)$ corresponds, at most, one solution r^* of (5.48) and consequently, one solution r_1^* and one solution r_2^*. □

Lemma 5.19. *Consider* $(b_1, b_3, b_5) = (0, 1, 0)$. *So, system* (5.49) *can have at most 224 zeros.*

Proof. Using $h_1 = h_4 = 0$ we obtain

$$r_1 = \frac{f_3(\theta_1, \theta_2)}{g_2(\theta_1, \theta_2)} r \text{ and } r_2 = \frac{f_4(\theta_1, \theta_2)}{g_2(\theta_1, \theta_2)} r,$$

and we get $r \neq 0$. Consider $\widetilde{r}_1 = g_2(\theta_1, \theta_2)^2 r_1/r$ and $\widetilde{r}_2 = g_2(\theta_1, \theta_2)^2 r_2/r$.

With the notations $\cos\theta_1 = x$, $\operatorname{sen}\theta_1 = z$, $\cos\theta_2 = y$, $\operatorname{sen}\theta_2 = w$, multiplying $h_5 = 0$ by $\widetilde{r}_2$ and considering $\widetilde{h}_2 = g_2(\theta_1, \theta_2)^2 z h_2/r + \widetilde{r}_1 x h_3$, we obtain a system with four equations and four unknowns (x, y, z, w) given by

$$\begin{aligned} \widetilde{h}_2 &= 0 \\ \widetilde{h}_5 &= 0 \\ x^2 + x^2 - 1 &= 0 \\ y^2 + w^2 - 1 &= 0. \end{aligned} \tag{5.51}$$

Using the software *Mathematica* we get that the first and the second equations of (5.51) are polinomial function of degree 8 and 7 respectively. By Bezout's Theorem, (5.51) have at most 224 solutions. Using the second equation of (5.49) and Lemma 5.17, to each solution $(x^*, y^*, z^*, w^*) \in (-1, 1) \times (-1, 1) \times (-1, 1) \times (-1, 1)$ corresponds, at most, one solution r^* of (5.48) and consequently, one solution r_1^* and one solution r_2^*. □

Lemma 5.20. *Consider* $(b_1, b_3, b_5) = (0, 0, 1)$. *So, system* (5.49) *can have at most 224 zeros.*

Proof. Using $h_1 = h_2 = 0$ we obtain

$$r_1 = \frac{f_5(\theta_1, \theta_2)}{g_3(\theta_1, \theta_2)} r \text{ and } r_2 = \frac{f_6(\theta_1, \theta_2)}{g_3(\theta_1, \theta_2)} r,$$

and we get $r \neq 0$. Consider $\widetilde{r}_1 = g_3(\theta_1, \theta_2)^2 r_1/r$ and $\widetilde{r}_2 = g_3(\theta_1, \theta_2)^2 r_2/r$.

With the notations $\cos\theta_1 = x$, $\operatorname{sen}\theta_1 = z$, $\cos\theta_2 = y$, $\operatorname{sen}\theta_2 = w$, multiplying $h_3 = 0$ by $\widetilde{r}_1$ and considering $\widetilde{h}_4 = g_3(\theta_1, \theta_2)^2 w h_4/r + \widetilde{r}_2 y h_5$, we obtain a system with four equations and four unknowns (x, y, z, w) given by

$$\begin{array}{rcl} \widetilde{h}_3 & = & 0 \\ \widetilde{h}_4 & = & 0 \\ x^2 + x^2 - 1 & = & 0 \\ y^2 + w^2 - 1 & = & 0. \end{array} \tag{5.52}$$

Using the software *Mathematica* we get that the first and the second equations of (5.52) are polynomial function of degree 7 and 8 respectively. By Bezout's Theorem, (5.52) have at most 224 solutions. Using the fourth equation of (5.49) and Lemma 5.17, to each solution $(x^*, y^*, z^*, w^*) \in (-1, 1) \times (-1, 1) \times (-1, 1) \times (-1, 1)$ corresponds, at most, one solution r^* of (5.48) and consequently, one solution r_1^* and one solution r_2^*. □

This completes the proof of proposition 5.4. □

Proof of Theorem 5.3. Consider $n \geq 6$ and $\overline{b} = e_1$. First of all, note that the function h is a composition of some elementary functions and function I_1. A direct study of I_1 shows that it is of class C^1 on $(0, \infty)$. The subsystem, obtained of (5.44), formed by all the equations $h_j = 0$, where j is even, is a $(n/2-1) \times (n/2-1)$ linear system in the variables r_i, $i = 1, \ldots, n/2-1$. By Cramer's Rule, we get $r_i = \Delta r_i/\Delta_n$, where Δ_n is the discriminant of the matriz (P_{ji}) with $P_{ji} = P_{ji}(y_{j/2}, w_{j/2}, y_i, w_i)$, a polynomial of degree 2, being the coefficient of r_i in h_j and Δr_i is equal to Δ_n replacing the row i by the vector $(B_j r)$, where $-B_j$ is the coefficient of r in h_j. An easy computation shows that $r_i = r f_i/\Delta_n$ where f_i is an appropriated function.

It is easy to see that, for each n, $\deg \Delta_n = (\deg \Delta_{n-2}) + 2 = n - 2$, where $\deg p$ is the degree of the polynomial p (note that Δ_n has $n/2 - 1$ rows).

Multiplying h_{j+1} by $(r_{j/2}(\Delta_n)^2)/r$, we obtain a polynomial of degree $2n-3$ in the variables $(y_1, w_1, \ldots, y_{n/2-1}, w_{n/2-1})$ where $y_k = \cos\theta_k$ and $w_k = \operatorname{sen}\theta_k$ for $k = 1, \ldots, n/2 - 1$. By Bezout's Theorem, the subsystem, obtained of (5.44), formed by all the equations $h_{j+1} = 0$, where $j + 1 \geq 3$ is odd, together with the equations $y_k^2 + w_k^2 - 1 = 0$ for $k = 1, \ldots, n/2 - 1$ has $(4n - 6))^{n/2-1}$ solutions $(y_1^*, w_1^*, \ldots, y_{n/2-1}^*, w_{n/2-1}^*)$. Using the first equation of (5.44), by Lemma 5.8, for each one of the previous solutions, we obtain at most one r^* and consequently, at most one r_i^*, $i = 1, \ldots, n/2 - 1$.

If $\overline{b} = e_j$ we replace h_j by h_1 in the evaluation to obtain r_i, $i = 1, \ldots, n/2 - 1$. As consequence we apply the Bezout's Theorem for polynomials of smaller degree. So, the number of solutions when $\overline{b} \neq e_1$ is smaller.

□

Remark 13. *Using the main result of [7] the stability of the limit cycles associated with the solution* $(r^*, \theta_1^*, r_1^*, \ldots, \theta_{(n/2-1)}^*, r_{(n/2-1)}^*)$ *is given by the eigenvalues of the matrix*

$$\frac{\partial(h_1, \ldots, h_{n-1})}{\partial(r, \theta_1, r_1, \ldots, \theta_{(n/2-1)}, r_{(n/2-1)})}\Big|_{(r,\theta_1,r_1,\ldots,\theta_{(n/2-1)},r_{(n/2-1)})=(r^*,\theta_1^*,r_1^*,\ldots,\theta_{(n/2-1)}^*,r_{(n/2-1)}^*)}.$$

Índice Remissivo

Bibliography

[1] A. Andronov and S. Pontryagin, *Structurally stable systems*, Dokl. Akad. Nauk SSSR **14** (1937), 247–250.

[2] M. di Bernardo, C.J. Budd, A.R. Champneys, P. Kowalczyk, A.B. Nordmark, G.O. Tost and P.T. Piiroinen, *Bifurcations in nonsmooth dynamical systems*, SIAM Rev. **50** (2008), 629–701.

[3] M. di Bernardo, A.R. Champneys, S.J. Hogan, M. Homer, P. Kowalczyk, Yu.A. Kuznetsov, A.B. Nordmark and P.T. Piiroinen, *Two-parameter discontinuity-induced bifurcations of limit cycles: Classification and open problems*, Internat. J. Bifur. Chaos Appli. Sci. Engrg. **16** (2006), 601–629.

[4] M. di Bernardo, C.J. Budd, A.R. Champneys and P. Kowalczyk, *Piecewise-smooth dynamical systems – Theory and Applications*, Springer-Verlag (2008).

[5] A. Buica and J. Llibre, *Averaging methods for finding periodic orbits via Brouwer degree*, Bull. Sci. Math. **128** (2004), 7–22.

[6] A. Buica and J. Llibre, *Bifurcation of limit cycles from a four-dimensional center in control systems*, International J. of Bifurcation and Chaos **15**, (2005), 2653–2662.

[7] A. Buica, J. Llibre and O. Makarenkov, *Asymptotic stability of periodic solutions for nonsmooth differential equations with application to the nonsmooth van der Pol oscillator*, SIAM J. Math. Anal. 40 (2009), 2478–2495.

[8] C.A. Buzzi, T. de Carvalho and P.R. da Silva, *Closed polytrajectories and Poincaré Index of non-smooth vector fields on the plane*, posted in arXiv:1002.4169v1 [math.DS].

[9] C.A. Buzzi, T. de Carvalho and M.A. Teixeira, *Generic* 3*−parameter families of piecewise smooth vector fields in the plane.*, preprint (2010).

[10] C.A. Buzzi, T. de Carvalho and M.A. Teixeira, *Generic bifurcation of certain piecewise smooth vector fields*, posted in arXiv:1005.3258v3[math.DS] (2010).

[11] C.A. Buzzi, J. Llibre, J.C. Medrado and J. Torregrosa, *Bifurcation of limit cycles from a center in* $\mathbb{R}^4$ *in resonance* $1 : N$, Dynamical Systems: An International J. **24** (2009), 123–137.

[12] C.A. Buzzi, P.R. da Silva and M.A. Teixeira, *Singular perturbation problems for time reversible systems*, Proc. Amer. Math. Soc., **133** (2005), 3323-3331.

[13] C.A. Buzzi, P.R. da Silva and M. A. Teixeira, *A singular approach to discontinuous vector fields on the plane*, Journal of Differential Equations, **231** (2006), 633-655.

[14] P.T. Cardin, T. de Carvalho and J. Llibre, *Bifurcation of limit cycles from a* $n-$*dimensional linear center inside a class of piecewise linear differential systems*, preprint (2010).

[15] P.T. Cardin, T. de Carvalho and J. Llibre, *Limit cycles of discontinuous piecewise linear differential systems*, preprint (2010).

[16] T. de Carvalho and D. J. Tonon, *Generic bifurcations of planar Filippov Systems via geometric singular perturbations*, preprint (2011).

[17] S.N. Chow and J. Hale, *Methods of Bifurcation Theory*, Springer-Verlag, Berlin 1982.

[18] B. Coll, A. Gasull and R. Prohens, *Center-focus and isochronous center problems for discontinuous differential equations*, Discrete and Continuous Dynamical Systems **6** (2000), 609–624.

[19] F. Dumortier and R. Roussarie, *Canard cycles and center manifolds*, Memoirs Amer. Mat. Soc. **121**, 1996.

[20] N. Fenichel, *Geometric singular perturbation theory for ordinary differential equations*, Journal of Differential Equations **31** (1979), 53–98.

[21] A.F. Filippov, *Differential equations with discontinuous righthand sides*, Mathematics and its Applications (Soviet Series), Kluwer Academic Publishers-Dordrecht, 1988.

[22] P. Glendinning, *Non-smooth pitchfork bifurcations*, Discrete and Continuous Dynamical Systems Ser. B **4** (2004), 457–464.

[23] J. Guckenheimer and P. Holmes, *Nonlinear oscillations, dynamical systems, and bifurcation of vector fields*, Springer-Verlag, Berlin 1983.

[24] M. Guardia, T.M. Seara and M.A. Teixeira, *Generic bifurcations of low codimension of planar Filippov Systems*, posted in http://www.ma.utexas.edu/mp_arc-bin/mpa?yn=09-195.

[25] M. Han, K. Jiang and D. Green Jr., *Bifurcations of periodic orbits, subharmonic solutions and invariant tori of high-dimensional systems*, Nonlinear Analysis **36** (1999), 319–329.

[26] V. S. Kozlova, *Roughness of a discontinuous system*, Vestinik Moskovskogo Universiteta, Matematika **5** (1984), 16–20.

[27] YU.A. Kuznetsov, S. Rinaldi and A. Gragnani, *One-parameter bifurcations in planar Filippov systems*, Int. Journal of Bifurcation and Chaos, **13** (2003), 2157–2188.

[28] J. Llibre and A. Makhlouf, *Bifurcation of limit cycles from a two-dimensional center inside* $\mathbb{R}^n$, Nonlinear Analysis **72** (2010), 1387–1392.

[29] J. Llibre, P.R. Silva and M.A. Teixeira, *Sliding vector fields via slow-fast systems*, Bulletin of the Belgian Mathematical Society Simon Stevin **15-5** (2008), 851–869.

[30] N. G. Lloyd, *Degree Theory*, Cambridge University Press 1978.

[31] A. L. Maciel and J. Sotomayor, *Bifurcações de Campos Vetoriais Descontínuos*, Tese de doutorado, IME–USP (2009).

[32] M. C. Peixoto and M. M. Peixoto, *Structural Stability in the Plane with Enlarged Boundary Conditions*, Anais da Academia Brasileira de Ciências, **31**(2) (1959).

[33] J. Sotomayor, *Lições de Equações Diferenciais Ordinárias*, Projeto Euclides, IMPA 1979.

[34] J. Sotomayor and A.L. Machado, *Structurally stable discontinuous vector fields on the plane*, Qual. Theory of Dynamical Systems, **3** (2002), 227–250.

[35] J. Sotomayor and M.A. Teixeira, *Regularization of discontinuous vector fields*, International Conference on Differential Equations, Lisboa (1996), 207–223.

[36] J. Sotomayor and M. Zhitomirskii, *Impasse singularities of differential systems of the form* $A(x)x' = F(x)$, Journal pf Differential Equations **169**, n^{o}2, (2001), 567–587.

[37] P. Szmolyan, *Transversal heteroclinic and homoclinic orbits in singular perturbation problems*, Journal of Differential Equations **92** (1991), 252–281.

[38] L. Perko, *Differential Equations and Dynamical Systems*, Springer-Verlag, New York 1991.

[39] M.A. Teixeira, *Generic bifurcation in manifolds with boundary*, Journal of Differential Equations **25** (1977), 65–88.

[40] M.A. Teixeira, *Generic singularities of discontinuous vector fields*, An. Ac. Bras. Cienc. **53** (1991), 257–260.

[41] M.A. Teixeira, *Perturbation theory for non-smooth systems*, Meyers: Encyclopedia of Complexity and Systems Science **152** (2008).

[42] F. Verhulst, *Nonlinear Differential Equations and Dynamical Systems*, 2^{nd} edition, Universitext, Springer 1996.

[43] S.M. Vishik, *Vector fields near the boundary of a manifold*, Vestinik Moskovskogo Universiteta. Matematika **27** (1972), 21–28.